INFORMATICS TISCO, INC.

EFFECTS OF HIGH POWER LASERS

Sponsored by

Advanced Research Projects Agency

ARPA Order No. 1622

December 7 1971

**Approved for public release;
distribution unlimited.**

110 R

EFFECTS OF HIGH POWER LASERS

Sponsored by

Advanced Research Projects Agency

ARPA Order No. 1622

December 7, 1971

This research was supported by the Advanced Research Projects Agency of the Department of Defense and was monitored by the Air Force Office of Scientific Research under Contract No. F44620-70-C-0081. The publication of this report does not constitute approval by any government organization or Informatics Tisco, Inc., of the inferences, findings, and conclusions contained herein. It is published solely for the exchange and stimulation of ideas.

ARPA Order No. 1622
Program Code No: OF10
Name of Contractor:
Informatics Tisco, Inc.
Effective Date of Contract:
January 1, 1971
Contract Expiration Date
December 31, 1971
Amount of Contract: $215,672

Contract No. F44620-70-C-0081
Principal Investigator:
Stuart G. Hibben
Tel: (301) 779-2850
Short Title of Work:
"Laser Effects"

Prepared by

Informatics Tisco, Inc.
6811 Kenilworth Avenue
Riverdale, Maryland 20840

December 7, 1971

EFFECTS OF HIGH POWER LASERS

Introduction

This report contains a compilation of abstracts and one survey article on Soviet research in high power laser effects, published in the June 1969 - June 1971 interval. While this has normally been included as one of the subject headings in the Effects of Strong Explosions reports, we feel that the volume of recent laser material retrieved has warranted separate treatment. The report represents an exhaustive search by Informatics Tisco analysts of pertinent literature over this interval and, together with the laser articles already covered in the first two Explosions reports, completes the coverage to date on the latest Soviet high-power laser developments.

Articles have been selected on the general criterion of laser breakdown or destruction in the target medium, and are generally grouped by type of medium. Within each group the abstracts are arranged chronologically, except where a more logical grouping by author or subject suggested itself. Reference to previously reported laser articles is included where applicable; we intend in this way to generate a cumulative picture of the people, activities and directions involved in Soviet high-power laser R & D.

A survey article has been appended which gives a detailed summary of recent laser beam-target research at the Lebedev Institute under N. G. Basov. This paper provides a useful description of the laboratory techniques currently being used, and also relates the results of Basov's group to other Soviet and non-Soviet findings.

It should be noted that an increasing amount of Soviet laser reportage is being devoted to controlled fusion studies, notably by the group at Lebedev. However, this subject is considered outside the scope of the present report, hence all articles directly involving laser CTR research have been purposely omitted.

Cumulative numbering of the abstracts is continued from the second Effects of Strong Explosions report, for indexing purposes. A principal author index and source list are included at the end.

Table of Contents

LASER BREAKDOWN OF GAS

0266. Korneyev, N. Ye., Yu. I. Pavlov, and I. A. Rumyantseva. Study of plasmoids formed by focused laser radiation. Teplofizika vysokikh temperatur, No. 1, 1969, 167-168.

This paper is evidently a short version of a report by Korneyev and Pavlov already published (Effects of Strong Explosions, Report No. 2, June 14, 1971, 31). Ruby laser pulses with peaks of 60-80 Mw were focused in air; electron density and temperature of the resulting plasma were determined from spectrographic analysis. Temperature was determined from the N II 5179 and 5045 A nitrogen lines, N_e from the N II 3995 line. Other data are the same as in the cited earlier report.

0267. Vladimirov, V. I., G. M. Malyshev, G. T. Razdobarin, and V. V. Semenov. Study of an electric discharge through a laser spark. ZhTF, No. 5, 1969, 906-910.

An experiment is described demonstrating that a high-current electric discharge can be generated within a laser spark, at voltages well below normal air breakdown levels. Fig. 1 shows the configuration, in which

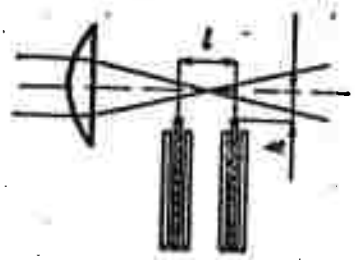

Fig. 1. Electrode positions relative to spark.

glass-clad tungsten electrodes were placed inside the spark region and fired by a 100 μf capacitor. By means of a second laser (normal to the plane of Fig. 1) the discharge was illuminated and shadow photos were made, an example of which is seen in Fig. 2. The threshold variations with ℓ and

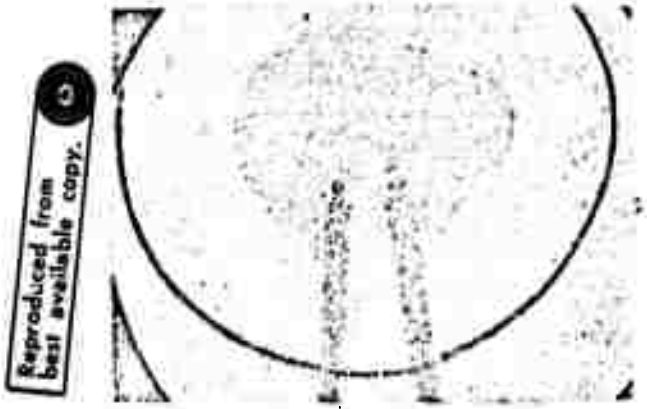

Fig. 2. Heated discharge region behind shock wave front.

h of Fig. 1 are plotted, showing a range of 50 to 550 v; no current figures are given. Data show that shock wave propagation velocity attained 3×10^5 cm/sec at 100 nsec following laser spark initiation. The condition obtained is seen to be essentially the same as for a self-sustaining arc discharge.

0268. Askar'yan, G.A., M.M. Savchenko, and V.K. Stepanov. Study of optical sparks and other nonlinear effects when focusing light with an axial aperture lens. ZhETF P, V. 10, No. 4, 1969, 161-165.

Photographic studies of optical breakdown in a variety of gases (He, Ne, Kr, air), liquids and glass are described. The method shown in Fig. 1 was used

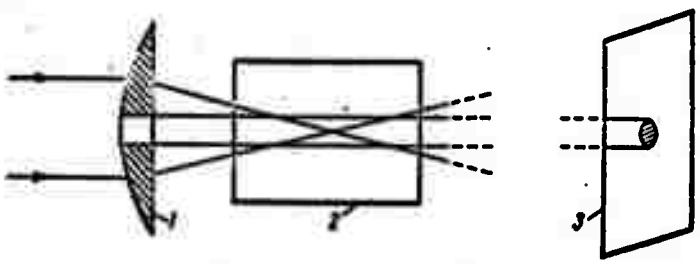

Fig. 1. Test configuration. 1-lens; 2-metal vessel with glass ports; 3-recordin film.

in which an axial portion of the incident beam passes through a lens aperture and is used as illumination for shadow photography of the spark. A Q-switched laser was used with 50 Mw peak power. Fig. 2 shows the distribution of darkening intensities on the film images for the gas specimens, atan initial pressure of 1 atm, which

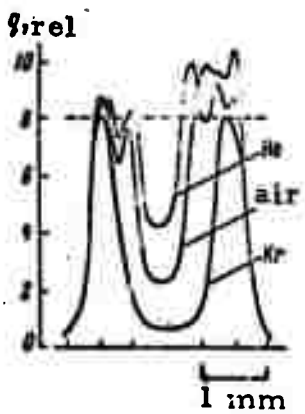

Fig. 2. Radial transmissivity distribution of sparks in He, Kr and air at one atm.

gives a qualitative picture of the absorption or reflection occurring in the spark. As a refinement the authors suggest inserting a doubler element in the lens aperture to generate a second harmonic illuminating signal, thus increasing the diagnostic effectiveness.

0269. Kovarskiy, V. A. Multiphoton transitions to an excited level of a hydrogen atom. ZhETF, V. 57, No. 4, 1969, 1217-1223.

A theoretical examination is given of multiphoton transitions to a degenerate level of the hydrogen atom, caused by irradiation with a powerful laser pulse. Transitions higher than the two-photon case are mainly considered. For calculation purposes, the model assumes both a fixed laser frequency ω and an auxiliary optical excitation source having a variable frequency Ω. A correlation is obtained between probability of transition and statistical radiation properties. Inhibition of resonant optical absorption at auxiliary frequency Ω by the laser radiation is also postulated.

0270. Generalov, N. A., G. I. Kozlov, and V. A. Masyukov. "Bleaching" and breakdown in molecular iodine under the effect of laser pulses. ZhETF, V. 58, No. 2, 1970, 438-440.
Safaryan, M. N. Bleaching of a molecular gas from the effect of laser pulses. Optika i spektroskopiya, V. 30, No. 4, 1971, 767-775.

An experiment is described in the first paper in which a pronounced bleaching process was observed in molecular iodine, as a result of focused laser radiation in the vapor. A ruby laser generating 50 ns, 10 Mw pulses was used, focused to a spot diameter of 3×10^{-2} cm by a lens with f=5 cm in iodine vapor at an ambient of 420°K. The bleaching effect was recorded as the ratio of transmitted to incident laser power through the focal region. Graphical results are given showing that for vapor pressures of 15 and 60 torr the focal region becomes almost fully transparent to incident laser radiation in a 10^7-10^9 w/cm^2 intensity range. The energy transition states governing the absorption effect are analyzed, and a theoretical threshold for the bleaching action is calculated and found to agree well with test results. It is concluded that the bleaching action, which corresponds to breakdown, results from photodissociation and excitation which causes spatial variations in refractive index within the focal region; this in turn can cause local breakdown at differing locations, at or near the necessary laser energy threshold.

In the second cited article Safaryan proposes a more detailed analytical model for the bleaching phenomenon in iodine reported by Generalov et al. It is assumed that a molecule under laser radiation undergoes an electron

vibrational transition and ceases to act as an absorption center; it returns to the initial state upon recombination of free atoms by triple collision. It is generally assumed that the characteristic duration of the radiation pulse and the photochemical reaction differ from vibrational relaxation time. For the case where all three intervals are of the same order of magnitude, the author uses his results to calculate effects in iodine vapor under the approximate test conditions of Generalov's group. Graphical data show good agreement between theoretical and actual test results. This analysis would be applicable both to a single molecular gas and to a mixture of it with an inert (non-absorbing) gas.

0271. Gernitz, E., R.M. Minikayeva, V. Ye. Mitsyuk, and V.A. Chernikov. Optical breakdown in gas mixtures. Vestnik Moskovskogo universiteta. Fizika, astronomiya, No. 3, 1970, 336-338.

Optical breakdown thresholds were monitored in Hg vapor with trace quantities of He or Ne. A Q- switched neodymium glass laser was used with a pulse width of 65 ns, energy of 1j, a dispersion of 5', focused in the vapor mixture at f=26 mm. The addition of He or Ne was found to lower the threshold level, even though the threshold for He or Ne alone is considerably higher than the mixture thresholds reported. The variation in threshold intensity was calculated on the assumption that lowering of the threshold depends on an increase in collision frequency of neutral atoms, as well as a reduction in diffusion losses.

0272. Arutyunyan, I.N., G.A. Askar'yan, and V.A. Pogosyan. Multiple photon processes in the focus of a high-power laser beam, with allowance for expansion of the active volume. ZhETF, V. 58, No. 3, 1970, 1020-1024.

Factors governing multiphoton processes at or near the focus of a laser beam in gas are analyzed. The total of events per unit volume, e.g. ionization, is expressed in terms of the probability of a single such event per unit time and at a given location, w(r, t). Here $w = AE^{2k}$, where E (t) = optical field amplitude, and k is the number of quanta required for ionization. Up through a certain range of optical field intensities it can be shown that the total of events N is related to E by $N(E) \sim E^{k}$. However for sufficiently great intensities $N \sim E^{3}$ and is independent of the quantization of the process. The results are cited as applicable for

determining the volume required for initiating multiphoton ionization in an optical spark. A similar theoretical treatment of multiphoton ionization is given by Delone et al (Role of field intensity and atomic structure in the process of multiphoton ionization. ZhETF P, V. 9, No. 2, 1969, 103), and was verified by observing laser ionization of Na atoms.

0273. Zel'dovich, B. Ya., B.F. Mulchenko, and N.F. Pilipetskiy. Observation of an extended optical spark. ZhETF, V. 58, No. 3, 1970, 794-795.

An experiment is briefly described in which spatially extended spark breakdowns were obtained in argon, using a conical rather than the usual spherical focusing lens. A ruby laser generating 15 Mw pulses was focused by a conical lens inside a pressure chamber and the resulting sparks were recorded as a function of argon pressure. Examples of spark formation are seen in Fig. 1. At 47 atm the spark geometry is similar to

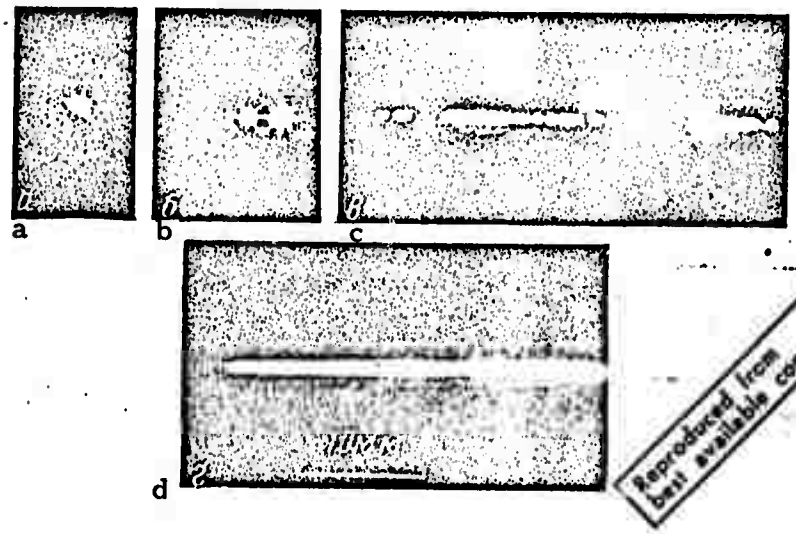

Fig. 1. Spark breakdown in argon. a-47 atm; b-(not given) c-60 atm; d-90 atm. Photos are side views.

that obtained by spherical lens; at increased pressure a spark train develops, leading to a continuous 30 mm line discharge at 90 atm pressure. An approximate calculation shows the focused power density to be 2×10^9 w/cm^2, which somewhat exceeds the threshold obtainable with a spherical lens under identical gas conditions. In the tested configuration the breakdown propagation velocity can exceed light velocity. It is concluded that this can be a useful technique for simulating line explosions and cylindrical shock waves. Similar results with a line-focused spark have been reported by Askar'yan and Stepanov (Effects of Strong Explosions, Report #2, 1971, 30).

0274. Krasyuk, I. K., P. P. Pashinin, and A. M. Prokhorov. Study of breakdown in argon and helium induced by a picosecond ruby laser pulse. ZhETF, v. 58, no. 5, 1970, 1606-1608.

The authors discuss experimental results of optical breakdown in argon and helium caused by high-power picosecond laser pulses. A ruby laser was used to generate 50 ps pulses focused at f = 2 cm to an area of 4×10^{-6} cm^2 in the tested gas. Breakdown was observed as a function of gas pressure over a range of 2 to 10^4 torr. As Figure 1 shows, the breakdown threshold is virtually independent of pressure up to some value, after which it decreases monotonically approximately as $1/\tau$. Within the precision limits of the measurement technique, the experimental and theoretical values for threshold intensities were in close agreement, e.g., 1.9×10^{32} vs 1×10^{32} photon/cm^2 /sec for argon. The results emphasize a fundamental difference in the breakdown mechanism from picosecond pulses as compared to longer duration pulses, namely that in the former case a direct multiphoton ionization occurs in place of the usual avalanche ionization mechanism.

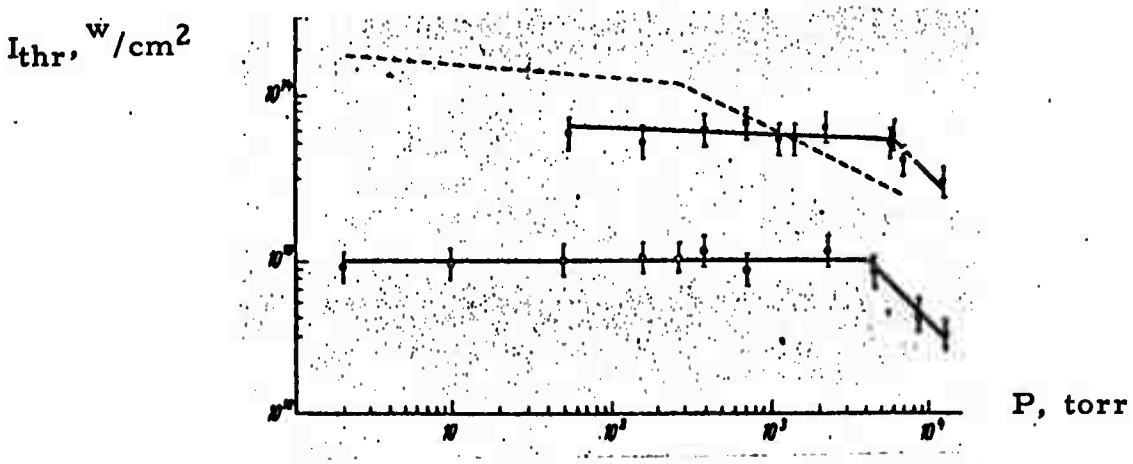

Fig. 1. Breakdown threshold vs pressure
o - argon; ● - helium

0275. Bunkin, F. V., I. K. Krasyuk, V. M. Marchenko, P. P. Pashinin, and A. M. Prokhorov. Structural study of a spark generated by a focused picosecond laser pulse in gas. ZhETF, v. 60, no. 4, 1971, 1326-1331.

With reference to the foregoing paper by Krasyuk et al (ZhETF, v. 58, no. 5, 1970, 1606), the authors have conducted further tests to

identify particular characteristics of picosecond optical breakdown in air, Ar and N_2 at atmospheric pressure. A ruby laser in the ring configuration of Figure 1 was used, generating pulse trains with individual pulse widths

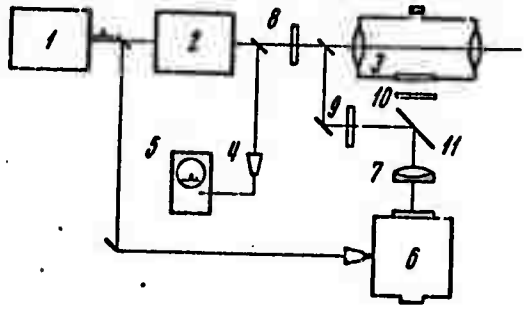

1 - ruby; 2 - amplifier; 3 - test chamber; 4 - photoelement; 5 - oscilloscope; 6 - electron-optical camers; 7 - lens; 8, 9, 10 - filters; 11 - deflector

Fig. 1. Gas breakdown experiment

of 20 - 100 ps. Additional recording equipment was used to get an exact time relationship of spark initiation, propagation and geometry with excitation pulse, lens focal length and focused spot dimensions. Typical photos of spark configuration are given, as well as streak photos of spark development. From the latter it can be seen that, following spark initiation, discrete subsparks continued to develop up to 160 ps after the end of the laser pulse. The authors note a lower threshold with their long-focus lens than the value reported by Krasyuk et al at f = 2 cm (3.5×10^{12} w/cm^2 vs 1.5×10^{14} w/cm^2, respectively). The results confirm that self-focusing is responsible for the discrete spark structure observed.

0276. Yevtushenko, T. P. and G. V. Ostrovskaya. Spectroscopic study of a laser spark. III. Continuous spectrum. ZhTF, no. 5, 1970, 1067-1071.

This paper is the third in a series reporting spectral studies of laser sparks in gas. Tests were made with atmospheric air and with He and Ar at pressures from 1 to 10 atm. Emission and absorption spectra were obtained over the 3000-7000 Å range, the technique for which is described. Figure 1 shows the comparative emission spectra obtained in the test gases at various pressures. Test data yielded a spark temperature on the order of 30,000°K in all three gases. Transmission and absorption coefficients were determined,

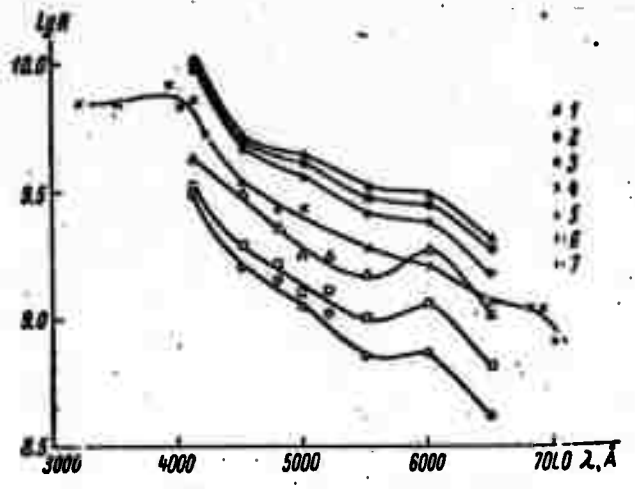

1 - Ar, 10 atm; 2 - Ar, 4 atm;
3 - Ar, 2 atm; 4 - air, 1 atm;
5 - He, 10 atm; 6 - He, 4 atm;
7 - He, 2 atm. H is in erg/cm

Fig. 1. Spectral energy distribution in a laser spark.

based on an electron density $N_e = 10^{19}/cm^3$ as observed 100 ns after initial breakdown. The authors propose the use of a laser spark as a continuous emitting source for absorption spectral studies, and illustrate with an example.

0277. Zubov, B. F., V. V. Kostin, T. M. Murina, and A. M. Prokhorov. Air breakdown from focused laser emission at $\lambda = 2.36\,\mu$. Kratkiye soobshcheniya po fizike, no. 11, 1970, 28-30.

A laser spark in air at atmospheric pressure, produced to date by ruby or neodymium lasers, is now reported by the authors with a $CaF_2:Dy^{2+}$ laser ($\lambda = 2.36\mu$). The experiment was done in a giant pulse mode at a pulse rate of 400 Hz, giving the appearance of a continuous glow breakdown; however, a photomultiplier monitor showed that breakdown occurred with each pulse and lasted approximately 100 ns. An expression for threshold laser intensity P_T is derived from experimental parameters. This showed that for $\tau = 40$ ns, a 400 Hz pulse rate and an average power of 1 watt, P_T was $10^9 w/cm^2$. The threshold was also strongly dependent on the number of excitation modes present. A typical spark spectrum is given in Figure 1, showing the NII line as seen in earlier ruby laser experiments. This would indicate a

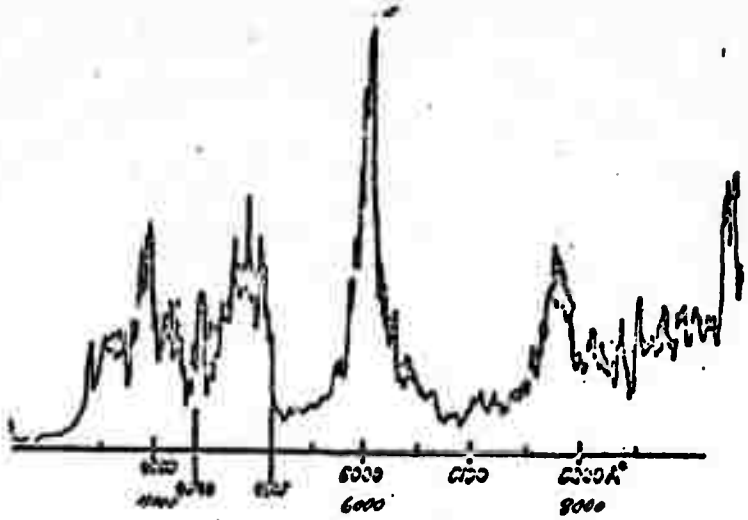

Fig. 1. Spark spectrum of air breakdown by a $CaF_2:Dy^{2+}$ laser.

temperature in the 30-40,000° range; however, some weak x-radiation was also detected, indicating a substantially higher initial plasma temperature.

0278. Mul'chenko, B. F. and Yu. P. Rayzer. Laser breakdown in an argon and neon mixture, and the role of photoionization of excited atoms. ZhETF, v. 60, no. 2, 1971, 643-650.

The authors are concerned here with the anomalous laser breakdown effect in a Ne-Ar mixture repor ted by Smith and Haught (Phys. Rev. Lett., 16, 1966, 1085), namely that over a substantial mixture range the breakdown threshold is well below the threshold for either gas in its pure form. The latters' results were duplicated closely, using a Q-switched neodymium laser; however, a qualitatively different threshold characteristic was found for ruby laser excitation, as shown in the graphs of Figure 1. Particular care was used

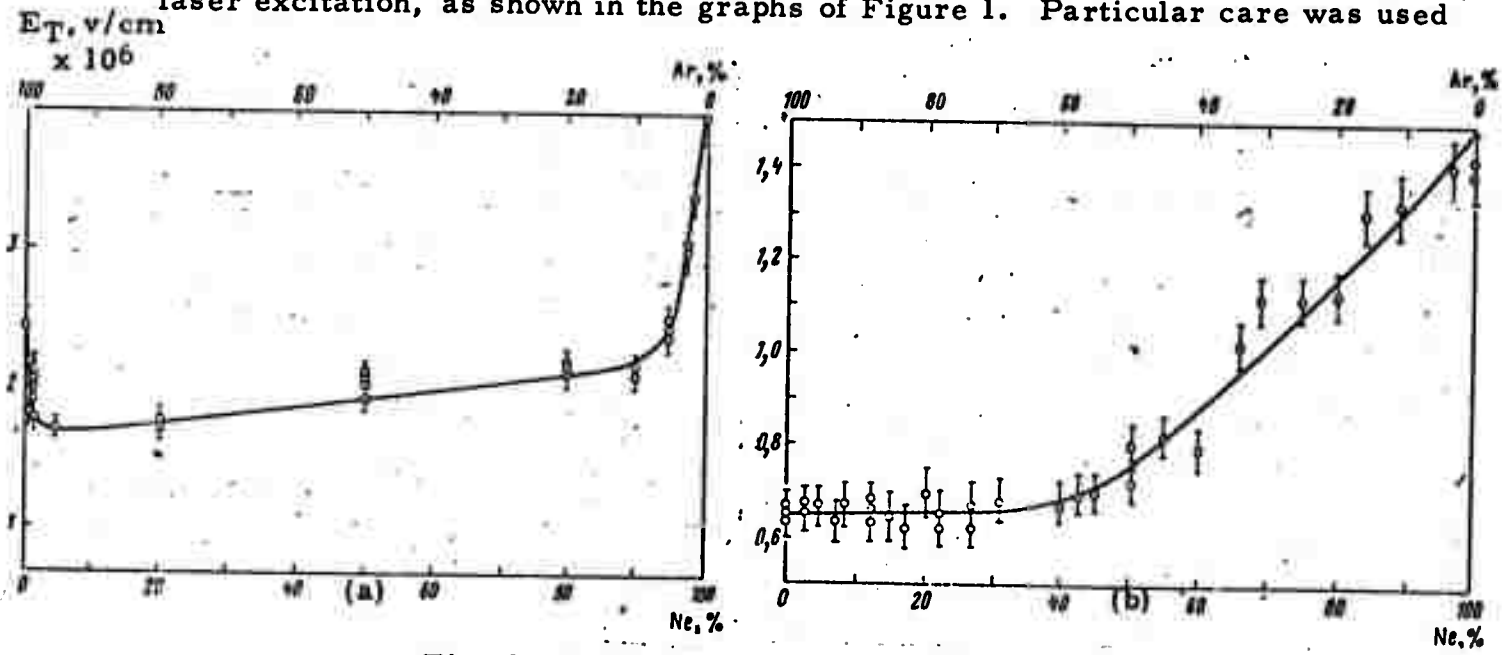

Fig. 1. Breakdown threshold in He + Ar.
p = 80 atm. a - Nd; b - ruby laser

to ensure the correctness of the gas mixtures and repeatability of the results, so that the difference between ruby and Nd laser effects could be established without question. Gas pressures were from 1 to 100 atm, with the bulk of the tests at 80 atm. The difference in laser responses is interpreted in terms of the high probability of Ne excitation at the ruby frequency, evidently from two-photon absorption, compared to the lower photoionization probability of the neodymium laser. In the former case the Penning effect is not a factor in accelerating the avalanching process, but is effective at the neodymium laser frequency. However, the authors do not consider the reduced threshold phenomenon to have been fully explained, and reject the "diffusion-like" loss mechanism proposed by Smith et al to account for it.

0279. Yeremin, V. I., L. V. Norinskiy, and V. A. Pryadein. Frequency dependence of optical breakdown threshold in air in the u-v band. ZhETF P, v. 13, no. 8, 1971, 433-436.

This experiment was designed to determine the optical breakdown characteristic of atmospheric air as a function of decreasing wavelengths, extending into the u-v region. To obtain the required laser intensities the authors used the frequency-doubling system first proposed by Norinskiy et al (Effective generation of powerful coherent u-v radiation. ZhETF P, v. 13, no. 4, 1971, 189-192), in which a neodymium laser fundamental is successively doubled to several higher harmonics. By strict control of experimental parameters this method produces peak powers up to 7 Mw for the 4th harmonic. The present authors used this technique to produce air sparks at 0.35 and 0.265μ, and report a nonmonotonic behavior of breakdown threshold with wavelength. Specifically, they found lower thresholds in the tested u-v range, in contradiction to the theory that threshold increases as the square of optical frequency. Their analysis of the electron-ion collision probabilities in the breakdown process shows that a lower threshold is to be expected at higher frequencies. Further clarification of this question will depend on applying single-mode emission, in order to eliminate the added variables introduced by higher modes.

0280. Ignatov, A. B., I. I. Komissarova, G. V. Ostrovskaya, and L. L. Shapiro. Holographic study of a laser spark. III. Sparks in hydrogen and helium. ZhTF, no. 4, 1971, 701-708

This paper continues a series of reports by the authors on experimental studies of optical sparks in gas. Use of a holographic method in the present

case enables a detailed picture to be obtained of spark parameters as a function of time and other variables. Figure 1 shows the test configuration.

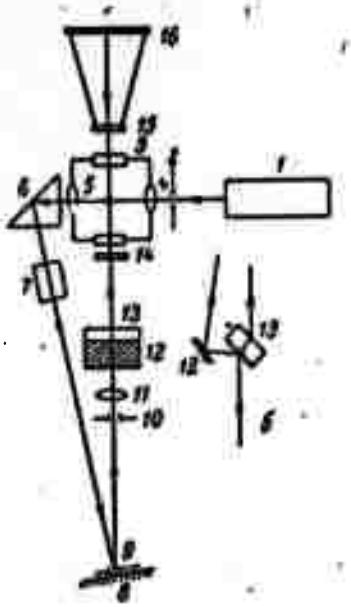

Fig. 1. Holography of a laser spark

The transmitted portion of a ruby laser beam (0.7j, 30 ns pulses) was frequency doubled in a KDP cell, divided into object and reference beams, and retransmitted through the spark region to form the hologram. Reconstruction was by a He-Ne laser at 6328 Å. Graphical data are given including electron density N_e, propagation velocity, and plasma geometry as functions of elapsed time after spark initiation. Figure 2 is an example of $N_e(t)$ in hydrogen for two gas pressures, while Figure 3 shows development of a spark profile in helium. The holographic method is thus seen as a powerful tool in identifying transient processes in laser-induced gas breakdown.

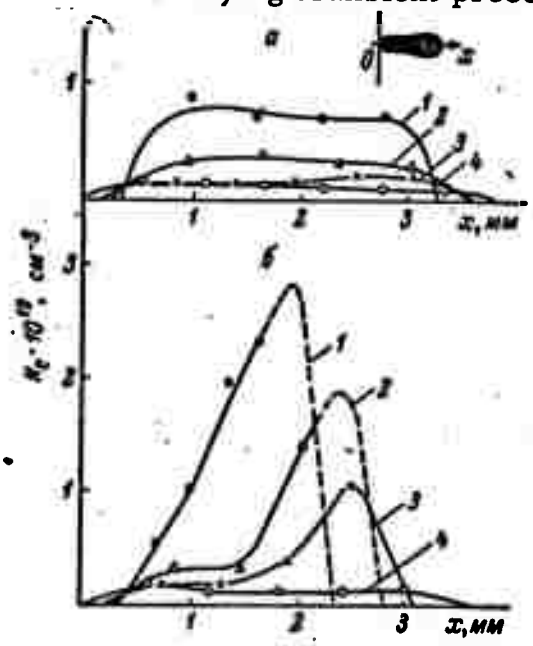

Fig. 2. N_e in hydrogen spark.
a - 1.75 atm; b - 11 atm;
1 - 20; 2 - 30; 3 - 40; 4 - 80 nsec

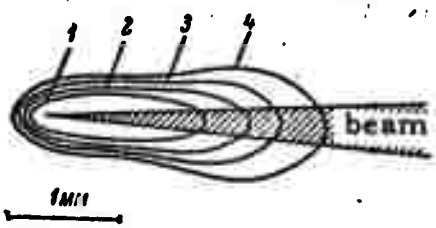

Fig. 3. Formation of spark in helium
1 - 4 as in Fig. 2

0281. Askar'yan, G. A. and N. M. Tarasova. Optical spark plasma in a gas envelope. Controlled propagation of the plasma and acceleration of the spark fireball. ZhETF P, v. 14, no. 2, 1971, 89-93.

A new version of a laser spark generator is described which provides control of plasma size and motion. A sketch of the configuration is shown in Figure 1. Pulsed emission from a Q-switched ruby laser (50-70 Mw) is focused within a vacuum chamber. At a selected interval after peak generation, the target gas is injected into the focal region at the desired pressure, by means of a high-speed valve. The resulting spark is controlled by an applied pulsed field of 10 koe and monitored by two SHF probes. Spark parameters are varied by means of initial static pressure of the gas, by changing the delay between laser pulse and gas injection, and by shifting the lens focus with respect to the inject port. Test data are given on spark formation in nitrogen and argon. Figure 2 shows the effect of reducing the

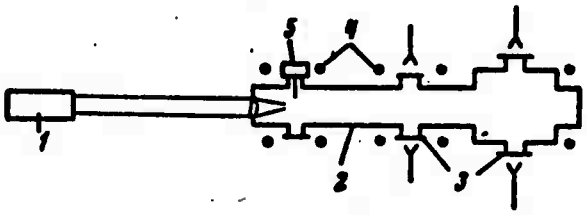

Fig. 1. Spark generator
1 - ruby laser; 2 - vacuum chamber; 3 - r-f probe ports; 4 - pulse coil (up to 10 koe); 5 - injection valve

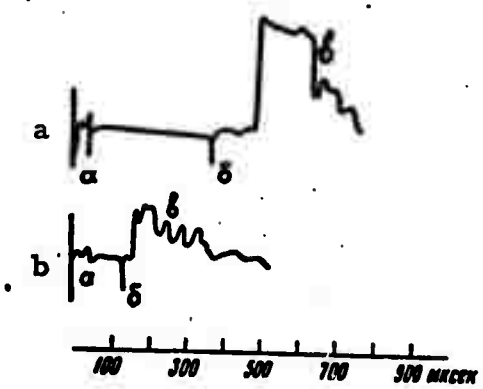

Fig. 2. Spark propagation for 300 (a) and 100 (b) microsecond delay

interval between the laser pulse and gas injection; in this case, shortening the delay from 300 to 100 μsec caused an increase in spark propagation velocity of an order of magnitude from 3×10^5 to 3×10^6 cm/sec. The method is simple and is cited for its advantages over the solid-target technique for generating a gas cloud.

0282. Generalov, N. A., V. P. Zimakov, G. I. Kozlov, V. A. Masyukov, and Yu. P. Rayzer. Gas breakdown from the effect of long-wave i-r radiation from a CO_2 laser. ZhETF P, v. 19, 1970, 343-346.

This is reported as one of the original studies of laser breakdown in gas from radiation in the infrared range. The authors used a flow-through CO_2 - N_2 - He laser mixture with discharge currents up to 90 ma, operated in a Q-switched mode. Pulse duration was 0.3-1.5 s with peak power of approximately 10 kw, and repetition rate was varied from 50 to 250 Hz. The beam was focused at f = 1.5 cm to a spot of 4×10^{-3} cm radius. Target gases were Ar, He, Ne and Xe, tested at static pressures up to 25 atm. Breakdown thresholds as functions of pressure and beam intensity are plotted, and spark photos are included. With the exception of Xe the data are somewhat inconclusive, owing to the uncertain impurity content of the other gases. A plot of threshold variation in Xe is shown in Figure 1.

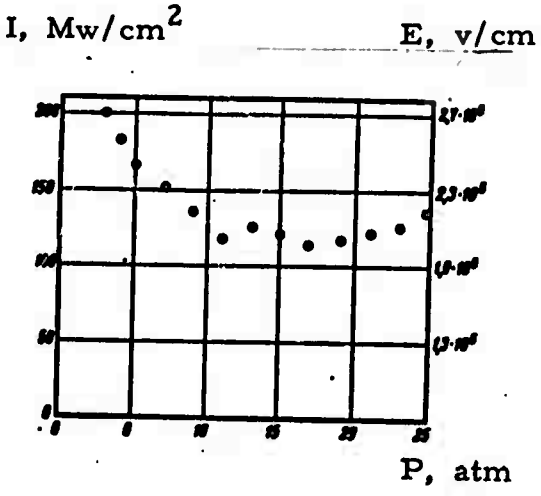

Fig. 1. Laser breakdown threshold in xenon

Figure 2 shows typical oscillograms of breakdown in Xe at p = 21 atm, including incident, transmitted and reflected pulse shapes. These all occur practically simultaneously at or near the laser power peak. The plasma glow was noted to exceed incident pulse width, but was considerably less than the period between pulses. An approximate expression is derived for threshold power density which agrees reasonably well with experimental findings.

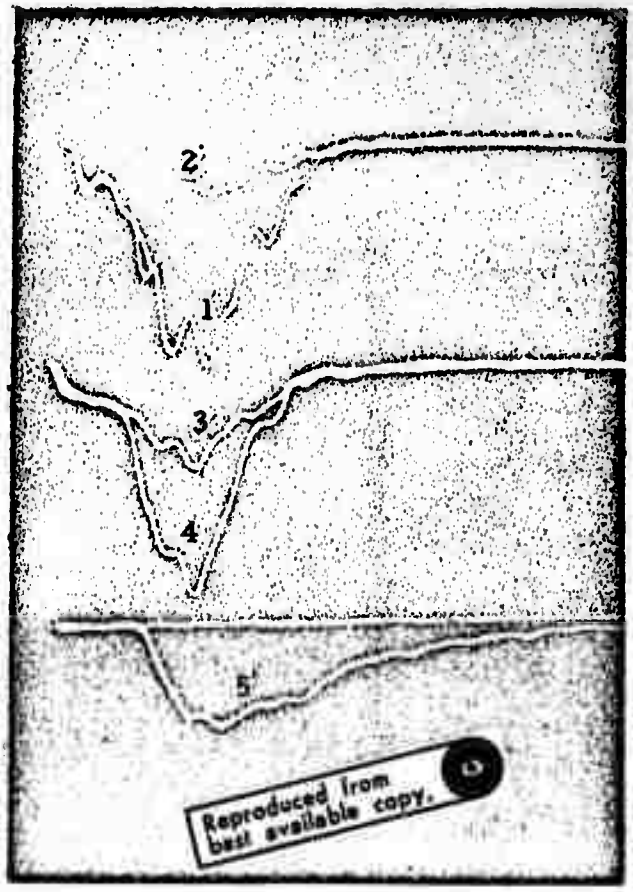

Fig. 2. Breakdown in xenon at 21 atm. 1, 3 - incident pulse; 2 - transmitted pulse; 4 - reflected pulse; 5 - plasma glow

0283. Afanas'yev, Yu. V., E. M. Belenov, O. N. Krokhin, and I. A. Poluektov. Ionization processes in a laser plasma. ZhETF P, v. 10, no. 11, 1969, 553-557.

A brief theoretical treatment is given describing the ionization processes which occur in a laser-generated plasma. Two general cases are considered, namely for incident radiation density q limited to values for which the plasma can be considered as in quasiequilibrium, and for higher values of q where thermodynamic equilibrium breaks down owing to rapid electron diffusion. The principal treatment is given to the latter case, and a model is postulated for it which yields approximate expressions for plasma parameters including electron temperature, ionization level, radiative output, and others. The cited case is characterized by an increasing divergence between electron and ion temperatures in the plasma; for example, for $q = 10^{12}$ w/cm^2, the difference may be on the order of 10^3 ev. The treatment given is directly relevant to interpreting laser plasma diagnostics in terms of bremsstrahlung output or ion radiation lines.

0284. Bunkin, F. V. and A. Ye. Kazakov. Compton mechanism in laser heating of an electron gas. DAN, v. 192, no. 1, 1970, 71-73.

A theoretical treatment is given to the problem of high-power laser absorption in a plasma, for the particular case in which a multiphoton Compton effect takes place. This has been shown to occur in energy exchanges in which a plasma is heated to thermonuclear temperatures within the focus of a sufficiently powerful laser beam. The authors derive expressions for energy absorption coefficient and rate for the assumed multiphoton mechanism. The rigorous equations for these are simplified for practical solution by assuming an initially relatively cool electron gas ($T \ll 10^8$ deg), such that electrons are nonrelativistic. With this assumption the approximate solutions for the energy equations were obtained by computer, over a wide range of test parameters; a neodymium glass laser was assumed as a source. The theoretical data show that for powerful e-m fields the electron gas can be strongly heated by multiphoton Compton effect; for example, for an incident laser intensity on the order of 10^{20} w/cm^2 and within a picosecond pulse width, the electron gas temperature can rise 10^7 degrees, or to thermonuclear temperatures.

0285. Bunkin, F. V. and A. Ye. Kazakov. Generation of electron-positron pairs from focused laser radiation in a dense plasma. DAN, v. 193, no. 6, 1970, 1274-1275.

The authors continue their analysis of the general case postulated in their foregoing paper herein, namely the production of relativistic energy levels in a nonrelativistic plasma by irradiation with a high-power focused laser beam. The conditions for generation of electron-positron pairs are analyzed quantitatively in terms of the parameter γ, where

$$\gamma = \frac{e}{mc^2}\frac{H_0}{H_{Cr}} = \frac{e}{mc^2}\frac{E_0}{E_{cr}}$$

in which E_0, H_0 = electric and magnetic field amplitude; E_{cr}, $H_{cr} = m^2c^3e\hbar$, and e = electron energy. For laser energies conceivably attainable in the near future, i.e., on the order 10^{19} w/cm^2, $\gamma \simeq 10^{-5}$. Hence the authors take $\gamma \ll 1$ and assume scattering effects by nuclei as well as interaction with free electrons, in formation of electron-positron pairs. From these assumptions an expression is obtained for the number of pairs formed in a given plasma volume at a given initial electron density and incident laser radiation energy. An assumed limiting case, determined by maximum tolerable electron density, is shown for $\lambda = 1.06\mu$ (Nd laser), radiation density = 5×10^{19} w/cm^2, a one-picosecond pulse and a focus volume of 10^{-7} cm^3. From this the maximum attainable number of pairs $N_p \simeq 8 \times 10^4 Z$ where Z is atomic charge. An expression for absorption coefficient is also derived. The authors note that the model does not require a prior ionization of the target volume since it can be shown that total ionization of the irradiated atoms can conceivably take place within the first period of the incident optical wave owing to tunneling action.

0286. Zakharov, S. D. and V. N. Fayzulayev. Bremsstrahlung absorption of powerful e-m radiation pulses in a fully ionized plasma. Kratkiye soobshcheniya po fizike, no. 5, 1970, 8-13.

The authors note that under high temperature heating of a plasma by laser radiation, absorption of light may be caused principally by bremsstrahlung emission, in which case the absorption coefficient K is independent of e-m field intensity. However, for powerful laser pulses in the picosecond range the field amplitude may have an appreciable effect on absorption; also, in this case the pulse width is comparable to the periodicity of electron-ion collisions, which would tend to reduce the absorbed energy. Assuming the latter case, the authors calculate K as functions of field strength E and pulse width τ, basing their work on an earlier paper by Bunkin et al (ZhETF v. 49, no. 10, 1965). A graphical solution for K(E) is seen in Figure 1 for two heating levels.

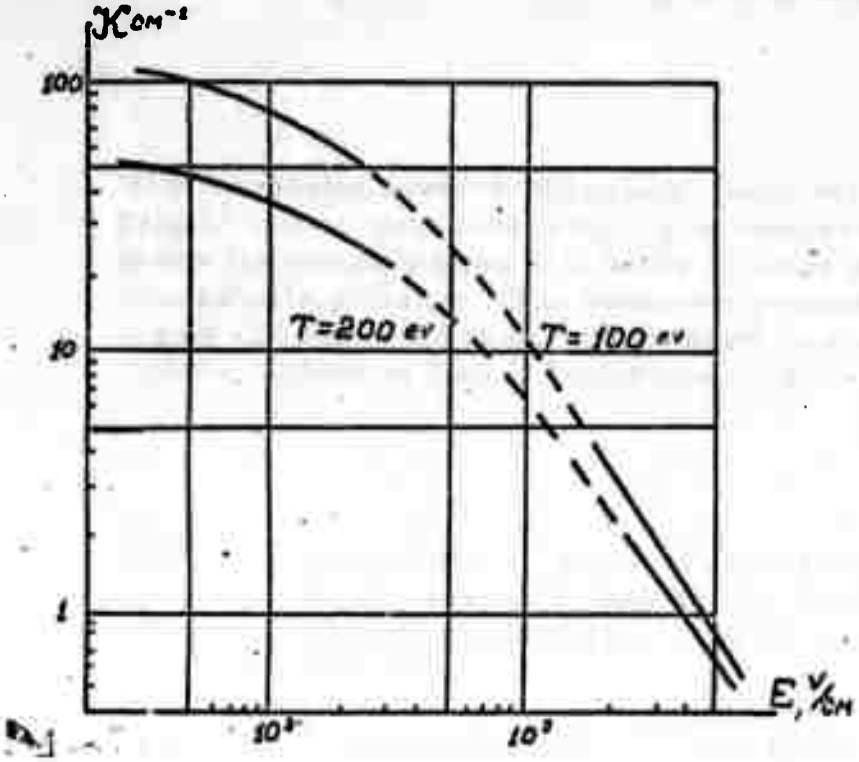

Fig. 1. Bremsstrahlung absorption vs field intensity

$\lambda = 1\mu$, $N_e = 5 \times 10^{20}/cm$
Z= 1

0287. Generalov, N. A., G. I. Kozlov, and Yu. P. Rayzer. Nonlinear absorption of laser pulses in a partially ionized gas. ZhPMTF, no. 1, 1970, 142-146.

This is a more detailed discussion of a previously published paper by the same authors (Effects of Strong Explosions, Report #1, Feb. 17, 1971, p. 45). The test described was designed to measure nonlinear absorption of a a laser beam when passed through a plasma behind a shock wavefront. A two-stage shock tube was used with hydrogen as the driver and xenon as the working gas; extra care was taken throughout to insure uniformity of plasma parameters and synchronization of laser transmission with shock wave position, so that maximum repeatability was obtained. Nominal conditions for the shock tube were a static Xe pressure of 10 torr, shock wave velocity of 1.82 km/sec, equilibrium temperature behind the shock wave of 11,250°K, and electron density $\sim 10^{18}$ /cm^3. The main phenomenon under study was the nonlinear absorption of laser energy over a certain range of intensities. This is seen qualitatively in Figure 1 which shows the relative absorption of beam power.

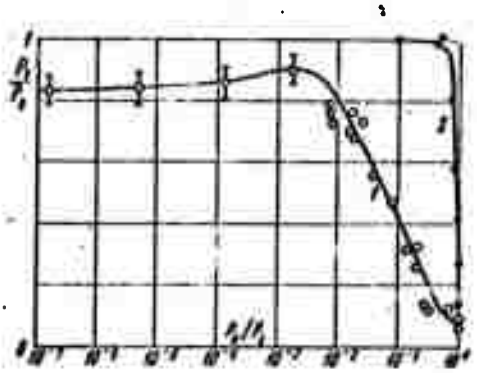

Fig. 1. Laser absorption vs incident power in xenon

P_0, P_1 and P_t = incident, transmitted and threshold levels respectively; 1-10 torr; 2-atmospheric

With increasing power a "bleaching" stage occurs, followed by a monotonic drop in optical transmissibility. For comparison, Curve 2 of Figure 1 shows the ordinary transmissibility of xenon at the same laser levels at atmospheric pressure. The ionization phenomena governing the nonlinear region are discussed here, and at length in a subsequent paper by the same authors (Effects of Strong Explosions, Report #2, June 14, 1971).

0288. Generalov, N. A., V. P. Zimakov, G. I. Kozlov, V. A. Masyukov, and Yu. P. Rayzer. Continuous hot optical discharge. ZhETF P, v. 11, 1970, 447-449.

The authors claim here the first continuous hot plasma generator, which uses a gas ignited and fed by two different lasers. The plasma region was maintained within the center of an enclosed gas volume, thus becoming the "optical plasmatron" suggested earlier by Rayzer (ZhETF P, v. 11, 1970, 195). The working gas was xenon in a steel vessel at varying pressures up to 10 atm. Initial breakdown was made by a Q-switched CO_2 laser, developing 10 kw, 0.3-1.5 μs pulses at a 50-250 Hz firing rate. The sustaining laser was a standard Lund 100 type, whose beam intersected the firing beam at right angles; it operated at 100 ma, 150 w, and was focused to a beam diameter of 0.08 mm in the plasma. Maintaining beam intersection and focal points was critical to the experiment, and admittedly complicated the method. However, this technique gives maximum flexibility in ignition frequency and duration, and furthermore does not contaminate the discharge region with electrode debris as is the usual case. The authors maintained a xenon plasma for periods of 10 minutes or more, terminating it only because of heating of the container, which was uncooled. A pressure threshold of 3 atm was determined for plasma generation; plasma shape and location were variable with increasing pressures. From i-r absorption data the plasma temperature was found to be about 14,000°K. This experiment was a variant of one reported earlier by Bunkin et al (Laser spark in the "slow burning" mode. ZhETF P, v. 9, no. 11, 1969, 609), in which the combustion phenomenon was obtained with a neodymium laser in atmospheric air. Combustion duration on the order of a millisecond was obtained at densities of 10^7 w/cm^2 under conditions where the density for optical breakdown would have been 10^9 w/cm^2.

0289. Mul'chenko, B. F., Yu. P. Rayzer, and V. A. Epshteyn. Study of a high pressure laser spark ignited by an adjacent plasma source. ZhETF, v. 59, no. 6, 1970, 1975-1982.

This experiment is a variant of the "optical plasmatron" described in the previous paper by Generalov et al (ZhETF P, v. 11, 1970, 447-449), in which the authors seek the optimum combination of conditions for igniting and sustaining a laser spark in gas. The present method is analogous to that of Generalov, except that rather than focusing both beams together in one plasma, Mul'chenko has used an offset igniter plasma to trigger the main plasma, as indicated in Figure 1. Ruby lasers were used in both cases, the

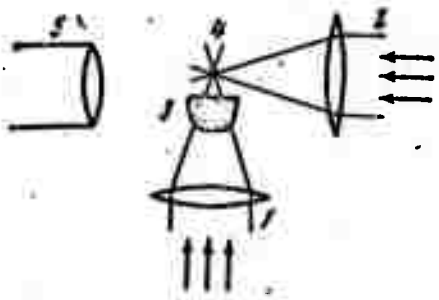

Fig. 1. Optical plasmatron

1 - sustaining beam; 2 - ignition beam; 3 - combustion plasma; 4 - ignition plasma; 5 - photorecorder

igniter operating in a free-running spike mode with 1.5-2 j pulses, while the sustaining laser operated in a quasi-cw mode with spike-free pulses of about 50 j. The working gas was mainly argon at pressures up to 80 atm. Extensive efforts are described in measuring ignition and sustaining laser power thresholds, gas pressures, beam focus diameters, plasma temperatures, spark propagation velocity, and light absorption. Figure 2 shows typical pulse shapes and time relations. Figure 3 shows the power threshold for sustaining the plasma as a function of gas pressure, while Figure 4 shows plasma temperature characteristics as functions of lifetime and distance from the beam focal point. For the lasers used, the pressure threshold was 16 atm; maximum temperature attained was determined photometrically to be 33,000°K.

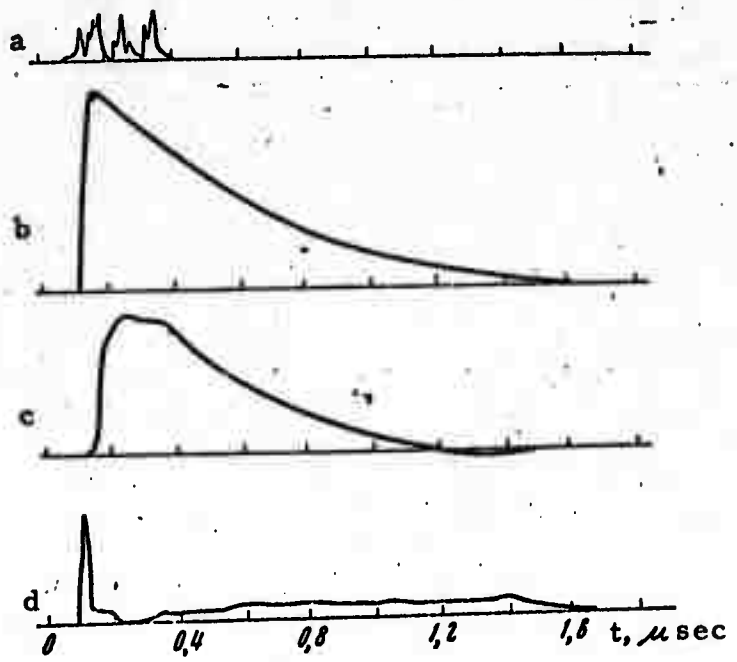

Fig. 2. Plasmatron pulse waveforms

a - spike pulse (1.5 j); b - spike-free pulse (40 j); c - plasma luminescence; d - transmitted spike-free pulse at p = 80 atm.

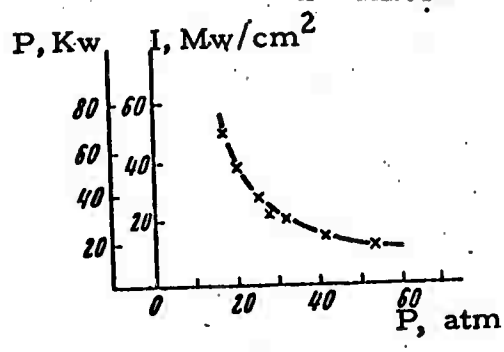

Fig. 3. Sustaining threshold vs pressure, argon

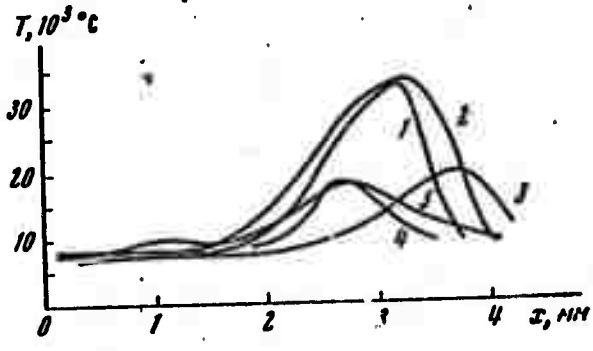

Fig. 4. Sustained plasma temperature vs distance from focal point. 1 - 50 μsec; 2 - 100 μsec; 3 - 500 μsec after sustaining pulse, p=80 atm; 4 - 50 μsec; 5 - 100 μsec after sustaining pulse, p=17 atm.

0290. Rayzer, Yu. P. Feasibility of an optical plasmatron and its power requirements. ZhETF P, v. 11, no. 3, 1970, 195-199.

0291. Rayzer, Yu. P. Subsonic propagation of an optical spark, and threshold conditions for maintaining the plasma by radiation. ZhETF, v. 58, no. 6, 1970, 2127-2138.

The author has investigated several variations on the standard electrode type plasmatron, leading to practical considerations for optically ignited and controlled plasmatrons. In an earlier paper (ZhPMTF, no. 3, 1968, 3-10), Rayzer gave a detailed analysis of the inductive type device in which a stationary discharge is produced within a solenoid. The possibilities of this and microwave plasmatrons suggested the use of lasers as an energy source, studies of which are reported in the two papers referenced above.

In the first paper Rayzer uses a simplified model to arrive at threshold intensity levels required for both a CO_2 and neodymium laser to maintain a controlled plasma. The levels sought are insufficient to produce optical detonation but can sustain slow combustion, i. e., subsonic propagation of the discharge against the beam by thermal conduction and radiation mechanisms. For the assumed tube geometry and heat losses using an air breakdown at atmospheric pressure, the author obtains a threshold of 1.3×10^4 kw/cm^2 for a neodymium laser, giving a peak plasma temperature of 17,000°K; for CO_2 the figures are 100 kw/cm^2 and 18,000°K, respectively. It is pointed out that the laser power requirement can be reduced by going to higher gas pressures, but at the expense of a more complex plasmatron construction.

The second of these papers is an expanded treatment of the same subsonic plasma problem, again referring to CO_2 and neodymium lasers in an air spark. For simplicity a one-dimensional case is assumed, with propagation only in the axial direction of the confining tube. Optical properties of the plasma as well as radiative and conductive losses are taken into account; also the reduction in laser threshold power realized by an optimally focused beam is defined. Propagation velocity of the plasma is calculated as a function of plasmatron parameters; for tube diameters on the order of a few millimeters, these values reach the order of 10 m/sec. It follows that the plasma can be moved by relocating the laser focus, providing this is done at rates not exceeding inherent propagation velocity.

0292. Zel'dovich, Ya. B., and Ye. V. Levich. Heating a plasma by opposed beams of coherent radiation. ZhETF P, v. 11, 1970, 497-500.

Theoretical considerations are briefly discussed for heating a plasma by two opposed laser beams, and a quantitative comparison is given with an assumed single-beam heating. In the two-beam case one beam must be assumed to have a sufficiently broad spectrum to achieve the necessary energy densities, so that both beams are not strictly monochromatic; the problem is analyzed with this approximation in mind. Ideally, plasma heating rate would then be proportional to the product of the two beam intensities, and independent of atomic change or plasma density. After numerous citations of previous papers on the subject, the authors assume a numerical case for lasers with 50 j outputs, pulse width of 10^{-11} sec, density of 5×10^{17} w/cm^2, and frequency of 3×10^{14} Hz. The data given show the advantage of the dual beam over the usual bremsstrahlung heating, even at lower laser beam intensities.

0293. Krasyuk, I. K., P. P. Pashinin, and A. M. Prokhorov. Experimental observation of stimulated Compton absorption of laser emission in a spark. ZhETF P, v. 12, 1970, 439-442.

An experiment is described which was designed to demonstrate the predominance of stimulated Compton absorption of laser energy in a plasma, at sufficiently high beam intensities. The test was based on the theory that the scattered spectrum of laser light passing through a plasma will be generally shifted to longer wavelengths, which is difficult to attribute to other than Compton absorption. The test method is shown in Figure 1.

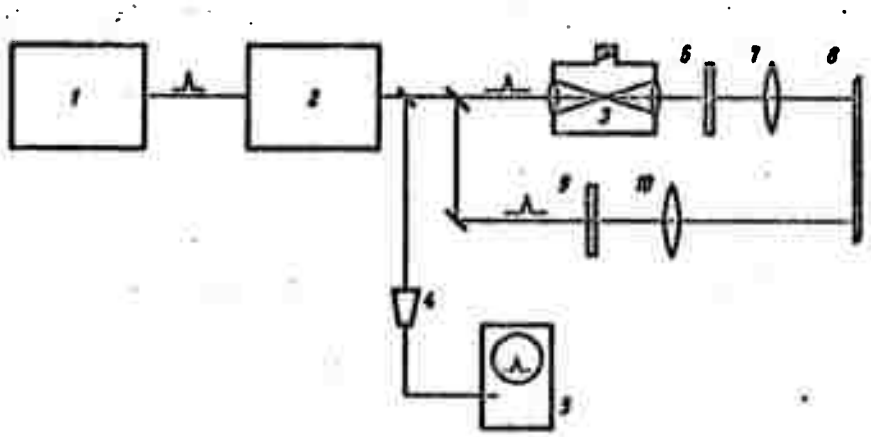

Fig. 1. Compton absorption experiment.
1 - ruby laser; 2 - amplifier; 3 - test vessel; 4 - photoelement; 5 - CRO; 6, 9 - filters; 7, 10 - collimators; 8 - spectrograph input

Amplified picosecond pulses from a ruby laser were focused in a helium vessel (3) to generate a spark; pulse width was 50 ns, with a density at the focal point of 2×10^{14} w/cm^2. The scattered spectrum of the transmitted beam was simultaneously compared to the original pulse spectrum in spectrograph (8). Typical shifts are seen in Figure 2 for helium and for a

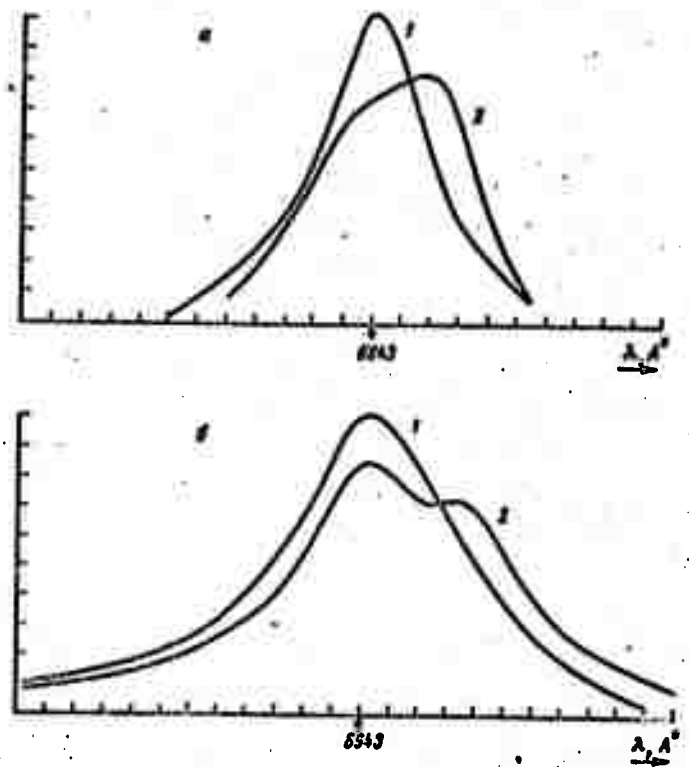

Fig. 2. Spectral shift in a laser plasma
a - He plasma; b - Al foil;
1 - incident radiation; 2 - transmitted radiation

150 Å thick aluminum foil target; the mean values of absorption coefficients were found to be $\alpha = 0.26 \times 10^{-2}$/cm and 2×10^{-2}/cm, respectively. In general the experimental values of α were less than those predicted by theory; however, the results are cited as evidence of the major role played by Compton absorption in this type of laser-plasma interaction. The results are also mentioned as confirming the theoretical findings of Zel'dovich et al (ZhETF P, v. 11, 1970, 497-500) in the foregoing paper.

0294. Anisimov, S. I. Self-similar thermal wave in a two-temperature plasma heated by a laser pulse. ZhETF P, v. 12, 1970, 414-416.

The author notes that in analyzing the physical processes taking place during laser heating of a plasma, a distinction must be made between ultra-short pulse and longer pulse effects. In the former case the main energy transfer mechanism is initially a thermal wave, which gives way to energy transfer by hydrodynamic motion. For longer laser pulse durations, however, this simplification is no longer valid and a more complex solution must be sought. Anisimov therefore develops a general analysis which shows that the heating and motion of a two-temperature plasma can have a generalized solution, if it be assumed that the energy absorbed by the plasma increases linearly with time, which is a reasonable approximation to the laser heating case. The system of equations presented is limited by several assumptions, e.g., viscous forces are neglected, and the plasma is treated as quasineutral. Several examples are given for varying ratios of electron and ion heating during the energy absorption process.

0295. Babenko, A. N., E. P. Kruglyakov, R. Kh. Kurtmullayev, and A. N. Papyrin. Thomson scattering of ruby laser light in a plasma behind a collisionless shock wavefront. ZhPMTF, no. 3, 1970, 38-41.

A plasma experiment is described in which a laser is used to assess the relative temperature levels attained by the electron and ion components of the plasma. The condition of primary interest is the "supercritical" case in a rapidly dissociating plasma, where ion heating becomes predominant. The test configuration is shown in Figure 1. An initial hydrogen plasma was

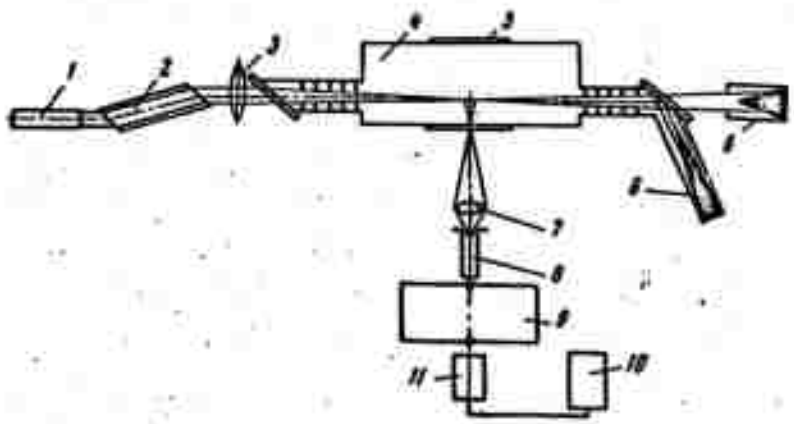

Fig. 1. Plasma temperature experiment
1 - ruby laser; 2 - ruby amplifier; 3, 7 - lenses; 4 - test vessel; 5 - shock coil; 6 - optical absorbers; 8 - lightguide; 9 - MDR-2 monochromator; 10 - CRO; 11 - photomultiplier

generated in glass tube 4, located in a quasistationary magnetic field of 400 oe. A shock wave was generated by a superposed pulsed field of 2.5 koe generated by a fast-rise current pulse through shock coil 5. Pulses from ruby laser and amplifier 1 and 2 ($Q = 1\text{--}4$ j, $\tau = 10\text{--}15$ ns) were focused at the midpoint of the shock coil; the portion of the beam reflected into the optical detection system 7-11 was then a function of electron scattering in the plasma. The laser pulse was synchronized to occur at the peak of the shock wave emission, thus ensuring that the registered scattering spectra were governed by electron temperature behind the shock wave. Test data showed that in the supercritical wave amplitude range, the actual electron temperature was consistently well below the levels predicted by a computer model, in which only electron heating was assumed. The experiment thus verified the appearance of ion heating and put a limit to the validity of the cited computer model.

0296. Gribkov, V. A., V. Ya. Nikulin, and G. V. Sklizkov. Increased plasma density from the collision of laser flares. Kratkiye soobshcheniya po fizike, no. 2, 1971, 45-49.

An experiment is described in which two opposed plasma flares are generated simultaneously to collide with each other. The objective was to measure the thermodynamic properties of the impact region. Figure 1 shows the test arrangement. A neodymium laser beam was split into two opposed beams of 12 ns and 30 j each, and

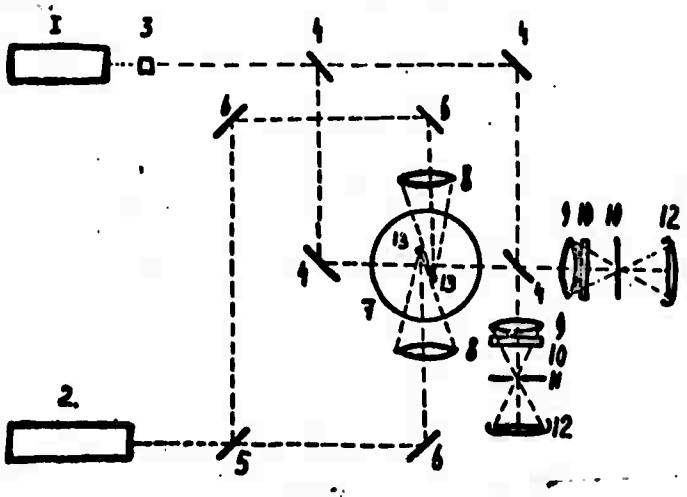

Fig. 1. Colliding plasma experiment.
1 - ruby laser; 2 - Nd laser; 3 - KDP cell; 4 - interferometer mirrors; 5 - splitter; 6 - mirrors; 7 - test vessel; 8, 9 - objectives; 10 - filters; 11 - diaphragms; 12 - photorecorders; 13 - targets

directed onto two slightly offset polyethylene targets, separated by 1 mm, so that the generated plasmas would intersect. A ruby laser was used for high-speed interferometry of the collision region; wavelengths of 0.69 and 0.35μ were used over an interval of 100 ns following the beam-target pulse generation. With this technique, the contribution of ions to the collision region could be discounted, since in this case the ion component was practically independent of optical frequency. From the combined interferograms it was possible to determine electron density profiles in the collision region, as shown in Figure 2.

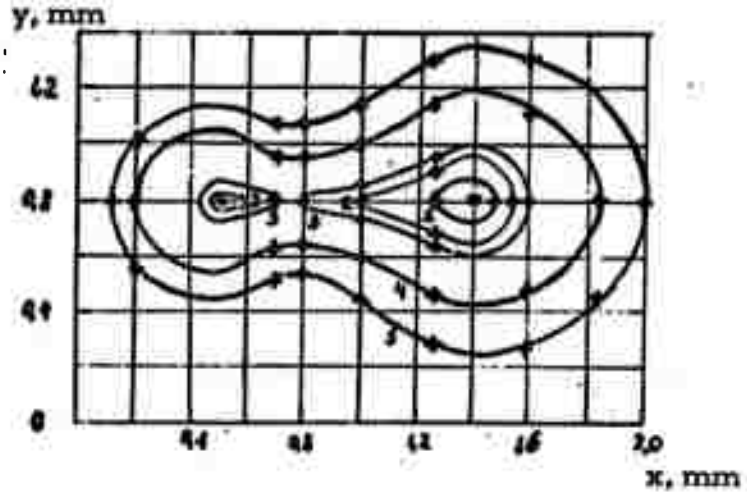

Fig. 2. Electron density profiles from colliding plasmas. 1 - $8.8 \times 10^{19}/cm^3$; 2 - $5 \times 10^{19}/cm^3$; 3 - $3.5 \times 10^{19}/cm^3$; 4 - $1 \times 10^{19}/cm^3$; 5 - $5 \times 10^{18}/cm^3$.

Figure 3 shows an electron density profile in a plane bisecting one target, for the two-beam case as well as for only a single target beam. A sharp increase is clearly evident in the colliding plasma case. The target specimens in this experiment were cubes, 0.2 mm on an edge; the authors suggest that substantially higher densities could be obtained by using cylindrical or spherical targets.

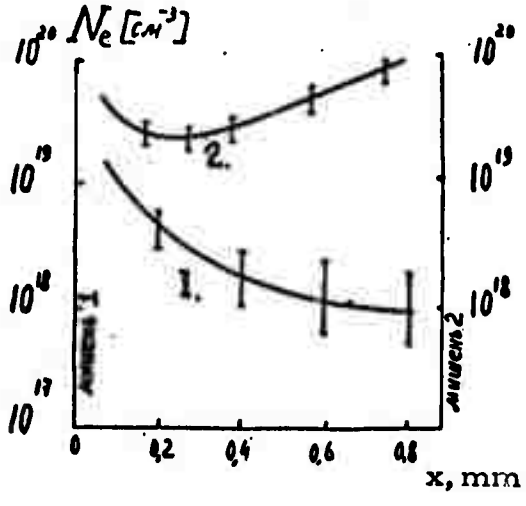

Fig. 3. Electron density for single-beam (1) and colliding (2) plasmas

0297. Zakharov, S. D., Ye. L. Tyurin, and V. A. Shcheglov. Dynamics of heating a fully ionized plasma by focused laser radiation. IN: Kvantovaya elektronika, (Moskva), no. 3, 1971, 106-108.

The authors derive expressions which define laser heating of a fully ionized plasma, for the symmetrical spherical optics case illustrated in Figure 1. The analysis assumes that gasdynamic expansion, electron-ion

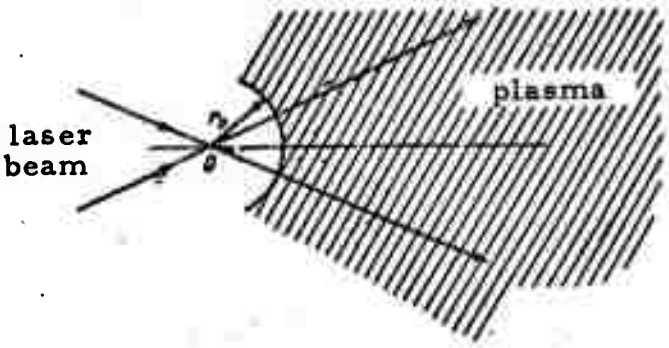

Fig. 1. Plasma heating model

relaxation, and conduction and radiation losses may all be neglected. This is the accepted case for a nominally dense plasma ($n \simeq 10^{20}/cm^3$) and for pulse widths in the ultrashort range ($< 10^{-10}$ sec). Following development of heat equations for the general case in terms of beam intensity I and plasma temperature T, the authors determine T(r, t) and I (r, t) for the specific case of interest of a sharply-focused beam such that the depth of the heated region $\gg r_o$ and plasma temperature in this region rises well above its initial value. It follows that an absorption wave of laser radiation will exist; an expression for the radius coordinate of this wave is given, from which a maximum effective penetration depth may be determined. The described model is applicable only on the condition that the length of the caustic of the focusing objective is substantially less than maximum penetration depth; otherwise a planar one-dimensional model must be used.

0298. Vinogradov, A. V., andV. V. Pustovalov. Optical absorption in a nonuniform laser plasma. ZhETF P, v. 13, 1971, 317-320.

The problem of laser plasma shielding of a target surface is discussed, and means of maximizing laser energy absorption in the plasma region are a analyzed. The model assumes laser pulses of $\tau < 10^{-8}$ sec and energies in the 10-100j range, which typically would produce plasma electron densities above critical for a neodymium laser. In such cases it is estimated that as

much as 60% of the incident energy may be reflected rather than contributing to further plasma heating. The authors show that absorption can be maximized by offsetting the target plane from normal to the beam, so that some conversion of an incident p-polarized wave to Langmuir oscillation takes place. This is a nondissipative process and independent of plasma temperature. The expression for conversion coefficient, i.e., absorption coefficient, is given and its limiting conditions are analyzed.

0299. Davydov, Yu.I., A. A. Zhukov, A. N. Kokora, and M. A. Krishtal. Variation in the structure of gray and white cast iron caused by laser radiation. FiKhOM, no. 1, 1969, 17-22.

Structural changes in metallic targets exposed to destructive laser radiation are discussed. The beam, described only as from a neodymium glass laser in a pulsed mode, was focused on specimens of gray and white cast iron, and the resulting crater geometries and structural effects were observed in detail. Figure 1 is a typical photo of a section through the bottom of a crater, and shows three distinguishable regions: a fused and

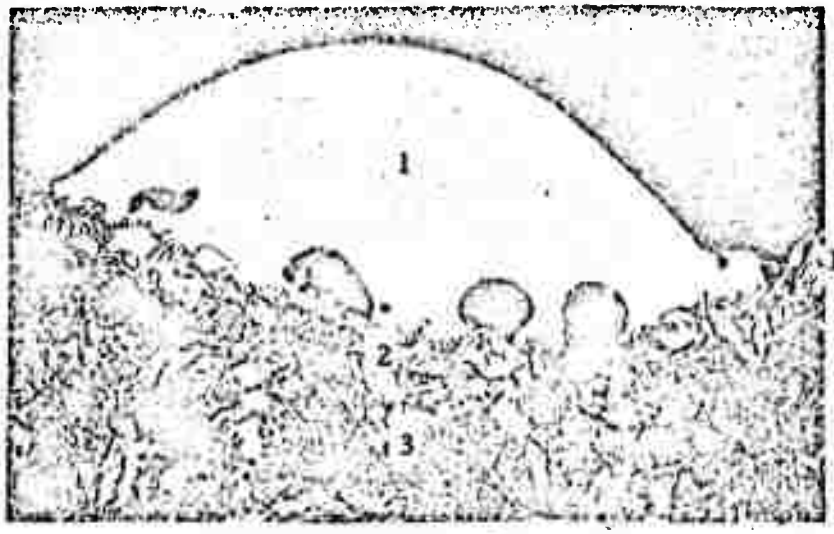

Fig. 1. Heating effects around crater. 1 - fused; 2 - partially altered; 3 - no effects

rehardened region; a secondary boundary region beneath it, showing some heat alteration; and a third unaffected region. The fused region had a droplet-like formation, with some porosity depending on the graphite content of the specimen. Portions of the second zone, owing to rapid heating and cooling, changed from a perlite to martensite structure. A number of other microphotographs are included showing the irregular pattern of the altered regions in radial directions from the impact point, and the cause for this is discussed. Data are also given showing the increased hardness of the fused impact region after cooling, as a function of cavity depth in the target specimen.

0300. Mirkin, L. I. On the possibility of saturating iron with carbon by means of a pulsed laser. DAN SSSR, v. 186, no. 2, 1969, 305-308.

The possibility of saturating a metal surface with carbon by means of intense laser heating is shown. Test data are given principally for cast iron which was given an initial overlay of carbon compounds, then subjected to pulsed radiation from an Nd-glass laser at 1.06μ. Overall pulse width was about 1 millisecond, comprised of several hundred spikes; energy was approximately 35 j. Focal distance was varied from 5 to 25 cm; in addition to exposure in the focal plane, specimens were offset up to 30% of the focal distance during exposure. The bulk of the experiment was devoted to measuring the increased surface hardness obtained by irradiation. In one case the surface hardness increased to 1400 kg/mm^2, compared to an untreated value of 150 kg/mm^2. A similar test using a tungsten base showed an increase to 700-800 kg/mm^2. The saturation mechanism is explained as follows: the irradiated surface carbon is heated to several thousand degrees and converts to a chemically active plasma, during some portion of the laser pulse. The remainder of the pulse evaporates and melts the exposed metal surface which combines with the carbon plasma, resulting in martensite and austenite formations with 0.6--1% carbon content. Microphotos of typical treated surfaces are included.

0301. Mirkin, L. I. Saturation of iron with tungsten by means of a laser beam. IVUZ Chernaya metallurgiya, no. 2, 1971, 98-101.

This is a continuation of the laser impregnation experiment described in the foregoing article by Mirkin (DAN SSSR, v. 186, no. 2, 1969, 305-308). In the present case the same test technique was used to combine iron with a surface layer of powdered tungsten. Pulses up to 30 j, presumably also from an Nd laser, were applied to specimen surfaces with the beam defocused between 10 and 20%, and the resulting structure was examined by metallography and x-ray spectroscopy. An alloy surface hardness of 650 kg/mm^2 was obtained in this manner; other data are given on the alteration in crystal lattice structure. The laser technique is found to form a solid solution of iron and tungsten, owing to the extremely rapid heating and cooling rates (on the order of 10^6 deg/sec). Similar results were obtained when the iron was in powder form as well as the tungsten. The reaction was more effective because of the increased contact area, but showed more lattice distortion than in the former case.

0302. Kramarenko, N. L., Yu. V. Naboykin, and Yu. A. Tiunov. Stability of lead oxide and cryolite dielectric coatings under laser radiation. IN: Sbornik. Kvantovaya elektronika, no. 3. Kiyev, Naukova dumka, 1969, 311-313.

Studies are reported on the damage resistance of lead oxide and cryolite coatings to radiation from a ruby laser operating in a spike mode. The stability of multilayer coatings was greater with fewer layers used and also increased with substrate heating during the coating process. As an example, for a mirror with 1 to 9 layers of coating and 40--57% reflection factor, the mirror damage threshold was in the 320--680 j/cm^2 range for a substrate temperature of 20°C, whereas at 200°C this range was increased to 640--2100 j/cm^2. Under the reported test conditions it was found that the stability of lead oxide and cryolite coatings was less than for similar coatings of zinc sulfide and magnesium fluoride. This is ascribed to the lower melting point of PbS (888°C).

0303. Zhiryakov. B. M., A. K. Fannibo, and N. N. Yuryshev. On possible technological use of quasistationary radiation from a ruby laser. FiKhOM, no. 3, 1970, 14-24.

This describes a comparative experiment on damage threshold of various metals, from laser radiation in spike and quasistationary free-running modes. A ruby laser was used generating 50 j pulses with an integral width on the order of 1 millisecond. Damage thresholds to specimens including niobium, brass, copper, stainless steel and aluminum were determined for a variety of focused spot sizes. For a given net pulse energy the threshold was appreciably lower for the spike mode, as predictable from the difference in heat transfer mechanisms for the two modes. This was emphasized by using rotating metal disks as targets and comparing the annular impact areas. Photographs of this are included showing the discrete sequence of craters caused by spike emission, contrasted with a smooth band of fused metal for the quasistationary emission. Streak photos of emission intensity and relative intensity distribution over the laser output face are also given, and used to explain the difference observed in surface heating behavior.

0304. Zhiryakov, B. M., N. N. Rykalin, A. A. Uglov, and A. K. Fannibo. Features of damage processes in metals under focused laser radiation. ZhTF, no. 5, 1971, 1037-1042.

This is a continuation of the previous effort reported by Zhiryakov et al on the dynamics of laser damage formation to metal targets. Although data are not specified, the article refers to effects of both spike and quasi-stationary emission, so the test conditions are presumably the same as in the former report. In the present case the authors focus attention on conditions near the damage threshold, i.e., at $q \simeq 10^6$ w/cm^2, where ejection in the form of liquid droplets begins to occur. From impulse and momentum equations defining drop motion, a characteristic time is calculated for formation of a droplet shield which effectively screens the crater surface from the remaining portion of the laser pulse. For the given test conditions, this figure was in the range of 2--6 μsec. Additional data are given on ejecta mass vs beam intensity, as shown in Figure 1 for several metals. This data shows that ejecta mass is strongly dependent on the purity of the target metal.

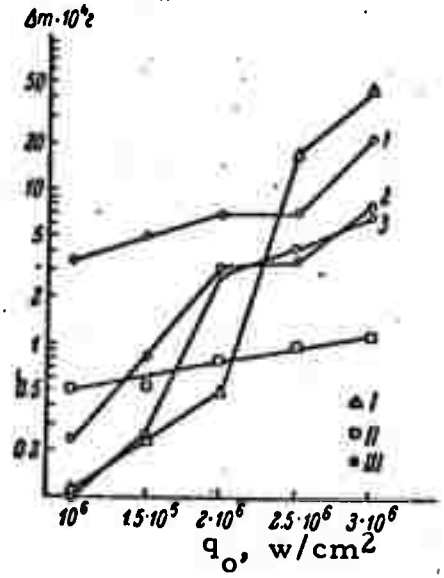

Fig. 1. Ejected mass vs beam intensity.

I - zirconium; II - chrome; 1, 2, 3 - blister, anodic and cathodic copper, respectively

0305. Apollonov, V. V., Yu. A. Bykovskiy, N. N. Degtyarenko, V. F. Yelesin, Yu. P. Kozyrev, and S. M. Sil'nov. Forming multiply-charged ions from the interaction of a powerful laser pulse with a solid. ZhETF P, v. 11, 1970, 377-381.

0306. Bykovskiy, Yu. A., N. N. Degtyarenko, V. F. Yelesin, Yu. P. Kozyrev, and S. M. Sil'nov. Mass-spectrometer study of a laser plasma. ZhETF, v. 60, no. 4, 1971, 1306-1319.

Spectral analyses are given of the multiply-charged ions formed by laser irradiation of Co, Ag, Ta, W and Bi targets. A neodymium glass

laser with two amplifier stages was used to generate maximum pulse powers on the order of 2 Gw; at a lens focus f = 5 cm, this yielded densities of 10^{13} w/cm^2. Other than this data, the discussion is concerned only with the spectrographic technique and analysis, based on a crossed field time-of-flight mass spectrometer. Identified lines ranged from Ag^{+16} to Co^{+25}, as well as high levels for trace C, N, and O. A theoretical calculation for Co ionization confirmed the experimental value, but was substantially higher for the other target materials. The authors ascribe the latter discrepancy to the fact that for calculation purposes the generated plasma was assumed to be in thermodynamic equilibrium, which may not hold for $q > 10^{12}$ w/cm^2, as in the present case.

A more detailed treatment of the same test is given by Bykovskiy et al in the second cited article. This includes additional ion energy spectra for each target metal as a function of laser energy density, as well as angular distribution patterns of the ejected ions.

0307. Gnoyevoy, Ya. N., A. I. Petrukhin, Yu. Ye, Pleshanov, and V. A. Sulyayev. Experimental study of shielding development in Al and Pb vapors. ZhETF P, v. 11, 1970, 440-443.

An experimental study is described which examines the shielding nature of vapor generated by laser impact with Al and Pb targets. The transition region in particular is treated, i.e., the region in which the vapor layer changes from optically transparent to opaque owing to the increased ionized mass. A two stage Q-switched ruby was used, generating 30--40 ns pulses and a maximum focused density of 15 j/cm^2. Care was taken to get maximum energy uniformity in the focused spot, which was achieved within 20%; spot diameters of 3.5 and 10 mm were used. In addition to laser power density, brightness temperature and pressure transients in the plasma were recorded; a time resolution of 3 nsec is claimed for the pressure recordings. Figure 1 shows the combined measured parameters for both metals as a function of time, taken at maximum laser intensity. The graphs show a peak brightness temperature of 46,000°K for lead and 30,000°K for aluminum. The transition to the shielding condition was determined to occur at approximately 1.5 j/cm^2 for Pb and 4.5 j/cm^2 for Al, corresponding to $T \approx 10^4$ deg K. It is emphasized that in this type of test allowance must be made for the time lag for the heated surface material to undergo phase change.

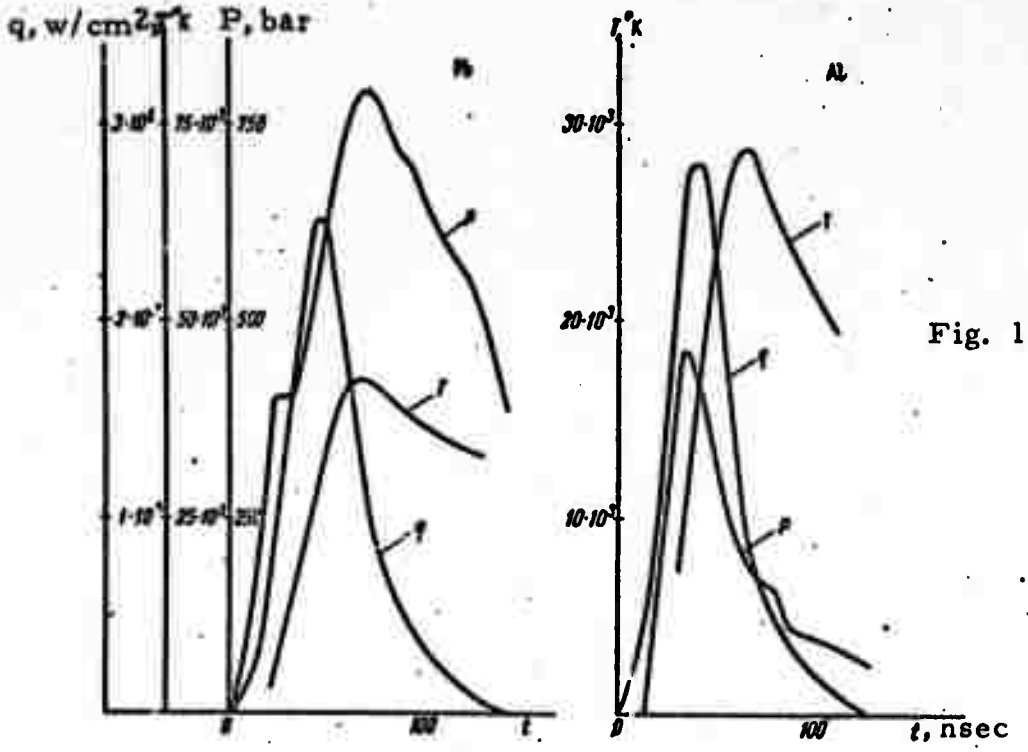

Fig. 1. Plasma shielding in Pb and Al targets

0308. Nemchinov, I. V. and S. P. Popov. The onset of shielding of a surface vaporized by laser radiation. ZhETF P, v. 11, 1970, 459-462.

The development period for vapor ionization, absorption of optical emission and shielding of a surface from laser radiation are analyzed. The discussion is based on the theory, developed by one of the authors, of the equilibrium "flash" at electronic temperature T_e coinciding with ionic (or atomic) temperature T_i. The basic assumptions of the theory are re-evaluated in view of the discrepancy between theoretical and experimental values of flux density q_* at which shielding begins. The experimental fact that shielding starts at a lower q than predicted by the earlier theory was taken into account in tentative calculations, in which the assumptions were made that $(T_e - T_i)(1/T_e) < T_e$ and the ionization rate is finite. Comparatively calculated q(t) plots, where t is the time of "flash" development, for Ta, W, Pb, Fe, Al, and Be targets exposed to q up to 1 Gw/cm^2 at 1.78 ev quantum energy (ruby laser), show that the "critical" q_* calculated with allowance for inequality of T_e and T_i is significantly lower than q_* calculated on the assumption of $T_e = T_i$. The application of the inequality condition T_e and T_i resulted in even shorter t in the case of an Nd glass laser (e = 1.16 ev). Therefore, it was concluded that shielding begins in the phase where heat conduction is still appreciable, and leads to some stretching of the pulse. Although the new calculations were in better agreement with experiment than the older ones, some discrepancy still remained. The authors note that the existence of shielding, if confirmed by experiment in the q = 2-20 Mw/cm^2 range, would allow generation of plasma by a laser in the range of very low flux densities.

0309. Andreyev, S. I., I. V. Verzhikovskiy, and Yu. I. Dymshits. Conditions for plasma formation from a solid target from the effect of single-pulse laser radiation. ZhTF, no. 7, 1970, 1436-1440.

A number of metals were subjected to 30 ns pulsed Nd-glass laser radiation at sufficiently intense levels to generate plasma. The test object was to determine the critical factor governing damage threshold, defined as the appearance of a detectable plasma in the focal area. The tests were done in vacuo with carefully cleaned target surfaces. The results confirm that energy density rather than power density is the critical factor determining the damage threshold. The comparative time characteristics for the laser pulse power and energy are seen in Figure 1, together with experimental data showing lag time in reaching threshold, as a function of pulse energy, for lead and graphite targets. The energy criterion also held true over a wide

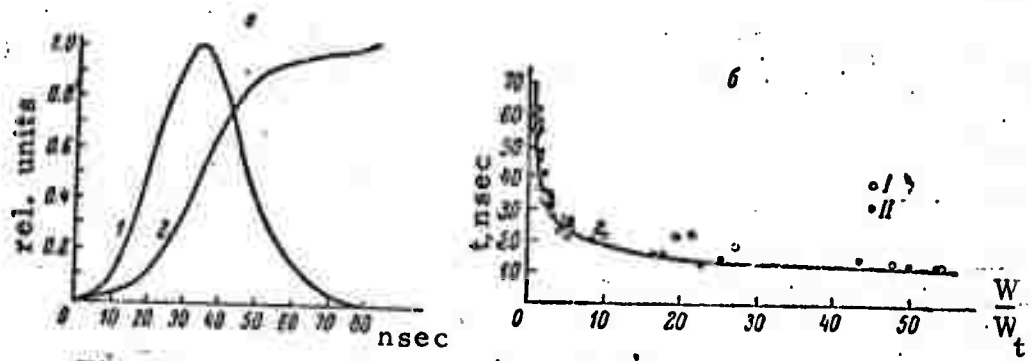

Fig. 1. Laser pulse and threshold characteristics.
a - Laser power (1) and energy (2) vs time;
b - Plasma development time vs threshold, for lead (I) and graphite (II) targets.

range of focused spot areas, up to 2 cm^2 for Al. Threshold energy density is shown to be that level required to ionize a layer of material to a depth of $1/\alpha$, where α is the laser beam absorption coefficient in the evaporated region. A summary of test and calculated data is given in Table I for all tested metals; discrepancies are not discussed.

Table I. Laser breakdown threshold in metals.

Material	Experimental threshold, j/cm²					$\frac{1}{\alpha} \times 10^{-6}$ cm	
	Calculated threshold j/cm²	Detectable plasma glow	Plasma Opacity	Filmed signal	Refl., R	T = 273° K	T = T_{vap}
Ag	0.20	0.20	0.18	0.24	0.33	1.15	5.05
Al	0.19	0.16	0.23	0.12	0.30	0.9	4.0
C	--	0.82	1.10	1.20	0.02	--	--
Cu	0.38	0.26	0.44	0.40	0.25	1.3	5.6
Mo*	0.81	0.74	0.79	0.79	0.20	1.25	7.4
Ni	0.67	0.17	0.27	0.31	0.35	1.5	7.7
Pb*	0.06	0.04	0.06	0.04	0.25	1.35	4.1
Pd*	0.40	0.29	0.37	0.24	0.27	1.6	6.7
Pt	0.52	0.58	0.76	0.82	0.30	1.35	6.4
Rh*	0.62	0.30	0.59	0.66	0.35	1.1	6.0
Ta*	1.00	0.30	0.18	0.16	0.31	1.7	8.8

0310. Komotskiy, V. A. On the maximum evaporation rate from a metal surface. ZhTF, no. 1, 1971, 220-221.

An experiment is briefly described which clearly defines the evaporative limit for laser radiation of a metal, i. e., the intensity level above which the energy absorption mechanism changes from basically evaporative to explosive destruction and ejection. This threshold is taken to be on the order of $q \approx 10^8$ w/cm². The criterion for transition was taken in terms of a characteristic dimension d of the evaporated region, as a function of relative incident intensity, i. e., the relation $d = f(P/P_t)$ was experimentally found, in which P_t is the evaporation threshold. A single-mode Q-switched ruby laser was used at $\tau = 1\mu s$, focused onto a thin Al film on a transparent substrate. Typical test results for a 100 Å film thickness are seen in Figure 1. The break in the vicinity of $P/P_1 \approx 10^4$ is taken to be the transition

from the evaporative to explosive mechanism. Expressed in terms of removal rate of n surface atoms, it is shown that limiting $dn/ndt \approx 0.7 \times 10^{13}$/sec, which is in reasonable agreement with earlier theoretical predictions.

0311. Yel'yashevich, M.A., V.K. Goncharov, L. Ya. Min'ko, and G.S. Romanov. Study of the physical state of destruction products from laser interaction with condensed media. ZhPS, v. 15, no. 2, 1971, 200-204.

Laser damage to a series of metals is described, principally with regard to parameters of the flares produced in the impact region. An Nd glass laser was used in both free-running and periodic modes, at energies up to 60 j. The beam was focused at f = 100 mm on a variety of metals at room conditions and in vacuo, including W, Li, Al, Cu, Fe, Pb, Zn, and alloys including brass and a type POS-40 (unidentified). In all cases care was taken to limit impact intensities to not over 10^8 w/cm^2, so that only a thermal destruction mechanism occurred. Photographic data are included comparing the size and brightness of plasma flares generated in several specimens. In some cases two discrete stages of flare propagation velocity could be distinguished. The most pronounced plasma absorption of incident flux was noted for W, Li and Al; for Cu, Fe, Pb, and Zn absorption was less, in accordance with theory.

0312. Krylov, Yu. K. and S. A. Volkov. Optical scatter in products formed by material evaporation by intense electromagnetic radiation. OiS, v. 30, no. 3, 1971, 517-523.

Theoretical and experimental treatments are given to optical parameters of the vapor region generated by intense laser irradiation of metal targets. The main object was to determine the effect of vapor products on coefficients of reflection and refraction of an auxiliary laser beam, passed at right angles through the target flare. The main laser was Nd glass generating 70 j, 600 μs pulses. The probe laser was He-Ne, collimated to a 10^{-2} cm^2 area beam, and registered by a photomultiplier. The relaxation process occurring in the flare generation is clearly seen in the transmitted pulse waveform of Figure 1. This correlates with a sequence of pulsations

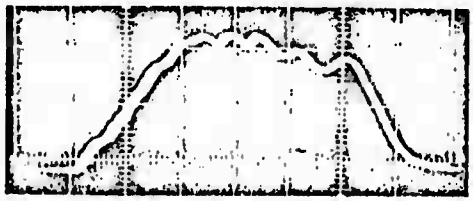

Fig. 1. Transmissibility oscillation in a laser plasma (Al target).

in the heating and cooling process of flare formation, with corresponding change in optical parameters. For the metals tested (Pb, Al, Cu, and Fe), the threshold for attenuation of the probe beam was in the range of 8×10^5 - 3×10^6 w/cm^2. The contribution of droplets in the vapor region to the observed optical behavior is analyzed.

0313. Arifov, U. A., V. V. Kazanskiy, V. B. Lugovskoy, and Z. A. Kayumova. Integral and spike emission caused by laser radiation. IAN Fiz, no. 3, 1971, 599-602.

This experiment was designed to clarify the nature of electron emission from a metal surface, generated by impact of a moderate-power focused laser beam. A Q-switched ruby laser was used, developing 8 j pulses at 2.8 ms duration; the impact pulse was limited to 10μs by a Kerr cell to prevent damage to the metal surface. A tungsten target was used, with Ni collector electrodes placed nearby to detect emission current. One minute between exposures was allowed, and the target surface was kept clean of absorbed gases; the tests were run at a 10^{-6} torr vacuum. Oscillographs show that the electron emission peaks correlate closely in time with the laser spikes; however, the electron spike pulse shapes suggest several possible emission mechanisms taking place. The data in fact indicate that a multiquantum effect, rather than a thermoelectric effect alone is mainly responsible for the observed spiked emission.

0314. Plyatsko, G. V., M. I. Moysa, and V. M. Zhirovetskiy. Some characteristics of the interaction of a laser beam with metals. F-KhMM, no. 3, 1971, 50-53.

An experiment is described whose object was to determine the optimum conditions for laser heating of a metal without causing ejection of the target material. Specifically, the physical processes taking place were correlated with the growth rate of the molten region, the laser beam intensity, and the

angle and focal distance of the beam relative to the target. The cited material was a 1 mm sheet of type 45 steel; a neodymium glass laser was used in a free-running regime, generating up to 70 j pulses at an overall duration of 3.5 μsec, focused at f = 30, 57.5 and 100 mm. Comparative photographic and graphical data are given showing the cavity geometries obtained at the various focal lengths, as well as at varying angles of incidence of the laser beam. The data show that at densities up to 15 j/mm^2, the beam incidence angle has a strong effect on rate and shape of the cavity formed.

0315. Rykalin, N. N. and A. A. Uglov. Internal vaporization from interaction of a laser beam with metals. TVT, no. 3, 1971, 575-582.

The effect of internal vaporization on destruction of nontransparent materials by a laser beam at $> 10^6$ w/cm^2 power densities is discussed, on the basis of earlier reported data. The resulting nucleation and growth of bubbles in molten metals are examined from the standpoint of statistical thermodynamics and equilibrium of vapor bubbles within the liquid volume. The importance is emphasized of artificial vaporization centers, such as gas cavities, nonmetallic inclusions and impurities, under conditions of heating by a laser beam at power densities up to 10^8 w/cm^2. The upper size limit of these vaporization centers was estimated to vary in the 1--100 micron range, depending on the depth of the molten layer. The lifetime and radius of a bubble developing around an artificial vaporization center in copper melt were calculated as functions of its depth and of radiation power density. In the early stage of vaporization by a laser pulse, the estimated maximum dimension of the molten drop ejected with the growing bubbles decreases with increase in power density, while in the more advanced stage of the process, ejection of larger drops becomes dependent on the melting process. The destruction mechanism is shown to be affected by internal vaporization via temperature distribution in the liquid layer adjacent to the vaporization boundary. As the pulse length is decreased while holding the power density at the same level ($< 10^8 - 10^9$ w/cm^2), the effect of internal vaporization is diminished with regard to the ejection mechanism. The cited phenomena may be observed also in the interaction of other energy sources, e.g., an electron beam or electric pulsed discharge with the solids and may lead to an explosive ejection of the target material.

0316. Goncharov, V. K. and L. Ya. Min'ko. Formation of successive shock waves by interaction of a controlled laser emission with absorbing materials. ZhPMTF, no. 3, 1971, 98-100.

A beam-target experiment is described in which a controlled laser emission regime was selected to produce shock waves and to study their

formation and propagation in absorbing materials, e.g., LS-59 brass. An Nd glass laser was used to produce a train of 1 μsec pulses with a 6 μsec spacing for a total duration of 700 μsec. The peak output energy was 150 j and peak power density was $\sim 10^7$ w/cm^2. The laser beam was focused on the material by a 100 mm lens. At atmospheric pressure a series of successive shock wave fronts were recorded by axial and transverse high-speed photography at the plasma region. The wavefront propagation rate decreased at increasing distance from the surface, but was always higher than propagation rate of individual plasmoids. A series of successive shock waves were also formed at a reduced ambient pressure (5×10^{-2} torr), but their propagation rate remained nearly the same with increasing distance from the surface. Spectroscopic studies indicated that shock waves are formed in the material vaporized by the preceding pulses. The existence of successive shock waves was confirmed by an experiment with a glass barrier placed at different distances from the target surface. The photographs clearly showed the shock waves reflected from the barrier. Proof was also obtained of a partial shielding of the target surface by an accumulation of discrete plasmoids.

0317. Levinson, G.R. and V. I. Smilga. Experimental study of damage threshold in thin metal films from effects of laser radiation. FiKhOM, no. 4, 1971, 124-128.

The authors derive expressions for laser damage threshold parameters for metallic thin films and compare them to test results obtained with Ag, Al, Au, Cr and Cu films. The films were vacuum-deposited on a quartz substrate, and exposed to focused pulsed radiation from a nitrogen laser at $\lambda = 337$ mm. Both power and power density were varied as functions of film thickness. Figure 1 shows two sets of calculated values of threshold power density for all tested metals. The beam intensity profile f(r) was also measured and its effect on damage threshold is discussed; discrepancies between calculated and actual values are also analyzed.

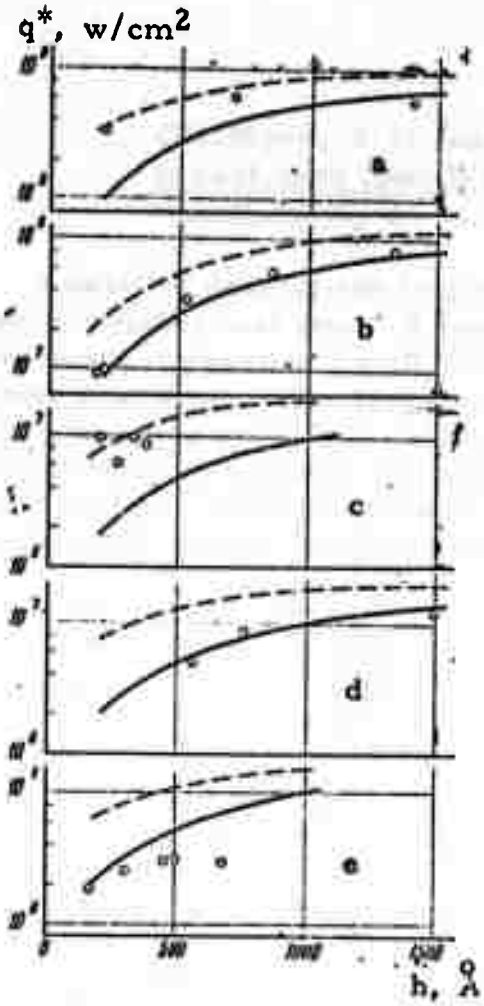

Fig. 1. Calculated breakdown threshold vs film thickness.

a - Ag; b - Al; c - Cr; d - Au; e - Cu. Dashed curve includes effect of heat loss in the substrate.

0318. Mezokh, Z. I., V. A. Yanushkevich, and L. I. Ivanov. Forming point defects in Ni by the action of giant laser pulses. FiKhOM, no. 4, 1971, 163-165.

Structural and electrical changes induced in laser-irradiated nickel are reported. Ni thin films on a quartz substrate were exposed to giant pulses from a ruby laser; the specimens were placed in a Dewar flask at liquid helium temperature. Change in resistivity was registered as a function of laser exposure, and the return to normal resistivity was observed as a function of annealing time and temperature. No other laser data are given; the test was evidently done below the damage threshold, and served primarily to demonstrate the generation and annealing of point defects in the metal lattice structure. In this case the concentration of point defects was determined to reach 10^{-2} at %, i.e., enough to significantly accelerate diffusion processes.

0319. Petukhova, T. M. and V. F. Senkevich. Pit formation in cast iron from laser radiation. IVUZ Chernaya metallurgiya, no. 6, 1971, 138-144.

A detailed description is given of the physical structure of pitting in a laser-irradiated cast iron. A type K-3M ruby laser was used in a free-running mode, focused at f = 10 mm; pulse energy was 1.5 j; overall pulse width was 3 millisec. The target types tested are identified as white, ductile, compound gray, and modified cast iron. The effects are also segregated by form of included graphite, i.e., bead, laminar, carbide or annealed carbon. Microphotos and relief profiles of pit formations are given and analyzed; Figure 1 compares pit profiles for four iron types. Results

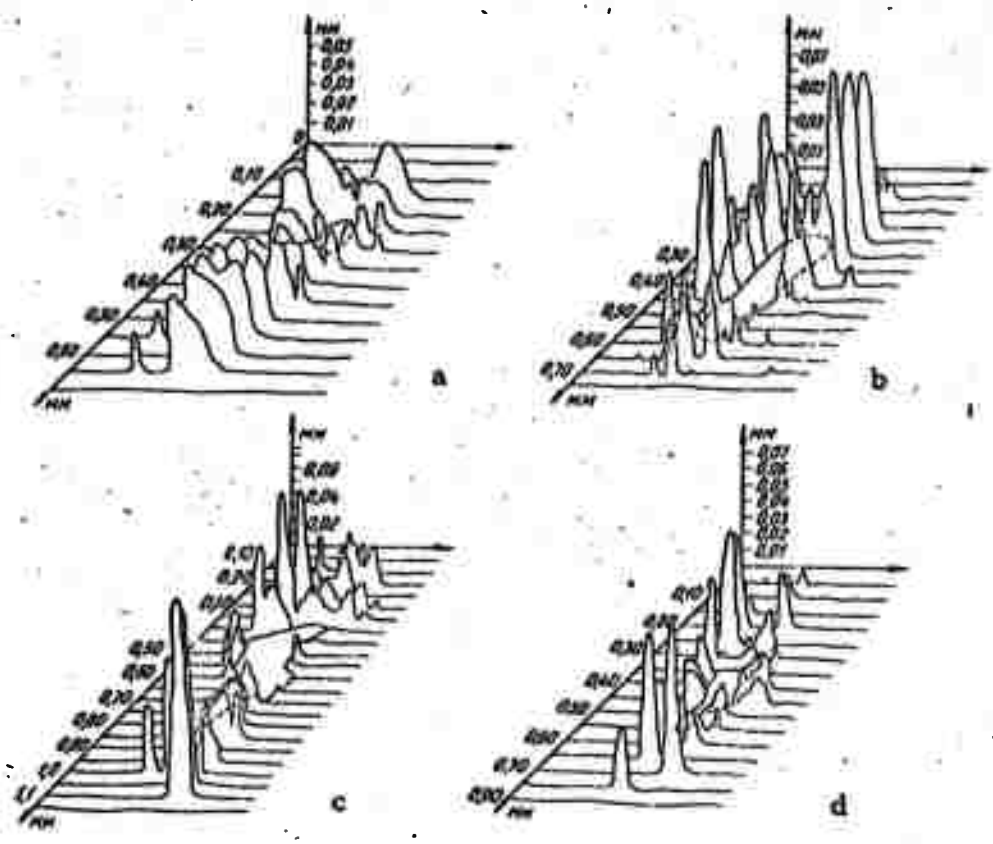

Fig. 1. Pit profiles.
a - laminar graphite; perlite structure; b - globular graphite; ferrite; c - globular graphite; perlite; d - carbon after anneal; perlite.

show that the type of graphite inclusion is a major factor in determining the pit geometry. This is seen in the figure, where a more uniform pitting action occurs with laminar as compared to bead-shaped graphite particles. Data on hardness change from irradiation is also given; on the average a surface hardness increase of 200-300 kg/cm^2 was obtained. Topographical maps of typical pits are included which correlate hardness variation with

pit profile over the target area. The authors note the similarity of their results to those obtained for steel targets, as reported earlier by three other cited authors.

0320. Chernenko, V.S., V.S. Kovalenko, and P. Yu. Volosevich. Effect of initial steel structure on heating by a photon beam. MiTOM, no. 7, 1971, 63-64.

A brief discussion is given of the correlation between laser heating effects on a steel surface and the initial structural condition of the steel. The cited experiment was performed with ruby laser irradiation of type ShKh 15 steel (1.02% C, 1.5% Cr), at intensities yielding surface heating rates on the order of 10^3 - 10^5 deg/sec. Target specimens were previously hardened in an oil bath at 850°C and tempered for two hours at temperatures from 200° to 600° C. Results show that the impact zone developed a martensite-austenite structure which was independent of the preliminary conditioning of the steel specimen. The depth of the heated zone, i.e., the depth to which the critical point was reached resulting in a discrete structural change, was found to be inversely proportional to tempering heat, as seen in Figure 1. The dependence of the critical point on initial dispersion of the steel structure is pointed out, and is concluded to be a major determinant in laser heating effect.

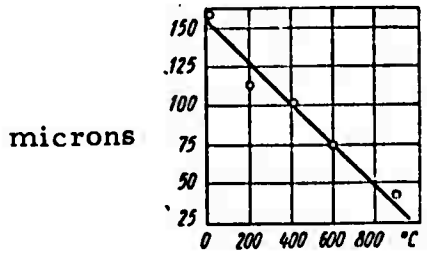

Fig. 1. Heat penetration vs prior tempering temperature. Ruby laser, steel target.

0321. Shchuka, A. A. Study of electron emission induced by laser radiation. PTE, no. 4, 1971, 177-179.

This article basically describes a vacuum beam-target apparatus designed to register electron emission from a laser-irradiated target. Both ruby ($\lambda = 0.69\mu$) and Nd glass ($\lambda = 1.06\mu$) with a KDP frequency doubler can be used, focused on a rotatable target in a vacuum vessel at 10^{-8} torr.

Tungsten and molybdenum are mentioned as the usual target materials; the laser mode is evidently free-running, at approximately 1 μs pulsewidth and energies in the 0.1 to 1 j range. Electron emission from both the impact face and rear face of a thin specimen is registered with identical opposed multiplier arrays having a sensitivity down to 10^{-12} a. A sample oscillogram shows frontal emission to nearly coincide with the laser pulse, whereas a detectable lag occurs in rear-surface emission. Variation of laser wavelength, at the same pulse energy, was found to have no significant effect on electron emission characteristics for the targets tested.

0322. Zverev, G. M., Ye. A. Levchuk, and E. K. Maldutis. Destruction of KDP, ADP, and $LiNbO_3$ crystals by powerful laser radiation. ZhETF, V. 57, No. 3, 1969, 730-736.

To establish the mechanism of volumetric optical destruction, the authors exposed KDP, ADP and $LiNbO_3$ crystals to focused pulses from a q-switched Nd-glass laser ($\lambda = 1.06\,\mu$) or its second harmonic, ($\lambda = 0.53\,\mu$) operating in a single mode regime. The output energy and pulse length were, respectively, 0.11 j and 14 nsec. at 1.06μ , and 0.03 j and 10 nsec at 0.53 μ wavelength. Also, 20 nsec pulses with 3 j output energy from a Q-switched multimode ruby laser ($\lambda = 0.69\,\mu$) were used. Spherical lenses with f = 7.5 or 33 cm focused laser radiation into the interior of the crystals. Microscopic observation of the cracks in the KDP and ADP crystals showed that their nature is independent of crystallographic orientation of the sample or of frequency of incident radiation. Thread-like defects were observed in pure $LiNbO_3$ crystal and, under certain conditions, in KDP and ADP as well. The threshold power density for damage in all crystals studied was measured to be strongly dependent on the focal distance of the lens, i.e., the radius of the laser beam. The absolute destruction threshold for KDP and ADP by 0.53μ radiation was double that from 1.06μ radiation. The thread-like destruction was ascribed to self-focusing; dependence of the destruction threshold on the lens focus was due to development of thermoelastic stresses. The most important factor in destruction of KDP and ADP was shown to be linear absorption by impurities. The observed dependence of destruction threshold of KDP and ADP on wavelength invalidates the earlier assumption of the decisive importance of multiphoton absorption. An identical conclusion applies to stimulated Brillouin scattering, which was not observed in any of the crystals undergoing destructive exposure.

0323. Yeremchenko, D. V. and B. N. Morozov. Thermoelastic stress generated in a transparent dielectric by nonfocused laser radiation. FTT, no. 3, 1970, 848-851.

A mathematical solution is presented to the problem of distribution of thermoelastic stress σ in a transparent medium subjected to short ($\tau \leq 10^{-6}$ sec) nonfocused laser pulses. Formulas were derived for δI as a function of σ where I is incident flux density and δ is absorption coefficient. The case was considered both with and without allowance

for "hot points" in intensity distribution and for self-focusing filaments in the medium. In both cases the order of magnitude of threshold intensity I_{lim} for destruction was calculated to be the same. Also, the I_{lim} for quartz glass was calculated to be of the sameorder of magnitude as the experimental I_{lim} for a focused beam, if the δ value (= 0.5 - 20) is calculated with allowance for heat initially released by a single photon absorption and nonlinear processes. A linear relationship between σ and the absorbed energy $(\delta I)_{eff} \Delta t$ indicated that laser beam energy can be measured by the method of thermoelastic stress, if the beam intensity is below the threshold value.

0324. Agranat, M. B., N. P. Novikov, Yu. I. Yudin, and P. A. Yampol'skiy. Generation of centers of visible destruction cracks by the action of laser radiation. FTT, no. 3, 1970, 924-927.

PMMA samples were irradiated by a free-running laser beam at $\lambda = 1.06\ \mu$, while subjected to a 100-300 kg/cm^2 tensile stress, to verify the hypothesis that the number of destruction cracks generated in the laser irradiated samples under tensile stress is much greater than in nonirradiated samples under identical stress. The power output of the laser was adjusted to produce 5-10 visible cracks per unit length. The beam axis was made either perpendicular or at a 45° angle to the direction of mechanical stress. The above cited hypothesis was confirmed experimentally. In addition, the numbers $n_{\perp}$ and $n_{45°}$ of destruction cracks were found to increase by several factors, and the numbers of luminescent centers to a lesser degree with increase in tensile stress. The experimental finding that the diameter of the cracks in the stressed samples was much smaller (0.5-1.5 mm) than in the original ones (5-7 mm) was explained by the existence of more voluminous open micropores in the stressed samples; therefore, a greater fraction of the laser pulse is absorbed before gas pressure in the micropore attains a critical value. It is postulated that, under the described experimental conditions, tensile stress mainly opens the micropores and generates additional centers of crack formation, while laser radiation generates destruction cracks centered on submicrocracks (micropores). The luminescent micro-regions accompanying crack formation are tentatively ascribed to breakdown in the micropores. Photos showing the combined damage effects are included.

0325. Agranat, M. B., I. K. Krasyuk, N. P. Novikov, V. P. Perminov, Yu. I. Yudin, and P. A. Yampol'skiy. Destruction of transparent dielectrics by laser radiation. ZhETF, V. 60, no. 5, 1971, 1747-1756.

The authors investigate the destruction of polymer samples (plastics, polystyrene) from the action of Q-switched laser pulses with intensities below threshold, and by picosecond pulses, It was found that there are threshold values for laser pulses (for $\tau \cong 2\text{-}10^{-8}$ sec) and destruction criteria which do not depend on the laser pulse duration, but instead depend on emitted wavelength and on the material of the sample. Polymer destruction was found to depend on a parameter which takes into account both the energy characteristics and the intensity characteristics of the laser pulse. The authors found no significant difference in the effect of Q-switched lasers or free-running lasers with the polymer samples. No nonlinear laser energy absorption effects were observed on transition through the energy threshold value. The light emitted by the irradiated polymer sample was investigated in detail. It was concluded that the emission and heating in the microregion which may be related to the emission cannot explain the cracks generated in the sample. It was also concluded that the damage to the sample was not caused by electric breakdown in the field of the laser emission. The experiment showed that the emission accompanying the destruction of the sample is localized in the microregion and that its thermal characteristics show a delayed response in relation to the initiation of destruction. The same test report is given by the authors elsewhere (Agranat et al, Mekhanika polimerov, no. 3, 1971, 436-444).

0326. Belikova, T. P., A. N. Savchenko, and E. A. Sviridenkov. Light absorption by ruby in the pre-breakdown state. ZhETF, v. 58, no. 6, 1970, 1899-1903.

An experimental study of breakdown produced in a ruby specimen by single-pulse emission from a Q-switched ruby laser is described. The test was designed to establish kinetics of light absorption and criteria for dynamic breakdown. The fact that absorption acquired a substantial value in a shorter time than pulse length is the basic cause of dynamic destruction of the specimen which occurs as follows: heating of the medium by the absorbed light leads to an increase in pressure in a finite volume. Propagation of a shock wave occurs when pressure reaches a critical value. Destruction of the medium starts when negative pressure behind the shock wavefront exceeds the strength of the material. A formula is derived for the shock wave pressure P as a function of intensity of the incident light. At the initial electron

concentration in the conduction zone of $N \cong 10^{16}/cm^3$, P was calculated to be $\sim 10^6$ atm, in good agreement with earlier estimates. It was concluded that formation and propagation of shock waves must be considered in any study of mechanical destruction of transparent dielectrics by laser radiation, which commences at a delay of over 10 nsec behind the shock wave. This delay makes it possible to observe nonlinear effects of the Brillouin type of stimulated scattering. Photographic and oscillographic records are included showing typical delays in the absorption leading to the destruction process.

0327. Volkova, N. V. Structural defects in transparent dielectrics caused by laser radiation. FTT, no. 7, 1970, 2182-2184.

The nature of structural defects which determine density n of the centers of optical destruction was studied experimentally in LiF single crystals and PMMA using a Q-switched ruby laser. Application of laser pulses with increasing energy E to LiF crystals resulted in an increase in n up to some n_{max} which then remained constant with a further increase in E, up to applied levels of 10-15 E_{thr}. The values of E_{thr} and n_{max} varied with the structural type of the crystal. The n_{max} of each crystal type practically coincided with the corresponding density N of dislocation centers. Both n_{max} and N were equally dependent on Mg admixture concentration in LiF. This fact pointed to an impurity or vacancy type of structural defect. Destruction centers in PMMA merged even before the saturation level of n_{max}. For that reason, the saturation value of n_{max} was determined after 20-30-fold irradiation of PMMA by laser pulses with E slightly above E_{thr}. The n_{max} also correlated with density of scattering centers. This correlation leads to the belief that a photo or thermal destruction mechanism is involved in the case of PMMA, in contrast to LiF crystal destruction by a photoelectric mechanism.

0328. Novikov, N. P. and A. A. Kholodilov. Destruction of thermoplastics by powerful heat fluxes. Mekhanika polimerov, no. 1, 1971, 122-130.

Destruction of PMMA, polystyrene (PS), and polycarbonate (PC) targets by 2--12 cal/cm^2 x sec beam densities from a CO_2 laser ($\lambda = 10.6\ \mu$) was studied to verify earlier assumptions made by the authors, and to expand their proposed theoretical model (ZhPMTF, 1971, 2). Micrographic analysis of the irradiated thermoplastic samples indicated a breakdown of supermolecular

microstructure along the domain boundaries in PMMA, or of globules in PS, but only randomly located subsurface cavities, without a clear-cut separation of the structural elements, in PC samples. Above the surface of the PMMA and PS samples a "vapor-liquid drop" zone was detected, containing solid polymer fragments, while the vapor zone above the PC surface did not contain such fragments. It was also established that destruction of PMMA and PS occurs at a surface temperature T_s only weakly dependent on the incident power density whereas T_s of PC samples was almost linearly dependent on power density. The measured linear rate of PMMA and PS destruction fluctuated around a certain mean value which is explained as the result of a periodical screening of laser radiation by the vapor-liquid drop zone. Theoretical calculations based on kinetics of depolymerization-polymerization processes confirmed the experimental data and the exclusively thermal nature of optical destruction of thermoplastics. Damage photos of PMMA as well as tabulated damage data for all three specimen types are included.

0329. Orlov, R. Yu., I. B. Skidan, and L. S. Telegin.
Study of dielectric breakdown by ultrashort laser pulses.
ZhETF, v. 61, no. 2, 1971, 784-790.

Experimental results of laser breakdown in air, KDP, glass and water are described. Picosecond pulses from a neodymium laser and its second harmonic were used and compared to breakdown phenomena from nanosecond pulses, under otherwise identical conditions. The breakdown characteristics for picosecond pulse duration are seen in Fig. 1, where transmitted beam intensity through the breakdown region is plotted against incident beam intensity. Relative absorption is also seen in the photodetector responses of Fig. 2 in which the transmitted level is superimposed on the incident level. The rapid, complete absorption by air breakdown is contrasted with the gradual absorption in glass and water breakdowns. A comparison with effects of a 30 ns single pulse is given in Table I. For the picosecond pulsewidths the breakdown threshold was lower for the second harmonic than for the fundamental (1.06 μ). It is concluded that multiphoton processes are a major contributing factor to optical breakdown in picosecond pulse fields.

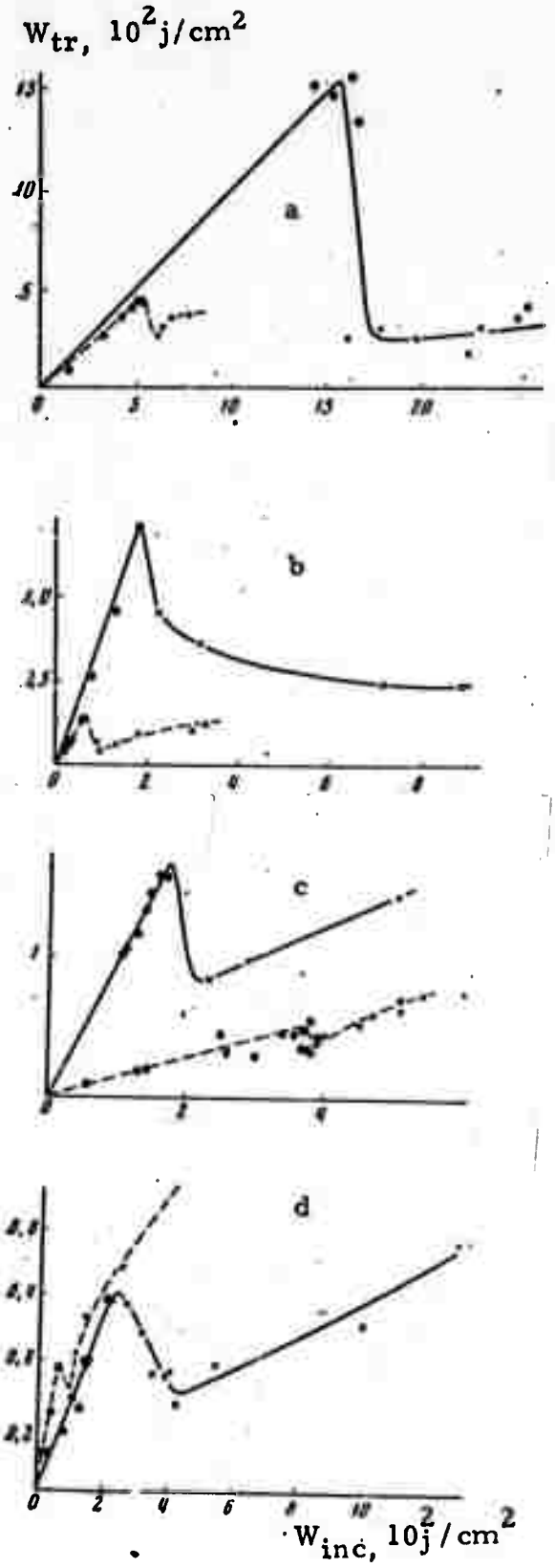

Fig. 1.
Breakdown from pulse trains. a-air; b-KDP; c-glass; d-water. Solid lines @1.06 μ; dashed lines @1.53 μ. • - breakdown; x - no breakdown.

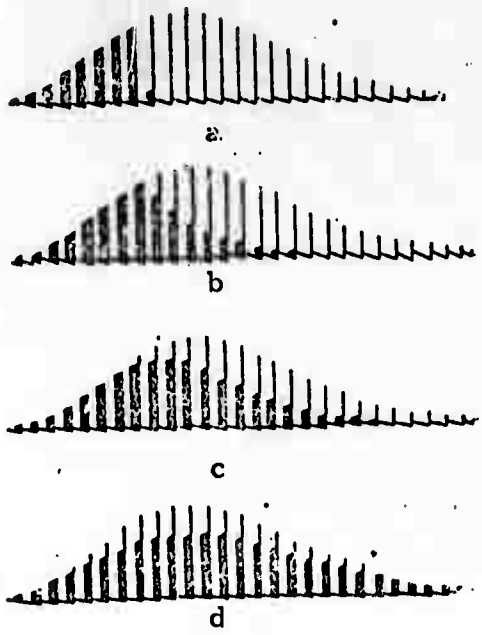

Fig. 2.
Incident vs. transmitted levels. a, b, c - breakdown in air, KDP, glass and water; d - prebreakdown absorption in air @ 0.53 μ

Table 1. Threshold density, 10^2 j/cm^2

	f lens	(1)	(2)		(3)
		λ = 1,06 мк	λ = 1,06 мк	λ = 0,53 мк	λ = 1,06 мк
Air	5		170		20
	35		20÷30	12	
KDP	70	25÷35	20	6	
Glass	70	5÷10	2	0,6÷0,9	0,2÷0,3
Water	70	10÷25	1,4÷2	1,1	0,3
	70	>50	1,5	0,8	0,15

(1) - Single pulse, τ = 30 nsec;
(2) - Pulse train, 10x3 ps;
(3) - Single pulse, τ = 3 ps

0330. Apshteyn, E. Z., L. G. Yefimova, and G. A. Tirskiy. Intense destruction of a vitreous body by radiation. MZhiG, no. 2, 1971, 131-134.

The destruction mechanism was analyzed of a body subject to fusing by radiation from a shock layer in supersonic gas flow, assuming an optically thin boundary layer. Given the parameters of the shock layer, destruction of a vitreous body may be described by a system of transcendental equations in an approximation of radiative heat conductivity of a fluid film near the critical point. Using the cited equations, the authors made calculations of destruction rate δ and degree of gasification Γ of a quartz-like thermal insulation material as a function of the body radius R_T, under specified flight conditions. The plots of δ, Γ (R_T) show that Γ decreases with decreasing R_T, owing to the increase in pressure gradient and consequently in the gas flow. At sufficiently great R_T, destruction of the coating proceeds on account of vaporization ($\Gamma \neq 1$). The minimum of the δ (R_T) plots also corresponds to an increase in pressure gradient, and hence in gas flow. The maximum effect of radiative heat conductivity appears at small values of R_T.

0331. Kalmykov, A. A., G. N. Rozental', and V. A. Rybakov. Surface phenomena in the interaction of laser radiation with transparent dielectrics. Zh PMTF, no. 2, 1971, 41-47.

Studies are reported on the mechanism and characteristics of laser-induced photoluminescence and photoelectric effect on the surface of several dielectrics, including quartz, K-8 inorganic glass, NaCl, plexiglass, and polystyrene. A single-pulse ruby laser of ~ 1 j output and 10-12 nsec pulse-width was used in the experiments. Photographic and spectral measurements show formation of a shock wave simultaneously with the luminescence induced by 10^8 - 10^9 w/cm^2 fluxes. Damage to the surface was not apparent at this level, confirming the conclusion that luminescence is caused by air ionization. The threshold flux density of luminescence was only weakly dependent on atmospheric pressure in the 1-760 mmHg range, a fact which indicates subsurface layers as the probable site of luminescence onset, possibly from absorbed gases. Two characteristic pulse spikes were noted on oscillograms of the current generated in the dielectric target by simultaneous illumination with laser pulse and application of a dc field in vacuum (10^{-6} torr). The laser and current signal peaks coincided while the luminous pulse lagged the laser pulse. A threshold value of flux density for the onset of current pulses was

determined. Discussion of probable causes of current generation and absorption of laser radiation led to a tentative conclusion that the free electrons liberated by laser radiation in dielectrics generate a current signal in the target, cause further absorption of laser radiation, and heating of the absorbed gases and adjacent air; this heating generates the flash. This mechanism is confirmed by the data on threshold flux density for generation of current and luminous flash in the inorganic dielectrics studied.

0332. Il'ina, K. N., A. A. Kovalev, A. Ye. Kuznetsov, A. A. Orlov, and P. I. Ul'kov. The initial phase of crack development in laser-irradiated polymethylmethacrylate. Mekhanika polimerov, no. 3, 1971, 551-552.

A finely divided zinc powder was introduced in a concentration of $\sim 10^7$ cm^{-3} into purified methylmethacrylate monomer before its polymerization, to prepare a PMMA sample with strongly absorbing particles after the pattern of inhomogeneities present in technical grade PMMA. The sample thus prepared was irradiated, together with the control of pure PMMA, by 2×10^{-3} sec. laser pulses at 1.06 μ in a spike mode. Microphotographs taken before and after irradiation showed formation of cavities or gas bubbles around Zn particles; cracks were observed at increased power density. The consecutive phases of destruction were found to be the same in the sample with Zn admixture as in the pure control sample. Characteristic plane cracks were formed by the gaseous products penetrating the cavity through a transition zone around a gas bubble. The similarity of qualitative destruction patterns of the technical grade PMMA and PMMA with the introduced absorption centers indicates that the interaction is independent of the nature of absorbing centers, after a certain stage in the destruction process. The authors note the similarity between the described damage and that typically observed in Nd glass lasers.

0333. Bonch-Bruyevich, A. M., I. V. Aleshin, Ya. A. Imas, and A. V. Pavshukov. Absorption of laser radiation in a subsurface layer of an optical glass. ZhTF, no. 3, 1971, 617-620.

Experimental proof was obtained of the existence of a subsurface layer in K-8 optical glass which strongly absorbs laser radiation. Radiation from a Nd glass laser generating quasicontinuous 800 j pulses of 700 μ sec length was focused on the glass surface; kinetics of surface cooling was recorded

in a 10 μ sec - 1 min interval after laser action was terminated. Temperature distribution along an axis perpendicular to the surface was the criterion of surface cooling kinetics, and made it possible to discriminate between the surface and internal absorption. The experiment revealed a relatively rapid temperature decrease, indicating radiation absorption in the subsurface layer. The depth of this absorbing layer was estimated to be of the order of 10-20 μ and the absorption coefficient in the subsurface layer to be 0.5 - 1 cm^{-1}. The linearity of the surface temperature dependence on power density of the laser pulse was an indication that the glass surface absorption is independent of nonlinear processes. Photos and graphical data in support of the findings are included.

0334. Pl'atsko, G. V. and Ya. S. Podstrigach. Stressed state caused by a laser beam in the process of destruction of transparent polymers. F-KhMM, no. 3 , 1970, 93-97.

Generation of stress waves in an infinite body, e.g., a transparent polymer is analyzed using the concept of mechanics of a deformable solid, and assuming instant absorption of electromagnetic energy in a thin circular region with maximum intensity in the center. The time and location of the destruction threshold of transparent polymers were formulated as functions of the principal stress parameters which determine destruction. Calculation of the stressed state indicated that the tangential stress attains its maximum at a certain distance from the beam axis, which depends on the absorption areas and stress parameters. The activation energy E_o of intermolecular bond breaking is expressed as

$$E_o = F_o (a) \nu \quad ,$$

where F_o is the pulse energy absorbed per unit area, a is a characteristic parameter of the area of intense absorption, and ν is the frequency of the generated ultrasonic wave. The calculated ν for plexiglass was nearly the same as the experimental values. It was concluded that the assumed mechanism of destruction adequately describes the actual physical process.

0335. Aleshin, I. V., A. M. Bonch-Bruyevich, Ya. A. Imas, V. L. Komolov, and V. S. Salyadinov. Surface destruction of K-8 optical glass. ZhTF, no. 4, 1971, 820-823.

The destruction of a glass surface by a focused laser beam was studied experimentally and the results have been interpreted in terms of a model of absorbing centers. An Nd glass laser ($\lambda = 1.06\mu$) emitting quasicontinuous pulses with $\sim$ 25% modulation, 500 j output and up to 800 μ sec pulse length was used to produce damage which was observed by illumination from a He-Ne laser beam. Successive steps of destruction at increasing power density of the laser pulse were described; formation and development of the flare was recorded with a SFR-2 high-speed photorecording camera. Heating of three glass samples of different surface states up to a critical temperature T_{cr} corresponding to destruction threshold was examined from the standpoint of the model of absorption centers. The derived relation between the threshold power density and characteristic time was verified for two of the samples, for which the average distance between two centers was found to be $\sim 10\mu$ in agreement with the electron microscopic data. The absorption coefficient of each center of 10^{-4} cm radius was evaluated to be $\sim$ 20 cm^{-1} at $T_{cr} \cong 2,000^{\circ}$ C.

0336. Makshantsev, B. I., R. K. Leonov, and P. A. Yampol'skiy. Destruction of transparent dielectrics by laser radiation. ZhETF P, v. 14, no. 3, 1971, 175-178.

The mechanism of the initial damage phase in transparent dielectrics is discussed in terms of electron excitation by the absorbed laser radiation and subsequent conversion of this excitation into heat. Heat evolution in impurity centers is concluded to be a consequence of radiationless electronic transitions in these centers. Formulas are derived in terms of temperature increase δ T in an impurity center and laser radiation intensity I which initiates optical destruction. The δ T dependence on time yielded the condition under which thermal explosion becomes possible. Thermal explosion may initiate destruction of the substance. In agreement with experimental data, the threshold I of optical destruction of fused quartz was evaluated to be $\sim 10^{11}$ w/cm^2, when destruction is initiated by Nd-glass laser pulses with a photon energy $\sim$ 1.12 ev. The thermal explosion model is thus used to explain the threshold characteristics of optical destruction in transparent dielectrics.

0337. Pilipetskiy, N. F., A. K. Fannibo, and V. A. Epshteyn. Heating dynamics of a damage center in a transparent medium irradiated by a quasistationary laser pulse. ZhPS, v. 15, no. 1, 1971, 33-37.

The initial phase of volumetric destruction of plexiglass by ruby laser pulses in a quasistationary mode was studied experimentally to establish the mechanism of destruction of transparent solids, hence to help formulate a criterion for optical strength of such materials. Quasi-stationary spikeless emission was obtained in an optical cavity formed by spherical mirrors at a sufficiently high relative pump rate. The brightness temperature of a damage center was measured photographically using the SFR ultra-high speed camera. Primary heating centers of two types, short-and long-lived, were detected. Evolution of both types was recorded during their existence in spherical or quasispherical form before the formation of plane cracks. During the short lifetimes (15 μ sec), the centers of the first type increased to $\sim$ 50 μ in diameter, before evolving into plane cracks. Temperature in these centers varied during lifetime from 2410 to a peak at 2730°, then dropped sharply to the initial value at the end of this period. The high-temperature (2520-2700°) phase of the second type lasted up to about 1 msec before evolving into a plane crack. During this time period the gas-filled cavity may expand along independently propagating branches. The tests stress the importance of high-temperature and high-pressure gaseous centers in the internal destruction of transparent polymers by powerful radiation.

0338. Pilipetskiy, N. F., N. F. Taurin, and V. A. Epshteyn. Heating dynamics of a damage center by laser. ZhTF, no. 7, 1971, 1502-1507.

Time-dependence of brightness temperature in a number of destruction centers was determined for LK-7 inorganic optical glass (PMMA), and polystyrene (PS) irradiated by multispike or giant two-spike pulses from an Nd-glass laser. Brightness temperature was recorded with an SFR ultra-high-speed photocamera with time-sweep as used in Pilipetskiy's earlier test described in the foregoing article. The photographs show formation of a multitude of small ($< 50 \mu$) luminescent damage centers of variable high temperature. The temperature of the gaseous phase in the centers rises and falls with time in the 3000-4000° range, depending on the radiation mode.

The lifetime of a damage center exceeded irradiation time (10^{-2} sec) in LK-7 glass and was about equal to spike duration in PMMA. Damage centers evolve from structural heterogeneities and microimpurities according to the sequence: preferential local absorption of light → heating → damage. More damage centers are thus generated in more heterogeneous materials, e.g., PMMA. The heat centers are concluded to be of decisive importance in the damage process of transparent solids.

0339. Fersman, I.A., L.D. Khazov, and G.P. Tikhomirov. Destruction stages in the surface of laser-irradiated transparent dielectrics. IN: Kvantovaya elektronika, Moskva, Izd-vo Sovetskoye radio, No. 3, 1971, 61-66.

A detailed description is given of precision experiments on the development of surface damage to laser-irradiated dielectrics. Target materials included polished K-8 glass, type KV and KU fused quartz, and sapphire. A ruby laser was used which generated 30 ns pulses, focused to a 110 micron diameter spot at the target surface. Delivered energy was controlled by neutral filters, with laser output held constant. The energy range of particular interest was $0.5\ W_{th} < W < Z\ W_{th}$, where W_{th} is in this case defined as the intensity at which a spark or luminous discharge first appears in the impact area. Electron microscopic observation of the impact area showed no visible effects at $0.5\ W_{th}$; surface deformation appeared at $0.8\ W_{th}$, followed by the luminous discharge. Irregularities in crater profile are discussed and results for the various target materials are compared. Initial surface quality was shown to have a pronounced effect, since highly polished specimens had damage threshold an order of magnitude higher than for other types. The experiment revealed a sequence of discrete stages in damage formation, summarized as follows for increasing laser intensity: 1) intensive absorption of radiation in local surface defects; 2) deformation of individual microregions in the surface layer to depths on the order of 1 micron; 3) formation of a high-temperature surface plasma in the process of structural breakdown; 4) surface fusion and further destruction by the shock wave from the spark discharge.

0340. Lokhov, Yu. N., V.S. Mospanov, and Yu. D. Fiveyskiy. Thermoelastic stresses generated in transparent solid dielectrics by a focused laser beam. IN: Kvantovaya elektronika. Moskva, Izd-vo Sovetskoye radio, No. 3, 1971, 67-72.

A theoretical analysis of laser-generated thermoelastic stresses in a transparent dielectric material is given for several possible variants in the critical parameters. The discussion is a continuation of an earlier

work by V'yukov et al (Effects of Strong Explosions, Report No. 1, p. 56) on the same topic. The model assumes a homogeneous isotropic dielectric with the laser beam focused to some internal point; the treatment is limited to pulse widths $\cong 10^{-8}$ sec. Breakdown with and without self-focusing is analyzed, and for the latter case expressions are derived for critical thermal stress and laser threshold intensities. In the self-focusing case a pronounced difference in the destruction mechanism is shown to exist, depending on whether linear or nonlinear absorption occurs. For the nonlinear absorption case, self-focusing will in all instances result in damage. A theoretical stress curve for the assumed model is given in Fig. 1, showing the non-monotonic characteristic of stress development. The inflection points are correlated to laser pulse duration and thermal parameters of the dielectric.

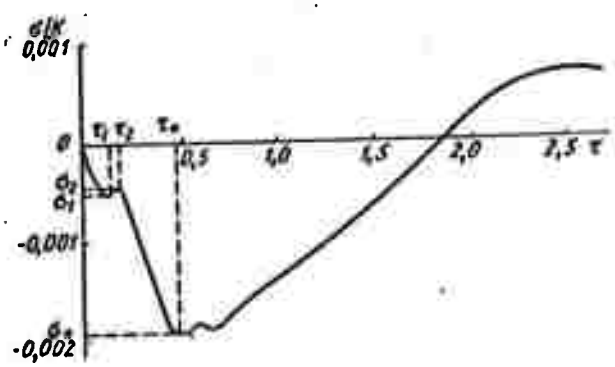

Fig. 1. Relative stress development vs. time along beam axis. Absolute maximum corresponds to laser pulsewidth.

LASER INTERACTION WITH SEMICONDUCTORS

0341. Brodin, M.S., P.I. Budnik, and S.V. Zakrevskiy. Destruction of "transparent" semiconductor crystals by powerful laser radiation. IN: AN Ukr SSR. Institut poluprovodnikov. Kvantovaya elektronika, Kiyev, No. 4, 1969, 107-114.

In a search for means of increasing mechanical strength of semiconductor crystals an experimental study has been made of the conditions and destruction mechanism of CdS_x - $CdSe_{1-x}$ ($x = 0.1-1$) and CdS_x - ZnS_{1-x} ($x = 0.9-1$) single crystals by giant pulses from a ruby laser. Destruction appeared on the crystal surface, at some threshold power density P_{th}, in the form of small cracks and fusion. The P_{th} for naturally cleaved crystals was higher than for polished crystals, and increased with the improvement in quality of surface treatment. Damage characteristics as functions of several laser and target parameters are discussed and tabulated. For example, P_{th} for $E \perp C$ polarized radiation was significantly lower than P_{th} for $E \parallel C$ polarized radiation, where C is the hexagonal axis of the crystal. The P_{th} dependence on pulse length (15 or 35 nsec) was inversely linear. A decrease in temperature from 190 to 4° K doubled P_{th}. Analysis of the cited data led to the conclusion that a rapid heating of the crystal lattice by energy transfer from the excited electrons, i.e. thermal shock, is a more probable mechanism of destruction than direct interaction of the optical field with the lattice. Also, the stresses generated in the crystal by thermal shock were estimated to be smaller than its tensile strength.

0342. Grasyuk, A.Z., and I.G. Zubarev. The interaction of semiconductors with intense optical pulses. FTP, No. 5, 1969, 677-680.

The authors describe a series of experiments to study the damage or strain at the surfaces of semiconductor materials, in this case GaAs, Si, and CdSe, by the application of intense laser pulses. Ruby lasers, neodymium lasers, and 1st and 2nd Stokes components of light from a ruby laser in liquid nitrogen were used as sources. The pulse widths ranged in duration from 20 to 30 nsec; wavelengths of 0.6943, 1.600 and 0.8280 μ were used. The intensity threshold of damage to the

semiconductor surface was determined for one-photon excitation as well as two-photon excitation. Various possible types of phenomena such as electrostriction, stimulated Brillouin scattering, avalanche-type breakdown, and thermal shock by which the semiconductor material could have undergone damage or strain are discussed briefly. Each phenomenon is described individually and by elimination all but the thermal effect are discarded as the most probable cause of damage. It was noted that, essentially, stability depended on the condition of the material surfaces. The presence of various microdefects and microcracks significantly lowered the surface stability of the materials. The authors observed that for each phenomenon investigated, the greatest strain created was due to thermal shock (~ 30 atm) and based on this concluded that thermal shock was also the most probable cause of strain or damage. The damage occurred only on the surface of the material and not the internal part of the irradiated area. This was ascribed to the fact that the geometry of the semiconductor material and the irradiated area was such that acoustic wave buildup was not likely to have occurred.

0343. Karpikov, I.I., R.O. Litvinov, and A.P. Lyashok. The effect of laser radiation on electrical parameters of metal-oxide-semiconductor structures. Sb. Poluprovodnikovaya tekhnika mikroelektronika (Coll. Semiconductor technology microelectronics), No. 4, 1970, 105-107.

Changes effected in electrical characteristics of MOS transistors and varactors by irradiation with pulses from a ruby laser were determined experimentally using a "Luch-1" type apparatus as a source of laser emission. The laser beam energy was below the threshold energy of visible surface damage. Transient responses of the MOS transistors irradiated at 8-9 kw/cm^2 show that the initial output current of p-type devices almost invariably decreased after irradiation, while that of the n-type devices always increased by an average of 200-300%. In MOS n-type varactors, leakage current typically increased and capacitance decreased as the result of irradiation. It was concluded that in most cases the characteristics of MOS devices are changed by laser irradiation, the devices of n-type Si being more affected than others. Preliminary measurements indicate that contact potential on the "real" surface of p-n junctions is also affected by laser radiation, hence the surface charge is changed. Presumably, a strong heating of the surface by the absorbed laser pulse is the principal mechanism of laser action. Treatment by

laser may therefore be the preferential method of controlling surface layer properties of a semiconductor and other parameters of semiconductor devices.

0344. Kazakevich, V.I., Yu.F. Babikova, A.A. Kozhemyakin, and N.N. Goryunov. Simulation of thermal breakdown in a transistor by heating with a laser beam. RiE, No. 3, 1971, 455-457.

An experimental technique using a laser as a source of localized heating is introduced to study thermoelectric negative feedback and subsequent thermal breakdown in transistors. Experiments are described in which this technique was applied to KT802 mesa-type silicon power transistors. A pulsed beam from a ruby laser, with 1 j peak energy, was directed alternately in the base, emitter, and the mesa-structure boundary of the collector junction. The length and shape of the light pulse and transistor current were recorded by a dual-wave oscillograph. A current jump, followed by a fusion channel at the heated spot on the surface, and mesoplasma were observed in all experiments, when flash energy reached a certain threshold value. The voltage-current characteristic of the collector junction and the short-circuit resistance measured after a breakdown indicated a metallic shunting of the collector junction had occurred. The fact that mechanical damage was not observed on the surface when current supply to the collector circuit was switched off, indicated that the observed damage must be connected with thermoelectric breakdown. Thus, the described laser technique is useful in detecting "weak" spots of local overheating in semiconductor structures and in studying the mechanism of short-circuit formations.

0345. Gulyayeva, A.S., B.A. Krasyuk, V.N. Maslov, and N.V. Troneva. Localized dissociation of gallium arsenide crystal by a laser pulse. FiKhOM, No. 3, 1971, 8-12

An experimental study was made of the effect of a 0.5 msec, 10j single pulses from an Nd glass laser on n- and p-type GaAs wafers. The 0.6--4 mm thick samples were exposed to the laser beam at some distance beyond the lens focus. The purpose of the study was to elucidate the earlier detected localized dissociation of GaAs, which might cause damage in laser microwelding of semiconductor devices. At an average

power density of 5.5×10^4 w/cm^2, damage was observed exclusively on the back face of specimens having 10^{16} - 3×10^{17}/cm^3 free carrier concentrations. No damage was detected on specimens with 10^{18}/cm^3 concentration, even as thin as 0.6 mm. Both the target face and the back face of the crystal exhibited similar damage at higher power density. A 50-70% decrease in As concentration on the damaged back face indicated a localized dissociation of GaAs. Consideration of the presence of free carriers in the allowed bands, and of the relationship between forbidden ΔE and laser radiation frequency, led to a tentative conclusion that the cumulative effect of acoustic waves is the cause of damage to the back face of the crystal via a dielectric mechanism, whereas the localized dissociation on the front face of GaAs is caused by absorption of laser energy on free carriers via a metallic destruction mechanism. Sample microphotos of damage to the target and rear faces are included.

0346. Arsen'yev, V.V., Ya. T. Vasil'yev, V.S. Dneprovskiy, and V.U. Khattatov. Destruction of cadmium sulfide crystals by picosecond light pulses. FTP, No. 3, 1971, 403-407.

An experimental study was made of surface damage to CdS crystals from nonfocused laser radiation of 3×10^{-12} sec. pulse width. An LG-55 Nd glass laser was used, generating a train of about 20 pulses at 8 nsec. intervals in a mode-locked regime. Laser beam diameter was $\sim$ 1 mm, its divergence was 5×10^{-4} rad, and emitted pulse energy was 0.1j. With the laser beam normal to the crystal surface, cleavage was observed on the exit surface only at a 30 Gw/cm^2 incident power density; cracks appeared on the front face of the crystal at a 150 Gw/cm^2 power density. The reflected light pressure P corresponding to a 30 Gw/cm^2 power density was calculated to be $\sim$ 20 atm. on the front face and $\sim$ 10 atm. on the exit face, although values as high as 100 atm were observed locally at the exit face. The threshold power density for destruction of the exit face was increased by immersing it in water, or by directing the laser beam at the Brewster angle to the front surface. In both these cases, P was decreased. Additional experiments and theoretical considerations of the damage mechanism to the exit face were able to eliminate the effects of hypersonic waves, generated either by direct interaction of light with the front face or by stimulated Brillouin scattering, or thermal shock, as possible causes of destruction of the exit face. This analysis led to the conclusion that the reflected light pressure is the most probable mechanism of destruction of the exit face of CdS crystal by ultra-short light pulses; thermal shock can contribute to destruction of the front face only.

0347. Gurevich, Yu. G., and O. N. Chavchanidze. Strong electromagnetic waves in a semiconducting plate. FTT, No. 4, 1971, 1091-1097.

A theoretical study is described of propagation of a plane monochromatic wave in a semiconducting plate bounded by z=o and z=a planes, the thickness a of which does not exceed the wave attenuation depth L. The study was limited to the case of weakly attemated waves ($\lambda \lesssim L$), and allowance was made for nonlinear effects resulting from heating of electron gas. Using the Maxwell and energy balance equations, the wave amplitude E_{ox} in the plate, transmission P_o and reflection R_o coefficients of the wave in null approximation were expressed as functions of the amplitude E_o of the incident wave and target thickness a. In the case of a strong heating effect in a thick ($a \cong L$) or a thin ($a < L$) plate with refractive index $n \cong 1$, it follows that P_o decreases or increases at increasing E_o depending on whether $q < 0$ or $q > 0$, respectively (q is a characteristic parameter of pulse transmission). The physical meaning of this conclusion is that electron temperature v rises at increasing E_o and hence $L \sim v^q$ decreases at $q < 0$ and increases at $q > 0$. Consequently, a wave at the wall z=a increases slower than E_o at $q < 0$ and faster than E_o at $q > 0$.

0348. Abrikosova, I. I., and O. M. Bochkova. Laser beam breakdown in liquid and gaseous He, and observation of stimulated Brillouin scattering in liquid He. ZhETF. P, v. 9, no. 5, 1969, 285-289.

Abrikosova, I. I., and N. S. Skrypnik. Laser breakdown and stimulated Brillouin scattering in liquid He^4. ZhETF, v. 59, no. 1, 1970, 59-63.

Laser-induced breakdown in liquid and gaseous helium is described. A ruby laser was used, developing 10 Mw pulses of 30-35 nsec and a focused spot radius of 10 mm. The beam was focused on the helium target in a Dewar flask, using equilibrium pressures up to 2.2 atm . Breakdown threshold vs He density is shown in Figure 1 for both liquid and gas phases, indicating their similar behavior. The authors conclude that breakdown is an avalanche

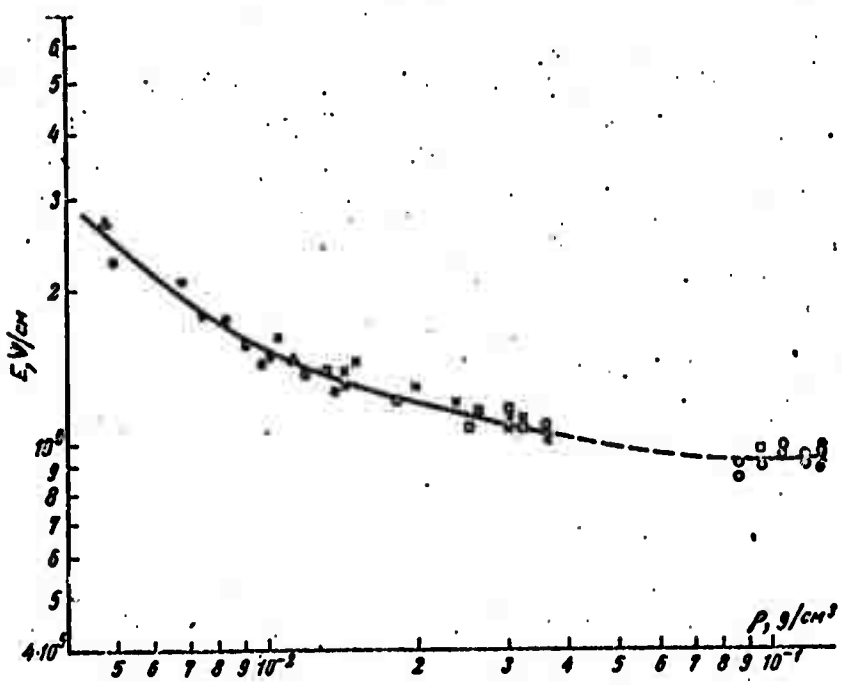

Fig. 1. Breakdown threshold in laser-irradiated helium.

phenomenon, starting with thermal emission from microscopic impurity particles suspended in the helium. The breakdown levels varied widely, even for identical laser beam and helium conditions; thresholds tended to drop with repeated exposure. For beam intensities exceeding 10^{10} w/cm^2 a pronounced Brillouin scattering was observed; the scattering threshold was above breakdown threshold. The intense Brillouin scatter could be used in the present case to measure the relatively low molecular scattering index

of liquid He. The second referenced article essentially describes the same experiment, with more details on test parameters. It also includes the sound velocities deduced from Brillouin component shift, as seen in Table 1.

Table 1. Sound Velocities from Brillouin Shift

Liquid He temp., ^{o}K	Brillouin component shift $\Delta\nu$, cm^{-1}	Calculated sonic velocity, m/sec
4.2	0.017	177
2.9	0.021	219
2.7	0.021	219
2.1	0.021	219
1.8	0.022	229

0349. Askar'yan, G. A. and V. B. Studenov. Banana-type self-focusing of a beam of light. ZhETF P, v. 10 1969, 113-116.

A theoretical and experimental treatment are given for self-focusing of a laser beam in liquid. Partial self-focusing of the beam, limited to a section of radius $r < r_m$ (r_m is the radius beyond which beam intensity is sharply decreased), and simultaneous loss of the peripheral beam portion at $r > r_m$ (banana-like peeling of a beam), were predicted theoretically for a variety of beams with a non-monotonic intensity distribution. The prediction was made by analyzing the refraction profile in several particular cases of self-focusing and the corresponding intensity distribution. An accompanying experiment evidenced for the first time self-focusing of a laser beam in water, and confirmed the theoretical analysis. The beam profile required for self-focusing was formed by directing a beam from a Q-switched unmodulated ruby laser through a glass plate with a screen in its center, then through water, or water with added copper sulfate. In the latter case, a spot of increased intensity appeared in the center, indicating the "banana-peel" effect. Thus, the range of media and beams (light, radio, and ultrasonic) capable of producing self-focusing may be expanded. It follows that the selection of the beam intensity profile of gas and solid state lasers may considerably affect spread of these beams in water or air.

0350. Kuzikovskiy, A. V., V. A. Pogodayev, and S. S. Khmelevtsov. Evaporation of a water drop by a light pulse. I-FZh, no. 1, 1971, 21-25.

Evaporation kinetics of a laser-irradiated water drop are described. The evaporation rate dr/dt of a water drop of initial radius r_o = 140-190 μ was determined experimentally at 2.4-15 cal/cm^2 effective energy density N of pulsed radiation of a GOR-027 ruby laser (λ = 0.69μ). The pulse output energy was 0.15 j and its length $t_p \ll r_o^2/a^2$, where a is the thermal diffusivity of water. Evaporation kinetics were measured by recording size dynamics of the drop on which the laser beam was focused. The recordings were made with the help of the SKS-1M and SFR-2L3 high-speed movie cameras, while the drop was suspended at the end of a glass or tungsten filament in a movable element. At N = 2.4-4.3 cal/cm^2, i.e., below the experimental explosion threshold value (5 cal/cm^2), an asymptotic form of r(t) curves was observed. The experimental r(t) and $\Delta r/r_o(N)$ plots were found to be in good agreement, over the studied range of N, with those calculated from theoretical formulas. Boiling without fractionation of the drop was observed for N in the 5-15 cal/cm^2 range. At N > 15 cal/cm^2 the r(t) dependence was practically linea to a critical moment (~1 msec), at which a sharp acceleration of the rocess confirmed the existence of an explosive regime. The experimental explosion threshold value of N was somewhat higher than the theoretical value because of interference of the suspension with the critical parameters in the center of the drop.

0351. Buzukov, A. A. and V. S. Teslenko. Sonoluminescence from focused laser radiation in a liquid. ZhETF P, v. 14, 1971, 286-289.

Sonoluminescence has been produced experimentally by collapse of cavities formed in a liquid by ruby laser radiation. Both 30-50 nsec single pulse and free-running modes were used, at an output energy of 0.5 j. With the laser beam focused in the liquid, luminescence signal and signal from a piezoelectric pressure pickup placed in the liquid at a 5-10 mm distance from the focus were simultaneously recorded on a OK-17 dual-channel oscillograph and photographed. The oscillograms of luminescence and of pressure pulses from a pulsating cavity in water show that the maximum luminescence intensity of 5-10 mw was produced in the 3750-4400 Å range by the first collapse of a cavity. The amplitude of sonoflash intensity in carbon tetrachloride was 1/2 to 1/3 of that in water. The free-running laser mode in acetone produced short luminescence pulses of small amplitude by pulsations from a quantity of small cavitation bubbles. The experiment confirms the emission of dynamic sonoluminescence in a liquid by the action of a focused laser beam; this effect must be taken in consideration in spectral investigation of stimulated Raman scattering.

0352. Trokhan, A. M., V. A. Belogol'skiy, and Yu. N. Vlasov. Surface boiling of a liquid. DAN SSSR, v. 196, no. 5, 1971, 1069-1071.

A brief description is given of surface boiling observed in still water irradiated by a 7w, 6 mm diameter beam from a CO_2 laser ($\lambda = 10.6\mu$). While surface temperature during irradiation was 100°C, the water was nearly at room temperature at 0.5-1 mm below the surface, indicating that radiation was completely absorbed in a subsurface layer of a few microns. The shadow and Schlieren photographs of the irradiated area show an intensive heat exchange occurring in a horizontal plane. Also 0.5-1 mm diameter cavities were revealed which extend in depth and generate laminar or turbulent flows. The flows propagate more than 1 cm in depth and last from several seconds up to several minutes. At a sufficient level of incident flux, the cavity extends by 2-3 diameters in depth, then collapses, typically leaving a starshaped trace on the surface. Formation of cavities and their collapse were found to occur more frequently in tap water than in distilled water, presumably because of the presence of foreign particles in the former.

0353. Askar'yan, G. A., Kh. A. Diyanov, and M. Mukhamadzhanov. New experiments in forming a self-focused filament from focusing a beam at the surface of a medium. ZhETF, v. 14, no. 8, 1971, 452-455.

An experiment in self-focusing of a ruby laser beam in liquid is described and analyzed. A Q-switched ruby at 6-30 Mw was focused at various depths in a container of nitrobenzol, and self-focusing was observed as a function of focal point distance from the liquid surface. A pronounced peaking effect is seen to occur in Figure 1 when the focus was ~5 mm below the surface. The filament generated was 100-150μ in diameter and more than 10 cm long, i.e., an order of magnitude below the diffraction scattering level. The depth of the focal point proved to be the controlling factor, irrespective of lens focal length or laser power. The authors emphasize the waveguide properties of the extended filament formation, and indicate its possibilities in propagation of highly concentrated optical flux in a nonlinear medium.

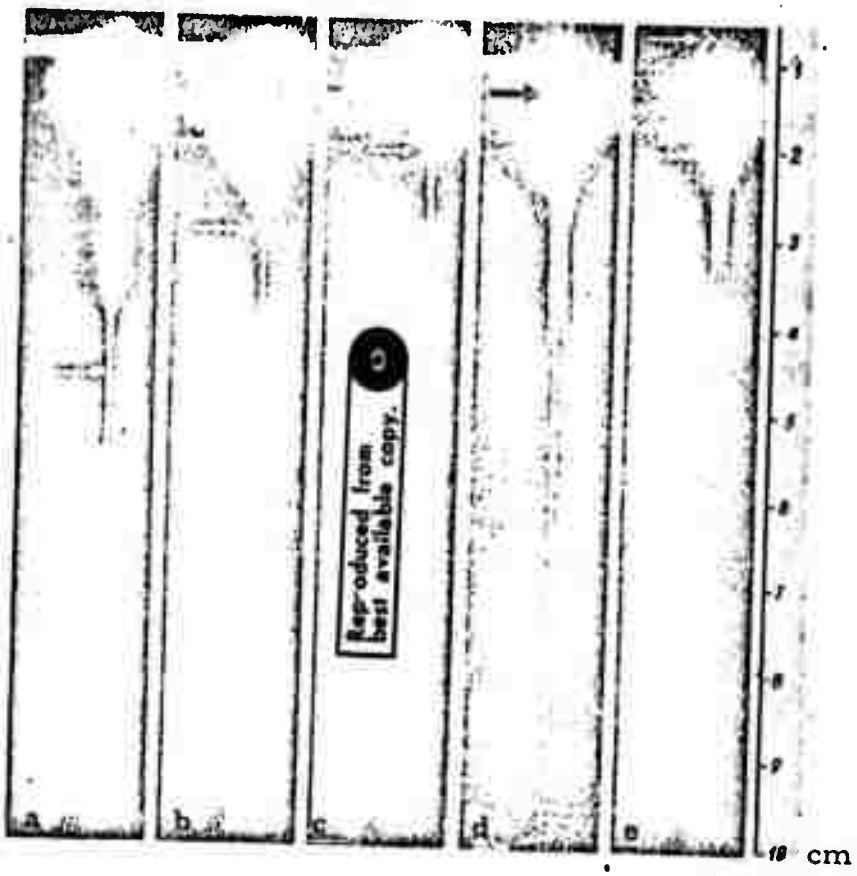

Fig. 1. Self-focusing in nitrobenzol

W = 6-7 Mw. Distances in mm from focus to surface and lens to surface, respectively; a - 40, 25; b - 23, 35; c - 15, 40; d - 5, 47; e - 3, 53. Arrow shows focal point.

LASER INTERACTION WITH MISCELLANEOUS MATERIALS

0354. Brodin, M.S., and A.M. Kamuz. Observation of self-bending of a non-uniformly intense laser beam in NaCl crystal. ZhETF P, Vol. 9, 1969, 577-580.

Experimental evidence is given for self-bending of a laser beam on passage through a solid medium. This effect was obtained by focusing the beam from a Q switched ruby laser (50-80 Mw average pulse power) obliquely on the face of an NaCl specimen, as shown in Figure 1, such that $A_1O_1 < O_1B_1$, resulting

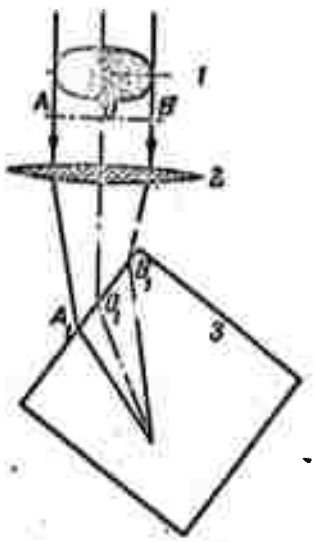

Fig. 1.
Self-bending experiment
1-section of beam; 2-lens;
3-NaCl target

in an intensity gradient at the crystal face. A cross-sectional view of the beam damage path in this case clearly shows the beam axis to be deflected approximately 6° in the direction of lower beam density, as measured at the focal point within the specimen. The experiment thus demonstrates a refractive index gradient and a self-focusing effect in the crystal.

0355. Poplavskiy, A.A., and L.D. Khazov. Anisotropic resistance of $CaCO_3$ to laser radiation (damage). ZhTF, No. 2, 1969, 407.

This paper briefly describes the distinct difference in the resistance of $CaCO_3$ crystal to intense laser radiation, as a function of beam polarity. Tests using a single-pulse ruby with a 0.5 mm diameter beam and 25 nsec

pulse width showed that the damage threshold for ordinary polarization was an order of magnitude higher than for extraordinary polarization. In both cases the laser beam was perpendicular to the crystal optical axis. The results evidently can be attributed to the known strongly anisotropic optical characteristics of $CaCO_3$, and could thus be expected to occur for other target materials of similar polarization anisotropy. The damage mechanism was not clear, since it was not typically of the self-focusing type common to these tests.

0356. Volkova, N. V. Structural features governing damage to alkali halide crystals from laser radiation. FTT, No. 2, 1970, 616-618.

This is an experimental study of Q-switched laser radiation damage to a number of akali halides, including pure and alloyed LiF; NaF; NaCl; KCl; KBr; RbI, and CsI crystals. The object was to correlate damage threshold to type of impurity inclusion and other inhomogeneities in the crystal lattice; inclusions on the order of 1 micron or less were particularly studied. Figure 1 shows the form of damage centers observed in NaCl.

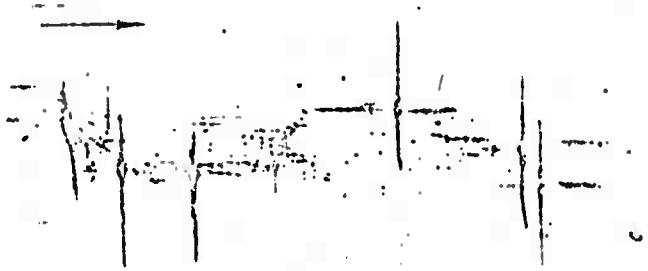

Fig. 1.
Damage centers in NaCl. Arrow shows laser beam direction; magnification is 400x.

From tabulated results relating damage threshold intensity to destruction center density, the authors arrive at three general factors which govern the laser damage resistance of alkali halides: 1) large ($> 1\ \mu$) opaque inclusions; 2) small ($< 1\ \mu$) scattering centers; and 3) crystallographic irregularities, e.g. density variations of trace elements or vacancies in the lattice matrix. A similar study on effects of optical irregularities in PMMA has been described in # 2 Explosion Effects Report (Volkova et al, p. 40).

0357. Suminov, V.M., and B.G. Kuzin. Hole configurations in single-pulse laser applications. Pribory i sistemy upravleniya, No. 4, 1970, 57-59.

Techniques of controlled hole formation in solids are discussed, based on experimental results with a single-pulse (unidentified) laser developing up to 70 j at 2 millisec duration. The target material is identified as type D 16 T sheet, presumably an alloy, 4 mm thick. Data are given on the growth rate and shape of the holes as functions of the number of laser pulses applied and of beam focus location. It is shown that these two are the primary factors in the controllability of hole formation. In particular a continuous adjustment method is proposed which synchronizes the focal distance to the increasing depth of the hole, thus maximizing growth rate. Differences between single- and multi-pulse hole formation are pointed out and analyzed.

0358. Batanov, V.A., B.V. Yershov, L.P. Maksimov, V.V. Savranskiy, and V.B. Fedorov. Laser system with energies up to 10 kj for studying the interaction of powerful optical beams with matter. KSpF, No. 4, 1970, 8-13.

This paper is concerned entirely with the design and operating characteristics of a powerful laser array specifically developed for high-level beam-target studies. The array consists of three parallel 3-stage Nd glass lasers whose combined output is synchronized to focus on a target surface. A net energy of 10 kj at 1 millisecond is thus developed, providing a density up to 10^7 w/cm^2 over a 1 cm^2 target area; focal distances up to 2 meters are used. Pulse shape, dispersion pattern and pump characteristics are discussed. It was attempted to build high reliability into the array; however experience over two years has shown that breakdown in the output faces of the resonator elements is a limiting factor, allowing only 5 to 10 pulses at the 10 kj level, or up to 50 times at the 5 kj level, before damaged elements must be replaced. No test results with target materials are mentioned.

0359. Goncharov, V.K., L. Ya. Min'ko, and Ye. S. Tyunina. Laser methods for generating plasma flows and shock waves. IN: Sbornik. Kvantovaya elektronika i lazernaya spektroskopiya. Minsk, 1971. 376-396. (RZh Radiot, no. 10, 1971, # 10D273)

A general review is given of recent progress in laser-generated plasmas and shock waves, from both condensed and gaseous media. Experience has shown that unmodulated laser radiation in the 10^6 - 10^9 w/cm^2 intensity range can produce relatively long-lived plasma states with controllable parameters. Beam-target studies with powerful giant pulse radiation will generate plasma flares with an accompanying spherical shock wave; the state-of-the-art now permits a wide range of control over the plasma and shock wave parameters in a localized region, for a variety of target materials. The technique has also yielded new information on the physics of gas and surface material heating by intense e-m flux. The term "laser plasmodynamics" is now applied to this field of study.

0360. Makarov, N. I., N. N. Rykalin, and A. A. Uglov. The temperature field in stationary vaporization. FiKhOM, no. 1, 1969, 23-26.

A detailed theoretical analysis is made of the temperature field in locally heated materials. The objective is to demonstrate the qualitative difference in heating effect between the general case of a surface heat source and a volumetric or penetrating heat source, as is the case of intense laser or electron beams focused on a solid target. In both cases the treatment is concentrated on the absorbed fraction of incident heat flux, assuming a stationary vaporization model. For the volumetric heating case the internal energy absorption is assumed to follow the Bouguer Law, i.e., to decrease exponentially with depth into the target material. The expressions for evaporation rate are shown to be identical for each assumed type of heat source. However, in contradiction to several cited earlier references, it is shown that for the volumetric heating case, the temperature field in the subsurface volume will not have a maximum at any depth.

0361. Rykalin, N. N., A. A. Uglov, and N. I. Makarov. Calculating the heating of a film by laser radiation. FiKhOM, no. 2, 1971, 3-8.

A general mathematical model is developed to define heating processes in a film-substrate combination, for the case of a localized heating source such as a laser beam. The model assumes the film thickness to be large with respect to beam penetration depth, so that the heat source may be treated as a surface phenomenon. The criterion of a thin film is taken to be satisfied if the temperature across the film layer is effectively constant, i.e., that the coefficients of thermal conductivity and diffusivity λ_1, $a_1 = \infty$. Temperature behavior in terms of pulse width and film and substrate thermal parameters is defined for several assumed cases, namely the one-dimensional case where thermal constants are invariant over the target surface; the two-dimensional case where variation of constants over the surface area is allowed; and for both unlimited and limited substrate thicknesses. A numerical example is included for an aluminum film on a ceramic substrate.

0362. Bunkin, F. V. Reflection of powerful ultrashort optical pulses from condensed media. ZhETF P, v. 10, 1969, 561-564.

The conditions are investigated under which a sufficiently short and intense laser pulse will be almost totally reflected from the surface of a condensed medium. More exactly, the case is considered in which surface ionization caused by the first several periods of the laser frequency is sufficiently great that the generated plasma is opaque to the remaining major portion of the laser pulse. It is thus shown that for picosecond pulses and a typically dense medium ($n_a \cong 10^{22}/cm^3$), laser wavelengths from the near-ultraviolet and longer may be effectively shielded from the surface, provided that the generated plasma does not appreciably dissipate over the duration of the pulse, i.e., that the thermalization process sufficiently exceeds the recombination process. A numerical example illustrating the effect is given based on Nd glass laser radiation.

0363. Barashev, P. P. and V. L. Tal'roze. The competition between thermal and photochemical mechanisms of material transformation in the field of a pulsed laser. KhVE, no. 1, 1971, 30-36.

A mathematical analysis is given of the effect of laser pulse length on the mechanism of laser-induced chemical reactions in a condensed medium. Two competing mechanisms, thermal and photochemical, are considered for the case of chemical reactions of the first and second order (mono- or bimolecular). Two model problems were accordingly solved for the criteria of pulse magnitude of τ_{cr}, below which the photochemical and above which the thermal mechanism of chemical reaction are predominant. The solution of the thermal problem gives the value of surface temperature ΔT_{max} at the end of the pulse action τ for a medium with a high or a low absorption coefficient. The solution of the photochemical case enabled formulation of a series of inequalities which determine the magnitude of τ_{cr} as a function of kinetic parameters α_1 and α_2 of the first and second order reactions, respectively. Also, an inequality is formulated for the critical value I_{cr} of optical flux density at which the rate of photochemical reaction is always higher than the rate of thermal reaction, i.e., at which the τ_{cr} concept is meaningless. A method is outlined for evaluating τ_{cr} by means of the cited inequalities. The τ_{cr} of the two-photon photochemical decomposition of AgCl is evaluated as an example of application of the method. The method

is applicable only on the condition that the photochemical reaction rate is independent of temperature and $\tau_{cr} > \tau_{rel}$, where τ_{rel} is the relaxation time of energy transfer from one to another degree of freedom.

0364. Chetverushkin, B. N. Numerical calculations of the spectral problem in heating of a substance by external radiation. ZhPMTF, no. 2, 1971, 48-53.

A theoretical analysis is presented on the problem of most usefully expressing the energy transfer between external beamed radiation, e.g., a laser, and a solid target. The advantages are demonstrated of assuming a spectrum of absorption constants which can be correlated to steps in the physical heating process following beam interaction with the material. For the assumed model, a five-group spectrum is concluded to be a sufficiently close approximation to a rigorous solution for practical purposes. The spectral calculations show that in the initial period of interaction the major part of absorbed radiant energy goes to increasing the internal energy of the material. This is followed by an increasing conversion to kinetic energy and growth of ejecta, together with formation of a compressional shock wave which precedes the thermal wave into the non-excited material region. The technique is shown to significantly reduce the number of independent parameters which must be considered, accordingly simplifying the problem solution.

0365. Askar'yan, G. A., and V. A. Pogosyan. Heat track and self-focusing of a powerful beam in a medium. ZhETF, v. 60, no. 4, 1971, 1295-1299.

A theoretical study is given of the effect of temperature distribution in time and space on absorption of a powerful optical beam. The case is considered of a special beam profile featuring an intensity dip near the center axis. In the case of refractive index of the medium n = 0, solution of the nonstationary heat equation exhibits a steady logarithmic increase in temperature with time. In the case of a square-parabolic near-axial intensity profile (n = 1), the temperature on the axis is always lower than off-axis temperature, i.e., the condition of beam self-focusing is satisfied

in a medium with derivative $n'_T < 0$. It is shown that self-focusing of the near-axis portion of the beam is the result of a nonstationary process even over a great time interval, i.e., this temperature regime under the given conditions is unstable. In the initial phase of heating at $\tau \leq 1$, the self-focusing conditions are satisfied at $r/a < 1$, where r is the beam radius and a is the radius of the heat emission region. At $r/a > 1$, a "banana"-type self-focusing occurs. The near-axial region of self-focusing shrinks continuously with increasing $\tau = \chi t/a^2$, where χ is the thermal diffusivity of the medium.

0366. Gusev, N. V., and A. A. Pyarnpuu. Quantitative study of the ejection of matter from a solid surface by the action of powerful radiation. ZhPMTF, no. 4, 1971, 127-133.

A detailed gasdynamic analysis is given of the physical behavior of ejecta from a solid surface irradiated by an intense laser beam. A normal incidence of the beam is assumed, and the geometry of Fig. 1 is used with cylindrical coordinates.

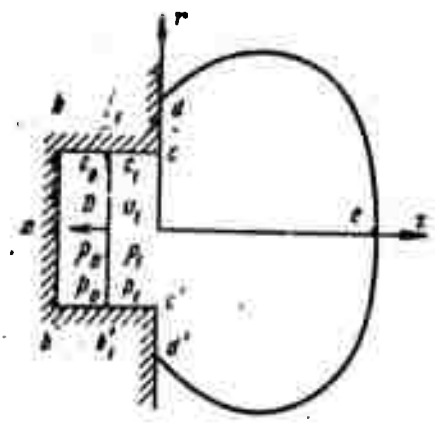

Fig. 1. Ejecta model

This is simplified to a problem in (r, z, t) only, by assuming a symmetrical ejection pattern about the z-axis. A general set of equations is given for the defined flare region in terms of velocity, pressure, density and optical absorption constant. The boundary conditions are then defined for the model of Fig. 1 for these variables. A numerical example is given for the assumed case of a graphite target subjected to a normal beam, with intensity increasing to the level where optical detonation occurs. Graphical solutions for this case are given for the variables as functions of z, an example of which is shown in Fig. 2; this gives the idealized temperature profile when

$q = 10^9$ w/cm^2, at 4 ns after laser interaction begins. The spike corresponds to intense heating at the flare boundary, resulting in shock wave generation. The analysis is generally useful in distinguishing differing stages of shock wave development typical for the assumed interaction.

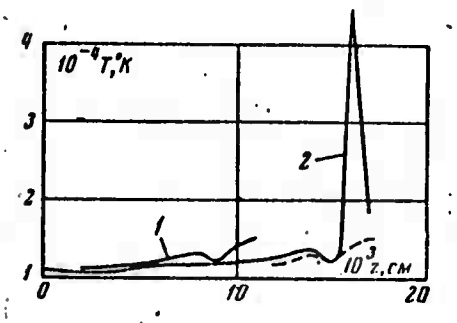

Fig. 2.
T (z) for $q = 10^9$ w/cm^2,
4 ns after start of laser pulse.
1 - using 10 initial data points;
2 - using 16 data points.

CONFERENCES

0367. Seminars of the Institute of Mechanical Problems, AS USSR. MZhiG, no. 1, 1971, 187-192.

Yu. P. Rayzer (Moscow) presented a paper on "Subsonic propagation of discharge and the optical plasmatron" at the 68th session of the General Seminar of the Institute of Mechanical Problems, AS USSR, on February 19, 1970. The author introduced an optical plasmatron in which plasma is formed and sustained by a laser beam without requiring special means of transferring electromagnetic energy. Propagation of the temperature-ionization wave generated in the plasmatron is described by gas dynamic and thermal conductivity equations. In contrast to combustion, the possibility exists here of achieving a stationary state, i.e. zero propagation velocity, at a threshold value of emission power. The threshold power for a Nd-glass laser was calculated to be 13 Mw/cm^2 (900 kw), in agreement with the experiment, and that of a CO_2 laser to be 7 kw. The threshold power decreases by more than one order of magnitude, if pressure is increased to 10 atm.

0368. Veyko, V.P., G.M. Kozlova, and M.N. Libenson. First All-Union School on Physico-technical Principles of Laser Technology. FiKhOM, no. 6, 1970, 141.

The First All-Union School on the title subject was organized by the Leningrad House of Scientific a d Technical Propaganda and the Leningrad Institute of Precision Mechanics and Optics. A series of lectures were presented from 9 to 14 March 1970 by leading specialists from Moscow, Leningrad and Gor'kiy to an audience of 140 people from 15 Soviet cities. Lectures on interaction of laser radiation with opaque media, transparent media, and thin films were given, respectively, by S.I. Anisimov, and Ya. A. Imas; V.A. Pashkov and M.N. Libenson. P.I. Ul'yakov lectured on destruction of materials by thermoelastic stress. Yu. K. Krylov and L. I. Mirkin discussed shielding of laser radiation by destruction products, and changes in properties and structure of materials by the action of laser radiation. N.N. Rykalin and A.A. Uglov, and L.M. Shestopalov gave lectures on the physical aspects of, respectively, material treatment in general, and heat-treatment and rapid hardening of metals by a laser beam. Ya. I. Khanin and V.P. Veyko lectured on methods of controlling

temporal and spatial structure of a light pulse, and methods of forming a laser pulse in the region to be treated. Technological applications of lasers were presented by V. P. Tychinskiy (gas lasers), B. N. Kotletsov (fundamentals of holographic technique), Ye. D. Vaks (dimensional treatment), V. Z. Vysotskiy (drawing on films by means of laser radiation), and L. N. Stepanov (laser welding). Finally, Yu. V. Lyubavskiy, lectured on powerful laser devices. The Second All-Union School on this subject is planned in 1971 in Gor'kiy.

0369. Ponizovskiy, Z. L. International Conference on Laser Plasma. Priroda, no. 1, 1971, 15.

An International Conference on Plasma Heating by Laser Radiation was held on 17-20 November, 1970 in Moscow under the direction of the Institute of Physics and the Scientific Council on Plasma Physics of the Academy of Sciences. The cited method, as noted in another article by N. G. Basov, O. N. Krokhin, and P. G. Kryukov, is expected to contribute to the solution of the problem of thermo nuclear fusion. Soviet scientists and guests from Great Britain, East and West Germany, Italy, Canada, Rumania, U. S. A., France, Czechoslovakia, and Japan attended the conference. Possibilities and the future outlook were discussed of achievement of conditions for thermonuclear fusion in a laser plasma, as well as heating processes from focusing a powerful laser beam on various targets; diagnostic methods for plasma; and the use of CO_2 lasers for heating. The problems of laser use in plasma injection and confinement in standard thermonuclear devices were examined. Some other uses of laser plasma were indicated, particularly in astrophysics and as a source of multiply-charged ions in accelerators.

0370. Uglov, A. A. Proceedings of the Seminar on Physics and Chemistry of Treatment of Materials by Concentrated Energy Fluxes. FiKhOM, no. 2, 1971, 166-167.

The 25th Seminar on the title subject was held October 1, 1970 at the Baykov Institute of Metallurgy, AS USSR under the direction of Academician, N. N. Rykalin and was devoted to the interation of laser radiation with metals, polymers, and semiconductors, as well as of electron beams with metals. Over 100 representatives of various organizations from Moscow, Leningrad, Kiyev, Minsk, Taganrog, etc. attended the proceedings. Papers on interaction of laser radiation with metals were

presented by A. G. Solov'yev, and V. M. Kirillov (The maximum vaporization rate of metals by laser beam); P. I. Ulyakov, (kinetics of metal surface vaporization by an optical beam), and B. M. Zhiryakov, N. N. Rykalin, A. A. Uglov, and A. K. Fannibo, (Certain characteristics of metal fracture by a laser beam). Breakdown of polymers by laser radiation was examined by A. A. Kovalev, A. Ye. Kuznetsov, A. A. Orlov, and P. I. Ulyakov, (On the initial propagation of cracks in plexiglass by interaction with a laser beam) and by N. F. Pileptskiy, (The mechanism of breakdown in polymers by a focused light beam). V. F. Brekhovskikh, A. V. Ovodova, A. A. Uglov, and A. K. Fannibo, presented experimental data and its interpretation in a paper on changes in dislocational structure of germanium exposed to a laser beam. Two experimental studies dealt with metals: on the behavior of an intense electron beam in a liquid (vacuum pump oil and mercury) by L. Yu. Vol'fson, A. N. Kabanov, A. A. Kafafov, Yu. N. Kushnir, and Ye. Ye. Chernova-Stolyarova, and on the effect of energetic and geometric parameters of an electron beam on the quality of machining by L. Yu. Vol'fson, A. N. Kabanov, A. A. Kafafov, A. I. Chugrinov, and Ye. P. Starostin.

DYNAMICS OF LASER INTERACTION WITH SOLIDS: REVIEW

Introduction

An extensive recent paper by Basov's group at the Lebedev Institute (1) is presented as a comprehensive up-to-date review of studies on high-power laser interaction with solids, based on both Soviet and Western sources. While it does not attempt exhaustive coverage of all significant non-Soviet reportage on the subject, it does give a detailed resume of experimental results obtained at the Lebedev Institute, where the most advanced beam-target studies in the USSR are taking place. Basov's report therefore may be taken as a Soviet state-of-the-art summary, and is the most detailed of its kind yet to appear in the open literature.

One major objective in these tests is to achieve the conditions for a controlled thermonuclear reaction (CTR), since the degree of ionization and plasma temperatures already attained suggest this to be an experimental possibility; the bulk of the beam-target reportage from the Lebedev group is now in fact oriented to CTR studies. However, although CTR is mentioned as one rationale, the present authors are not writi .g from that express viewpoint; rather a more general attempt is made to discuss the best techniques for generating a laser plasma from a solid target, and for measuring the parameters of most interest during plasma lifetime. The paper therefore includes detailed descriptions of plasma generating and monitoring apparatus, and a large number of photographs illustrating plasma development for a variety of conditions.

1. Statement of the Problem

Questions of laser interaction with material came under study directly with development of the solid-state laser, since such interaction still represents a limiting factor to solid-state laser output. However, the main impetus to advanced beam-target studies was the development of the Q-switched laser, generating giant pulses which could be focused to give surface power densities of 10^8 w/cm^2 or more, i.e., on the order of intra-atomic bonds. With present methods it is possible to introduce energy into the resulting plasma at a rate of 10^{10} - 10^{12} watts, which is an order of magnitude faster than possible with electric discharge techniques. A number of early studies showed that this could yield plasma flares with electron densities of 10^{19} - 10^{20}/cm^3, and with temperatures on the order of a million degrees.

A variety of direct and indirect methods have been developed for measuring plasma flare parameters. As pointed out by the authors, the physical demands on such measurements, e.g., time resolution, have been an impediment to obtaining a clear picture of flare processes. Two main approaches are mentioned here; in the generally earlier studies cited (2-8),

particle emission from the plasma was monitored for type, energy and spectra, from which some aspects of the heating process could be deduced.

More recent experiments have emphasized optical methods to observe plasma kinetics and spectral characteristics (9-15), most of which involved high-speed photography with the laser operating in a spike mode. Tests of this type have shown that the ejection rate of material from the target surface can reach 10^6 cm/sec. In (10) a giant pulse mode was used on a carbon target and observations of the luminous boundary showed it to accelerate from 4.8×10^5 to 7×10^6 cm/sec over a 3 mm travel, at an applied energy density of 700 j/cm^2. Single and dual-beam laser interferometry has been widely used in this type of study; with the high optical intensities available this permits very rapid photosequences, on the order of a few nanoseconds per frame. In (14, 15) the authors examined multiply-charged plasma ions in the vacuum u-v range and reported a new range of ion lines with a large effective charge.

Another approach briefly mentioned is measurement of the recoil pulse as a function of mass and rate of ejecta (16, 17). In (16), for example, the authors found the specific impulse to peak at a density $\approx 10^9$ w/cm^2 but decrease with higher intensities; it was further concluded from this test that the crater at the target surface was formed after laser pulse termination due to shock unloading.

The foregoing results, together with others omitted herein, are presented by Basov et al only as a sample of trends in laser plasma research, and are not intended to be comprehensive. Furthermore, it is emphasized that the kinetics of heating matter by focused Q-switched laser pulses still remains to be adequately explained. Apparent conflicts exist in evaluation of ion temperatures, for example; data have been reported showing ion energies in excess of 1000 ev, whereas ion temperature averaged by mass seldom exceeds 100 ev in a plasma flare. Other unanswered questions include the nonuniform heating of the plasma and contradictory evidence on the mass of ejecta.

2. Gas Dynamics of Plasma Heating and Dispersion

A large body of theoretical literature has appeared on the heating and motion of the laser plasma flare. Basov summarizes the essentials of those considerations briefly, both for an idealized approximation and for more rigorous cases which account for actual processes occurring in plasma formation. The basic parameters in any case are expressed in terms of the absorption coefficient k of incident radiation, or k (ρ, t), where ρ and t are instantaneous plasma density and temperature.

In a first approximation a spherical plasma is assumed with an initial radius R_o; equations of motion and heating are then derived using mean values of R and plasma velocity v. This yields Eq. (1) for plasma temperature,

$$T = \frac{1}{4} \frac{Q_0 t}{1{,}5 N_0 k}. \tag{1}$$

where Q_o is laser energy absorbed and N_o is the number of particles in the plasma. Eq. (1) is thus useful for giving the approximate maximum T attainable in the plasma for a given absorbed energy.

A more precise solution accounts for the fact that the heated mass is time-variable. The most useful model cited for this is a spherically dispersing plasma in which the dispersion rate is a linear function of radius, attributed to Sedov (18). This has the advantage of allowing the gas dynamic equations to be solved in analytical form. Basov refines Sedov's model by substituting Eq. (2) for velocity,

$$v = v_1 + \frac{\dot{R} - v_1}{R} r, \tag{2}$$

where v_1 = gas velocity in the center and $\dot{R}$ = velocity of the plasma boundary; he then derives energy and motion equations for the expanding plasma. It follows from this treatment that if the equation of state of the evaporated mass is known as a function of density and temperature, then for a given internal energy one may arrive at the plasma temperature attained by the end of the laser pulse.

A still more rigorous analysis requires including the effect of the focal area of the laser spot on the plasma surface, as pointed out by Nemchinov (19). Introducing this factor, Basov develops expressions for energy density ϵ, density ρ and evaporated mass M of the plasma in terms of focused spot radius d and incident Q. For the fully-ionized case, these parameters would reduce to the approximations of Eq. (3).

$$\begin{aligned} \varepsilon &\approx 0{,}45 k^{1/4} d^{-1/4} Q^{3/4}, \\ \rho &\approx 0{,}53 k_0^{-1/4} d^{-1} Q^{1/4}, \\ M &\approx 1{,}1 k_0^{-1/4} d^{1/4} Q^{1/4} t. \end{aligned} \tag{3}$$

Finally, for interest, Basov determines the time t_1 at which the self-similar planar model should yield to the spherical model; this is done by equating the expressions for ϵ for the two cases. For reasonable assumed values ($Q = 10^9$w, $q = 10^{12}$ w/cm^2, $d = 2 \times 10^{-2}$ cm), $t_1 \approx 10^{-9}$ sec, which may be considerably less than pulse duration τ. However, since ϵ is so weakly dependent on time, its values calculated from both models are reasonably close, even when $\tau > t_1$ by an order of magnitude.

3. Experimental Measurements of Laser Plasmas

The balance of this report is devoted to the experimental methods used by Basov's group in current laser plasma research. As already mentioned, the most useful results in this work are being obtained by optical observations, generally comprising high-speed laser photography and laser interferometry. Some additional discussion is given on particle emission and recoil measurement techniques for assessing plasma parameters.

a. Study of Plasma Dispersion Dynamics by High Speed Photography with Laser Illumination.

One test configuration widely used for the beam-target tests is shown in Fig. 1. A Q-switched Nd laser (5) with two amplifier stages was

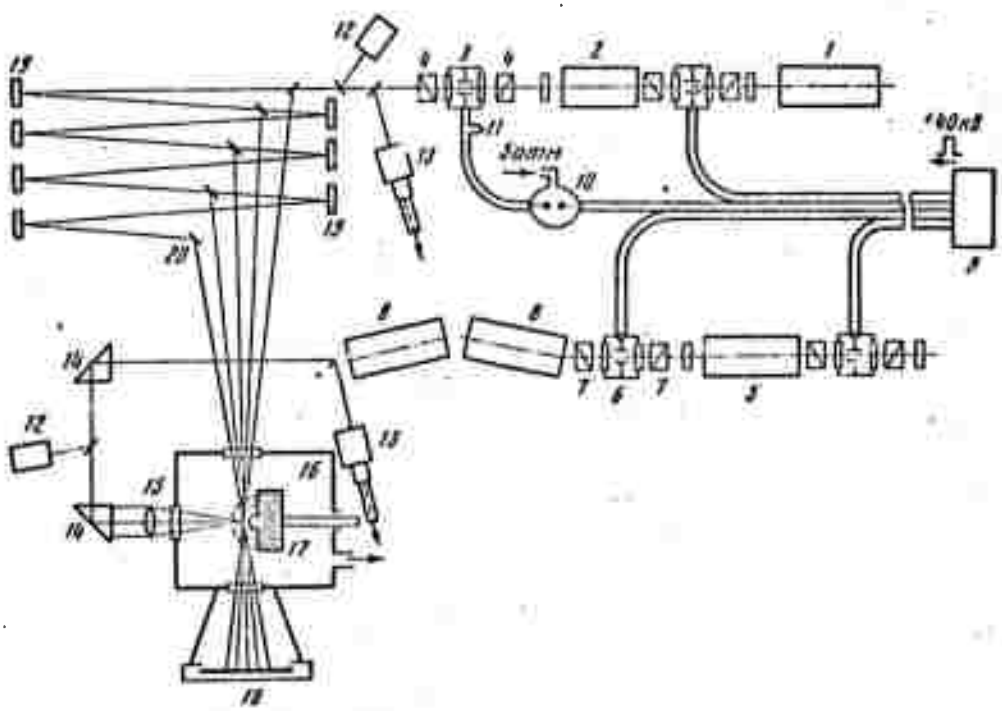

Fig. 1. Laser plasma experiment

1-gas laser; 2-Q-switched ruby; 3-pulse shaper; 4,7-polarizers; 5-Q-switched Nd laser; 6-decoupler; 8-amplifiers; 9-pulse generator; 10-shaper; 11-coax matching element; 12-calorimeters; 13-photoelements 14-deflectors; 15-focus, f= 150mm; 16-vacuum chamber; 17-target; 18-photofilm; 19-mirrors; 20-optical wedges.

used as the target beam, developing 20j pulses at durations under 15 ns. The beam was focused as shown on the target surface in a vacuum chamber, whose pressure was variable from 2×10^{-6} to 50 torr. There were some admitted problems in beam control, e.g. the delay between Q-switching and giant pulse generation was unstable, varying between 50 and 80 nsec, which complicated the synchronization problem with the illuminating optics. Also, although pulse energy remained effectively constant, there was a variation of some 8 nsec in pulse duration.

Plasma illumination was furnished by ruby laser (2) whose output was divided by optics (19) into five sequential beams, all focused to a common point in the plasma. In order to improve the photographic resolution the basic 20 nsec ruby output pulse was shortened by a special Kerr cell (3) and polarizers (4), such that the cell polarity was switched by π immediately following arrival of the pulse leading edge. This yielded narrowed outputs of about 3 nsec, but at a cost of attenuating the pulse energy by a factor of 30. The pulse narrowing feature imposed especially hard demands on the polarizers, which in the closed state were required to attenuate incident flux by 10^4 times, in order to keep background illumination on the film below a few percent. All four Kerr cells were synchronized from a master trigger as shown in the figure.

By splitting the ruby beam into five parts of equal incremental length and redirecting them onto the recording film after passing through the plasma, the authors obtained an unbroken sequence of photos with a time differential corresponding to the incremental path length for each beam. The dimensional resolution of this method is ultimately limited by interference caused by reflections, and by diffraction, in the plasma. An additional inherent uncertainty factor is the variance in dispersion among the five beams; in Basov's test, however, this was compensated for by an additional optical correction. In this case it is shown that resolution δ varies with cumulative incremental frame time τ, i.e. $\delta = \ell_1 a/c\tau$, where ℓ_1 is the distance from focus to film and a is effective aperture of the ruby laser. In the example given, with frames separated by $\tau = 50$ nsec, the resolution increased successively per frame from 0.8 to 0.04 mm. In any case the nominal flux for all five beams was the same at the film surface. The time resolution per frame was determined by the pulse width at the half-energy point; this occurred roughly at the 0.3 pulse amplitude level, resulting in a frame exposure time of 4 nsec and a resolution of 2 nsec.

With this equipment Basov et al report results of plasma generation studies for several target materials and ambient conditions. In the first described a carbon target was used in a 10^{-6} torr vacuum. In a typical 5-frame photo sequence (Fig. 2), the first two frames show an opaque

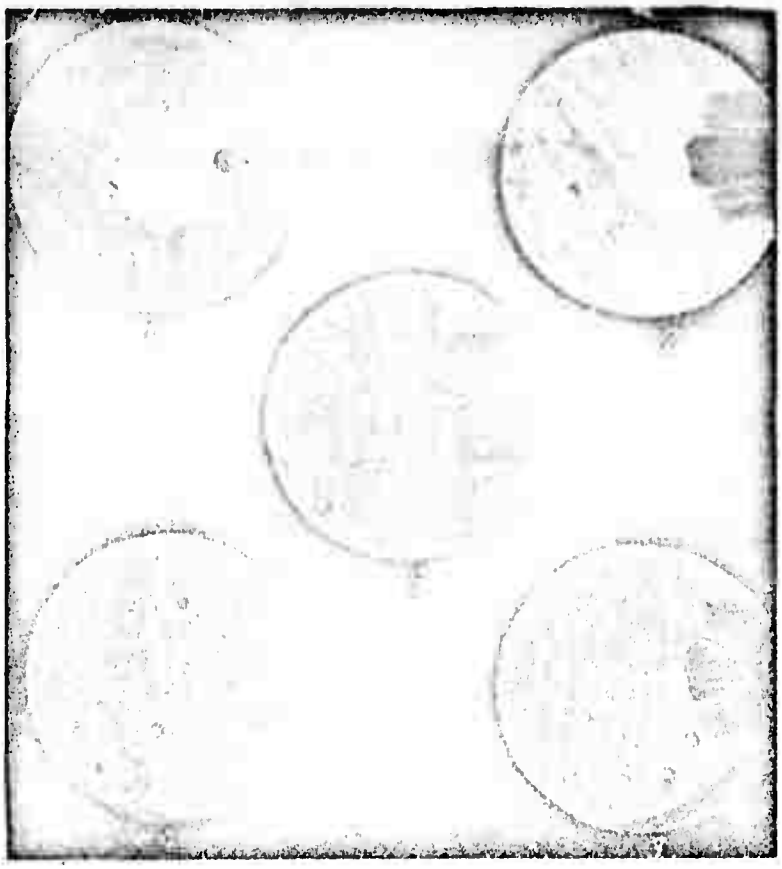

Fig. 2. Five frame sequence of flare expansion in vacuum, carbon target.

Frame diameter = 22 mm
Time between frames ≈50 nsec

region expanding at 3×10^6 cm/sec. By the third frame, this motion has stopped and in the fifth frame the opaque region has begun breaking up. Interference rings and refractive index gradient are evident in the sequence. The refractive effects indicate a diminishing electron density gradient in the direction of the target surface; this could be accounted for by recombination in an adiabatically expanding plasma.

The results of Fig. 2 were obtained with use of the decoupler cell in the Nd laser beam, as shown in Fig. 1. With this cell removed the effect is markedly different, since evaporation of the target surface begins some appreciable time before the arrival of the giant pulse; hence the plasma does not expand in a vacuum but into an atmosphere of the evaporated mass. An experiment of this type with carbon showed that the gas buildup 1 cm from the surface, generated over some 100 μsec prior to main pulse arrival, reaches densities on the order of $10^{17}/cm^3$. This results in shock

wave generation, whose progress can clearly be detected in a 5-frame sequence (Fig. 3).* For targets with lower heats of sublimation, the

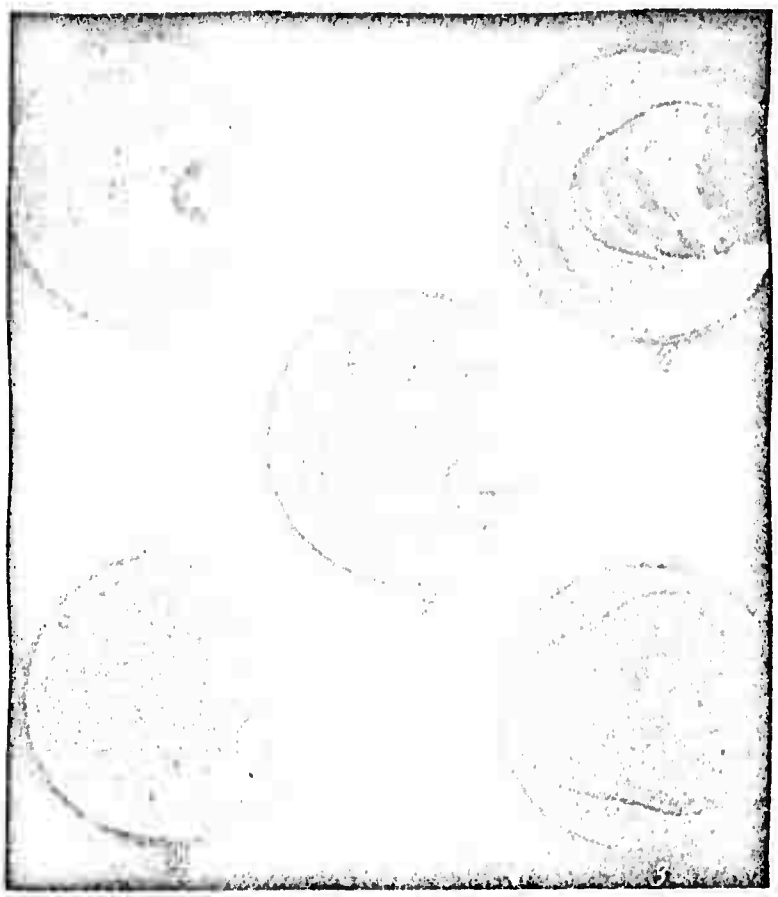

Fig. 3. Flare development with decoupler removed from Nd laser beam; carbon target. Pulse energy = 10j

pre-plasma evaporation is more intense, as in the cited cases of ebonite and plexiglass. Here the local density rose to $10^{18}/cm^3$ and was accompanied by strong turbulence which distorted the shock wavefront. In the case of plexiglass (Fig. 4), local spark breakdowns were also observed within the vapor cloud.

* In Fig. 3 and subsequent shadow photos, frame exposure time is 3 nsec.

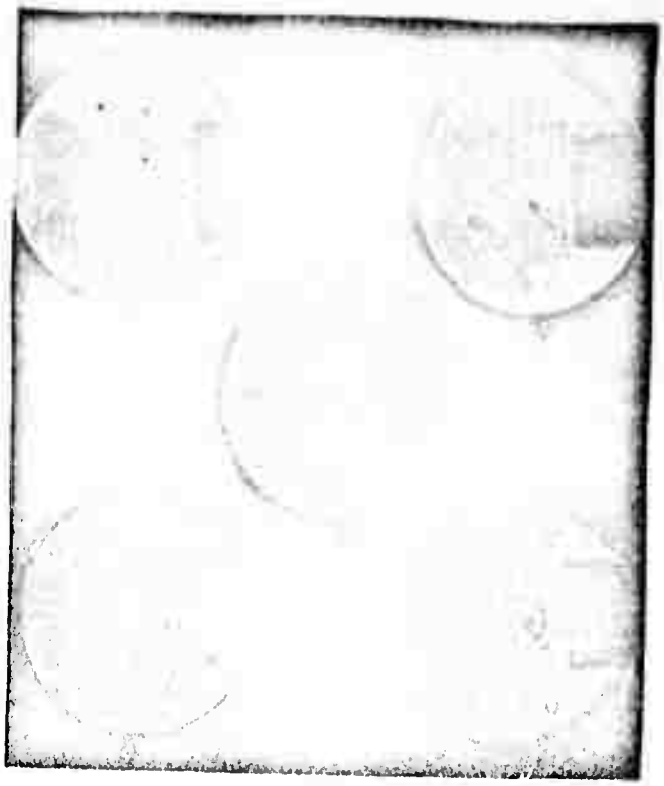

Fig. 4. Flare development from plexiglass target. Pulse energy = 7j.

A similar series of tests is described in low ambient gas pressures rather than in vacuo, using the same target materials and recording technique. Again the shock wave propagation is clearly discernible; plasma flares typically reached a characteristic dimension of 0.2 cm. The shock wave contour was close to spherical, but with a slightly increased radius in the direction of the focusing lens; this is owing to the fact that the focused spot has a finite area, so that initial evaporation occurs over a plane rather than from a point. These tests showed a weak dependence of shock wave velocity on target material; also the flare radius was practically independent of ambient pressure over a range of 0.1 - 10 torr (Fig. 5). A predictable limit here

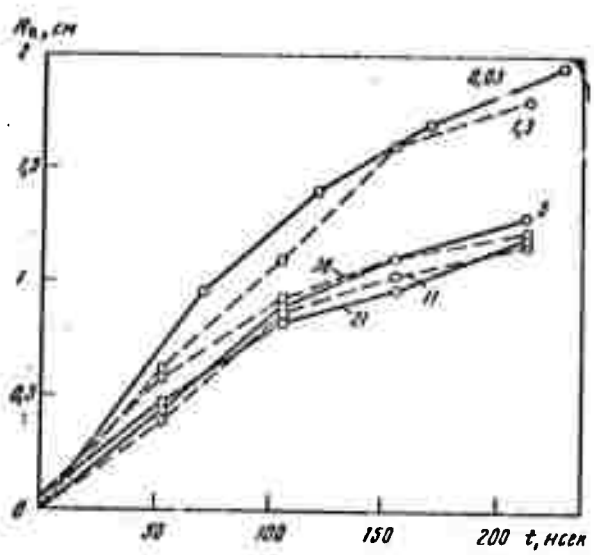

Fig. 5. Flare radius vs. pressure, radius vector in bea direction. Curve figures = pressure, torr.

was optical breakdown in the gas atmosphere, which began at about 40 torr (Fig. 6) with consequent shielding of the beam from the target surface.

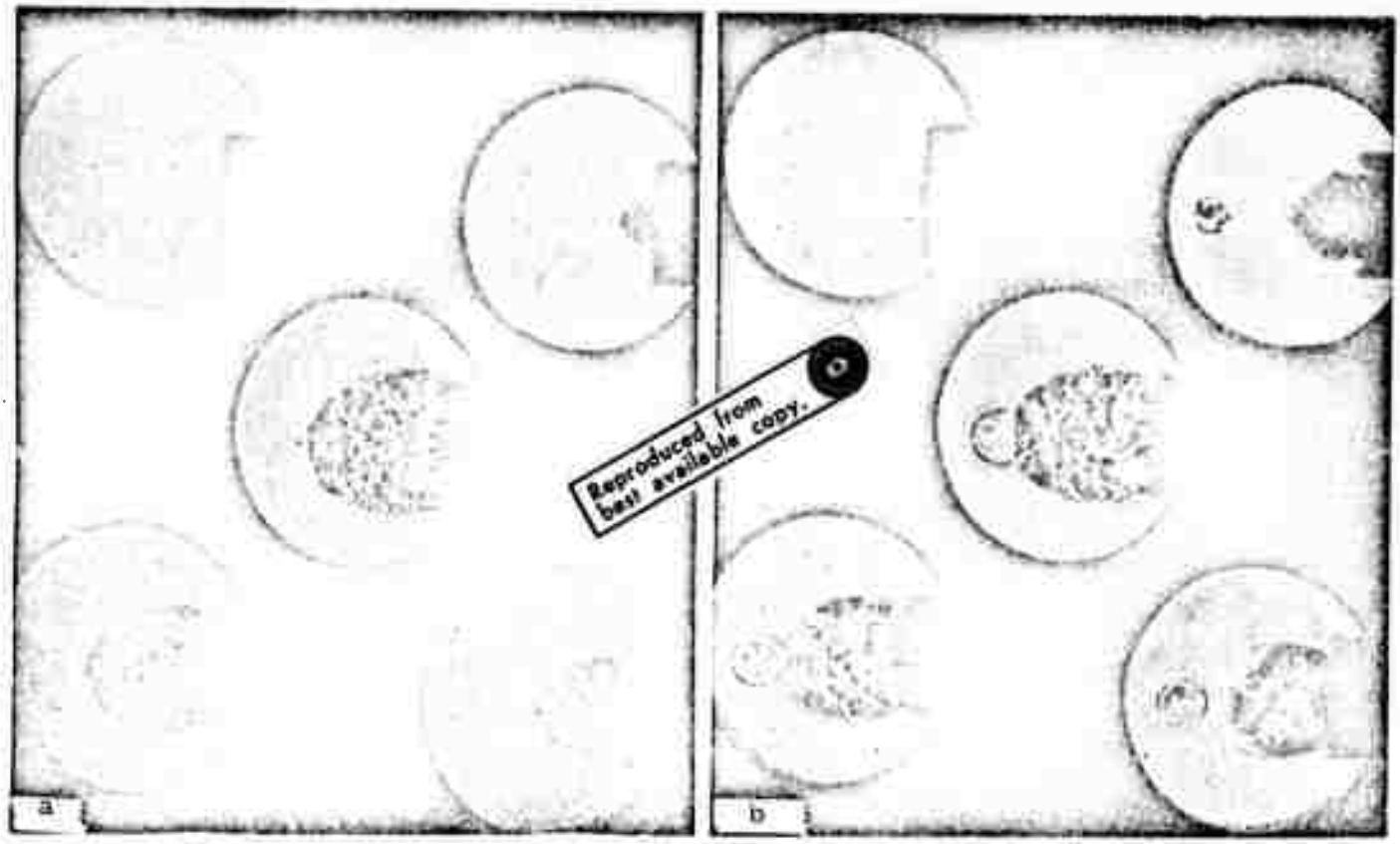

Fig. 6. Shock wave propagation, carbon target in air. a - P = 11 torr; b - P = 37 torr, breakdown occurs before target.

Fig. 7 shows shock wave propagation vs. time for four values of incident pulse energy taken at a gas pressure of 0.2 torr.

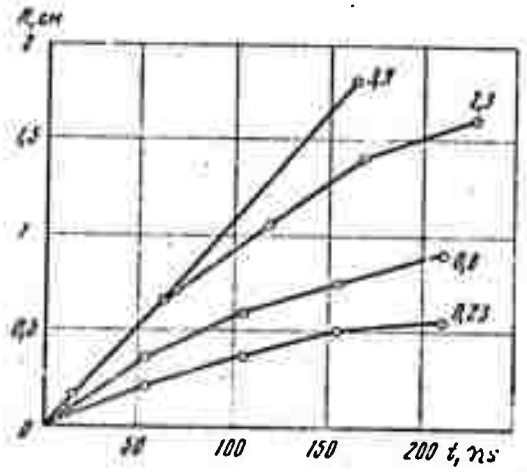

Fig. 7. Shock wave R(t) normal to target surface. Curve figures are pulse energies in joules; P = 0.2 torr.

Other steps in this series included irradiation of an aluminum foil target, and effects obtained with inclined incidence of the beam on the target. An interesting effect was obtained by using a notched impact surface, resulting in simultaneous generation of flares from two surfaces, and their collision (Fig. 8).

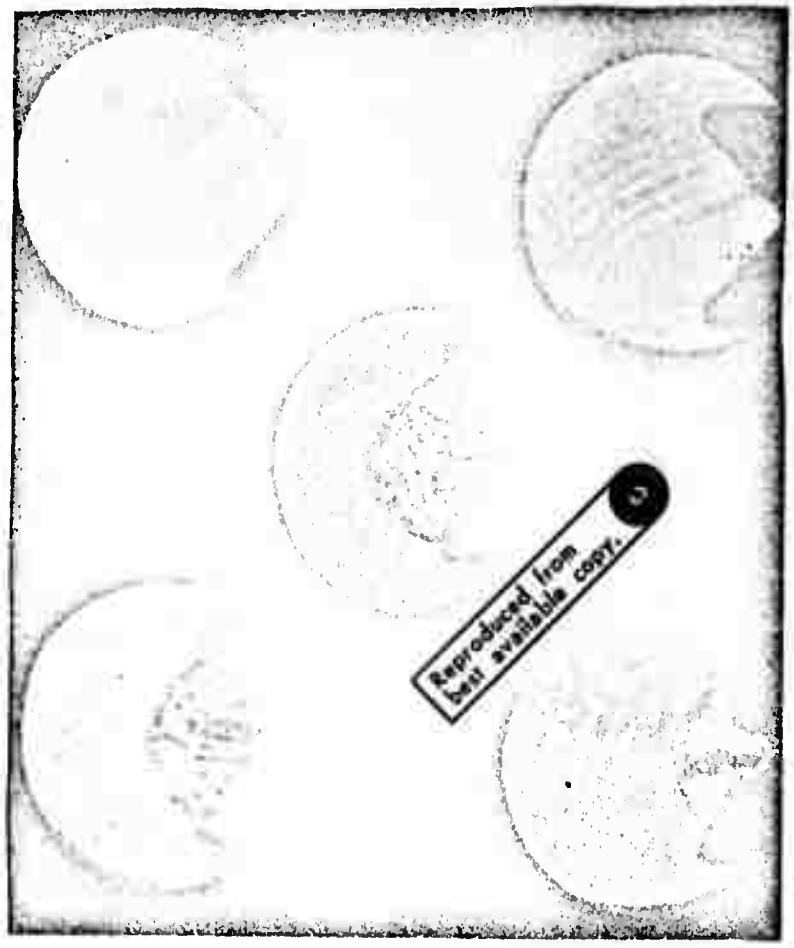

Fig. 8. Colliding shock waves from notched target. P = 10 torr, energy = 1.5j in each beam, impact points 7 mm apart.

Another high-speed method was used by Basov's group to photograph shock wave propagation in the plasma, for the case of trace gas in the test chamber. For static pressures greater than 0.2 torr the luminescence of the shock region was strong enough to register on film; the method for doing this is shown in Fig. 9. A standard high-speed SFR-2M camera was used, with the slit and rotating mirror arrangement shown in the figure; by raising the mirror rate to 90,000 rpm and increasing the mirror-to-film

distance to 1.25 m, the authors obtained a photo sequence with 2 nsec resolution.

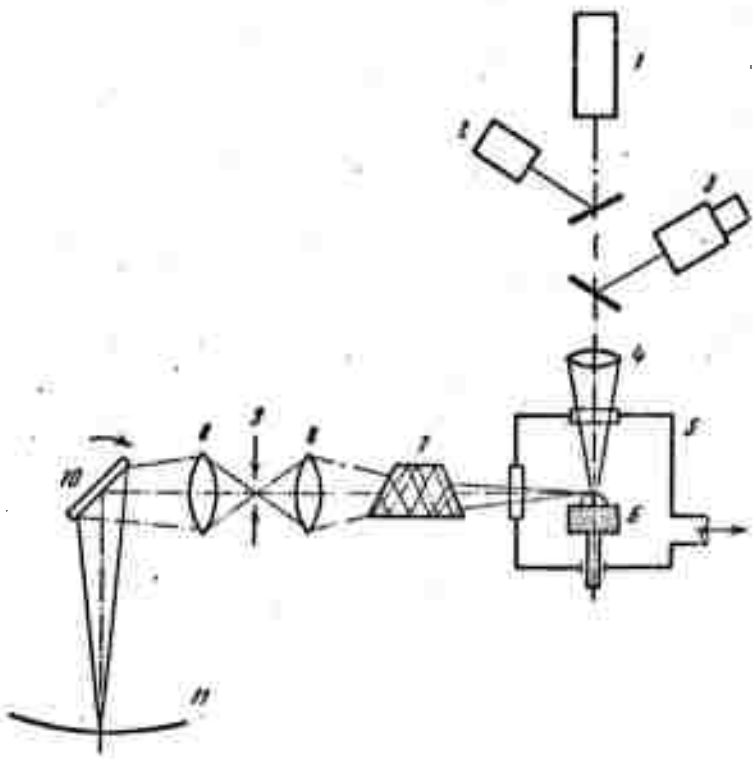

Fig. 9. Apparatus for measuring velocity of luminous front.

1-Nd laser; 2-calorimeter; 3-phòtoelement; 4-focal lens, f=100 mm; 5-chamber; 6-target; 7-rotating prism; 8-objectives; 9-target; 10-rotating mirror; 1-film.

The results showed that at lower pressures ($\sim$1 torr) the shock wave was not completely formed until near the end of the applied pulse, and the recorded luminous region represented the more slowly expanding plasma boundary; at low pressures a characteristic break between the shock wave and luminous boundary was thus evident. At increased pressures the shock wave formed more rapidly, and at 20 torr the luminous region practically coincided at once with it. Some of these effects can be seen in the photos of Fig. 10. The maximum shock wave velocity was recorded as 200 km/sec in

air at 1 torr. Similar experiments conducted in vacuo, including measurement of lateral flare propagation rates, are briefly mentioned here.

Fig. 10. Luminous shock wavefront

a - 1 torr; b - 7.2 torr; c - 19 torr.

Table 1 correlates the shock wave propagation rates with gas pressures for the carbon and lithium deuteride targets used.

Table 1. Shock wave velocity vs. pressure

P, torr	E, joules	v x 10^{-7}, cm/sec (carbon)	v x 10^{-7} cm/sec (LiD)
0,25	2,9	1,3	--
0,52	2,5	1,3	2,0
0,95	2,6	1,2	2,0
4,0	2,5	--	1,5
7,2	1,7	0,7	--
9,6	2,8	0,75	1,3
20,0	2,7	0,55	1,2

b. High-speed Interferometry Methods

For determining densities in a rapidly moving plasma, the interferometry method has become established as most useful. Basov describes three variants of interferometers used in the present series of tests, shown schematically in Fig. 11, including combined interferometry and shadow photography.

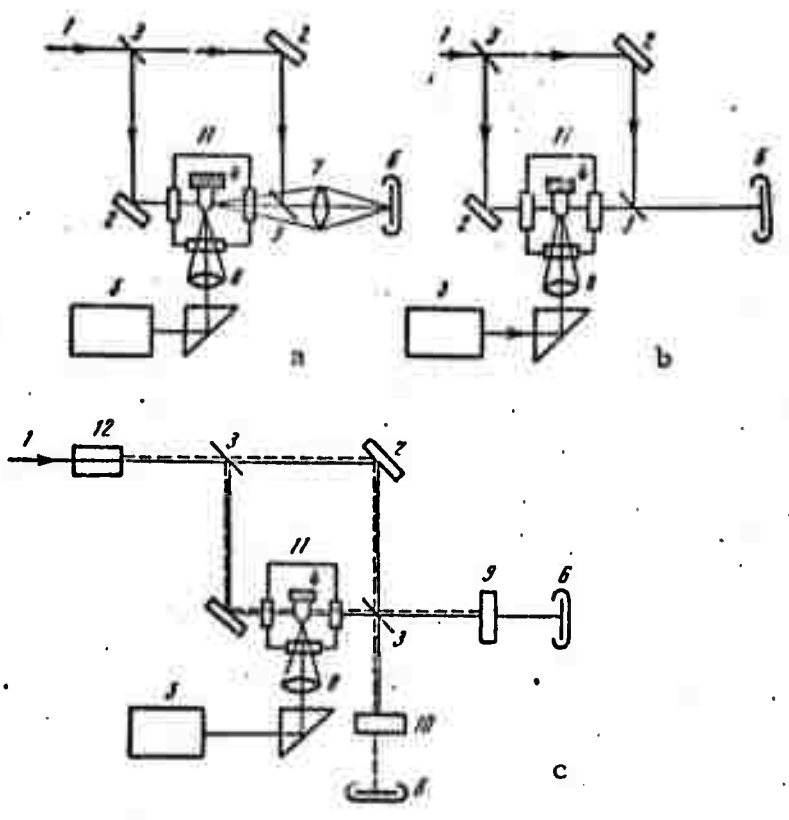

Fig. 11. Mach-Zender interferometer schemes.

1-narrowed ruby pulse; 2-deflector; 3-splitters; 4-target; 5-Nd laser; 6-film; 7,8-focussing lens; 9,10-filters; 11-chamber; 12-second harmonic generator

With the assumption of axial symmetry in the plasma flare, the process is simplified, since parallel-beam methods may be used rather than the multidirectional or holographic methods required in the general case. However, because of the minimum tolerable film exposure time the authors were constrained to use a Mach-Zender rather than the more accurate Fabry-Perot interferometer. The rapidity of flare propagation ($>10^7$ cm/sec) imposed a practical limit to interferogram interpretation, which was nominally accurate to 0.1 band; thus even with a 3 nsec resolution, some smear in the bands was present. The other inherent errors in the method are mentioned and evaluated for the present experiment.

The third variant of Fig. 11 is a dual beam method, using the ruby and its second harmonic. This has the added advantage of determining the dispersion of refractive index in the plasma. The cited case was somewhat complicated by the need to use quartz optics in the SHG beam path, and the lack of interference filters in the u-v band; this could be avoided by substituting a neodymium laser for the ruby. In spite of these limitations, Basov's group reports a frame resolution of 2 nsec for their dual-beam technique.

Results from several interferometry tests are described in which electron density N was determined directly from known laser wavelength λ and measured refractive index ν; for the ruby laser case, this reduced to $N = 4.67 \times 10^{21} \nu$. As before, tests were done both in vacuo and at various trace air pressures to register the shock wave. Figures 12, 13 and 14 are presented as typical of the results, taken about 100 nsec after the end of the laser pulse.

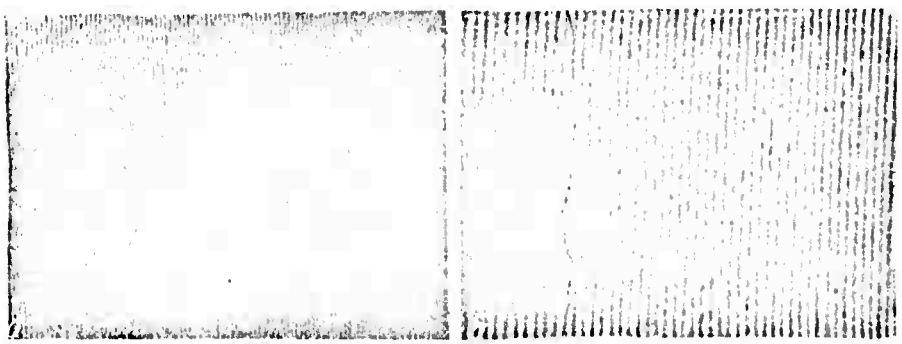

a b

Fig. 12. Simultaneous interferograms at fundamental and second harmonic

a - λ = 347 nm; b - λ = 694 nm

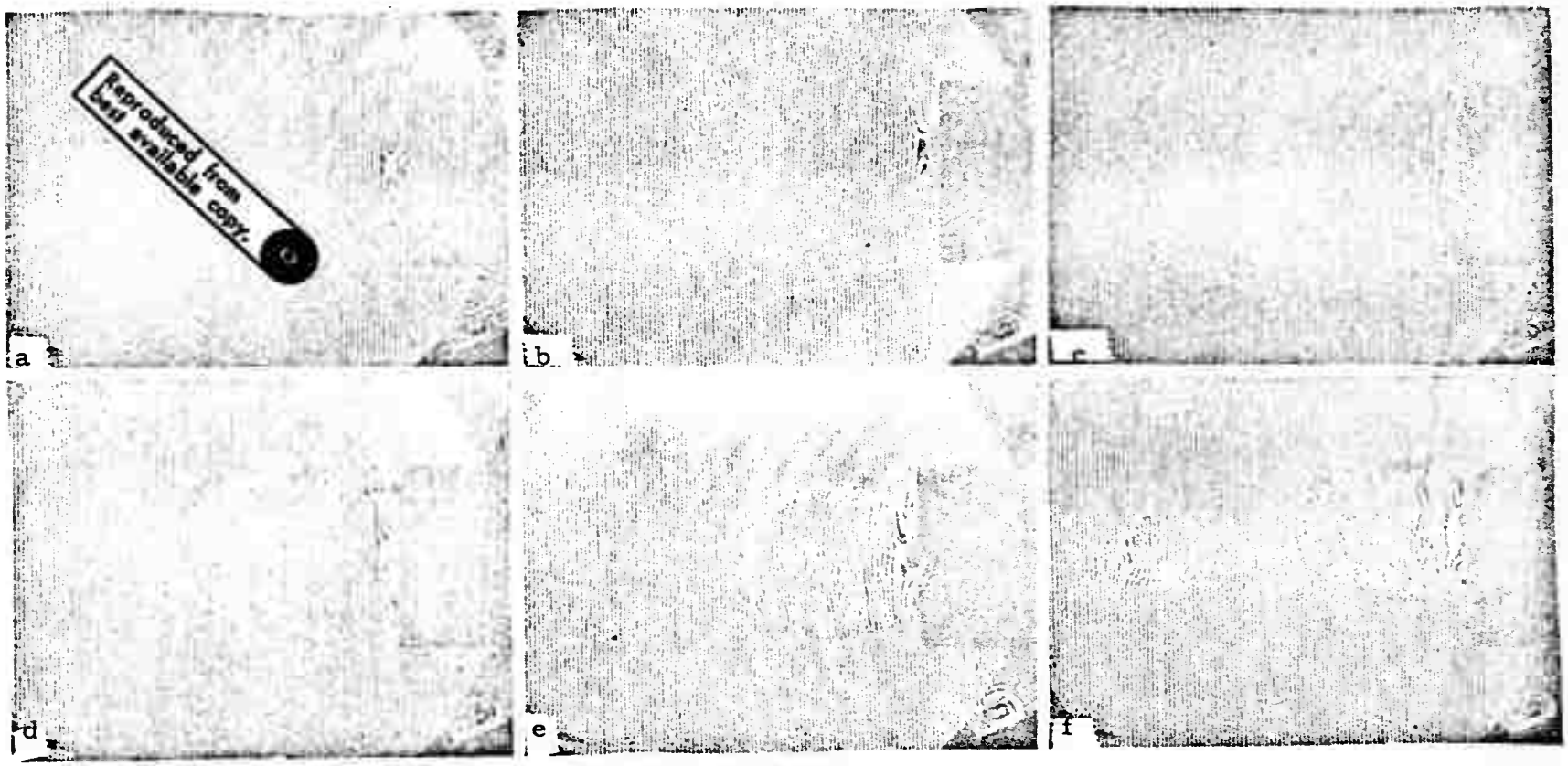

Fig. 13. Interferograms of shock wave from carbon target, 100 nsec after end of laser pulse. Ambient pressures for a-f are respectively 1.5, 2, 5.2, 12.3, 20 and 33.3 torr. Exposure time = 3 nsec.

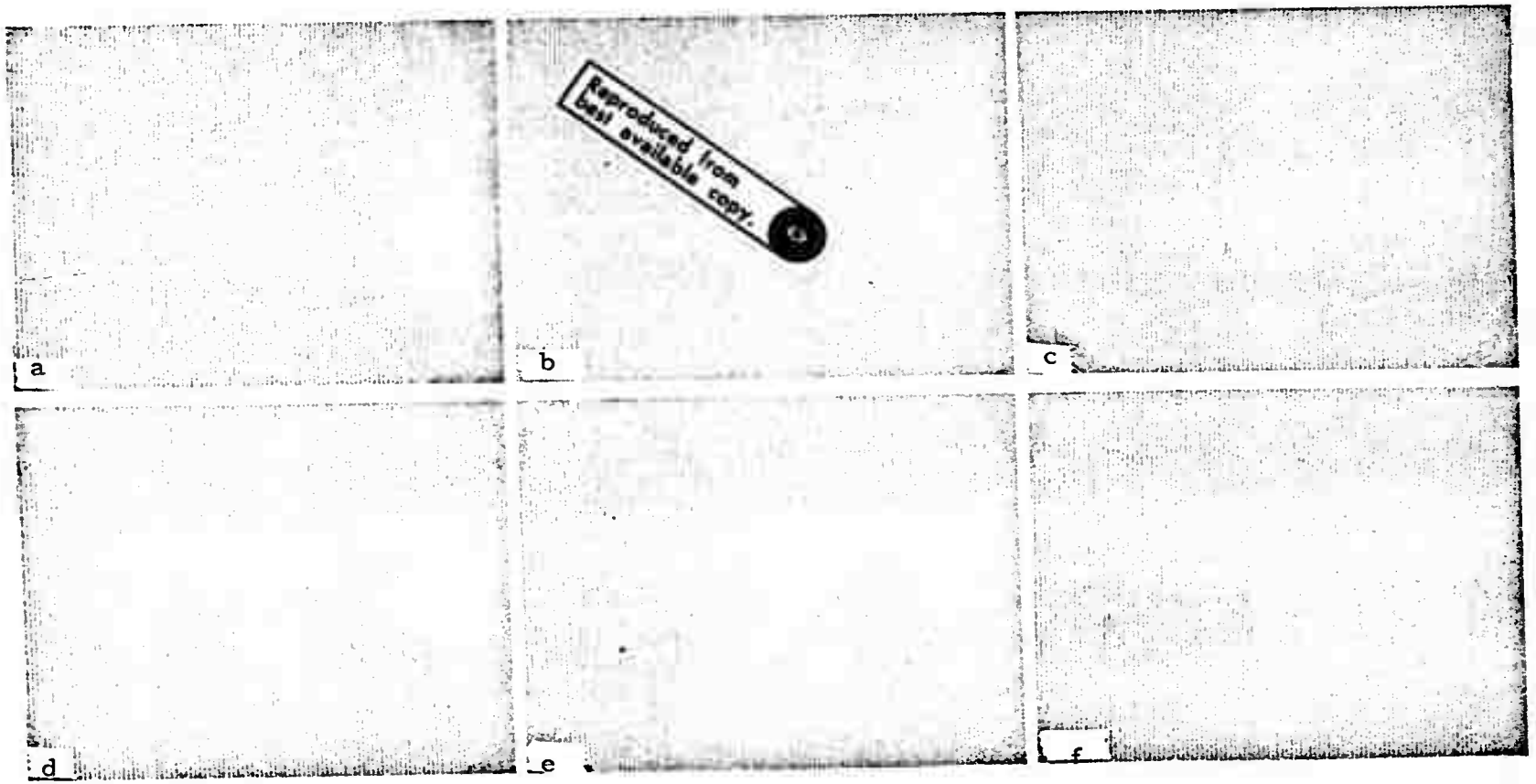

Fig. 14. Combined interferograms and shadow photos of shock waves, conditions similar to Fig. 13.

The dual-beam interferogram, for example, verifies that in the time intervals involved, ions and neutral atoms do not have a significant effect on plasma polarization. N was found to have a nearly spherical distribution in the plasma; on this assumption the isolines of N were plotted in Fig. 15 for a carbon target in vacuo.

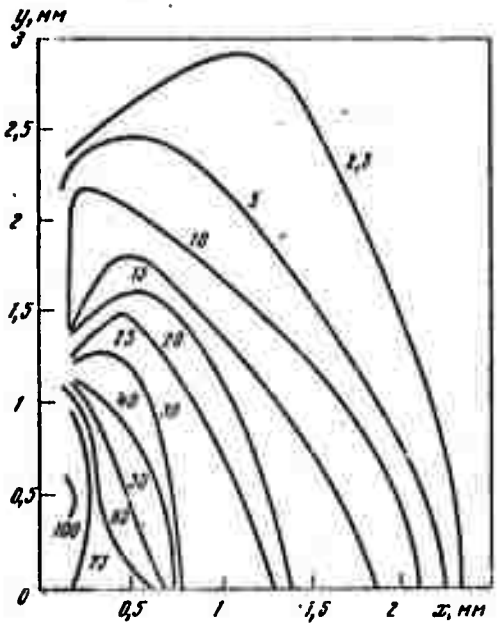

Fig. 15. Density isolines in laser plasma, x 10^{17}/cm^3. x || beam axis, y || target face.

Another useful application for the interferometry method is investigating conditions in the shock compression region. Basov discusses at length the ionization processes occurring in this region, and points out the difficulties in a rigorous quantitative analysis of them. However, by combining the interferometer and shadow techniques as shown in Fig. 11, it is possible to obtain images in which the compression region is well defined, and from which electron densities may be determined; Fig. 14 is an illustration of this. The exposure time had to be optimized so that the shadow portion would be clearly defined without obscuring the interference band. At pressures above 10 torr, refraction from the compression zone becomes strong enough to obliterate the bands, at which point the technique becomes ineffective. With some assumptions on symmetry, the authors arrive at the shock wave electron profile of Fig. 16. At a distance of 1 mm behind the wavefront, mean density was thus found to be 2--4 x 10^{18}/cm^3 over a wavefront velocity range of 0.8--1.4 x 10^7 cm/sec.

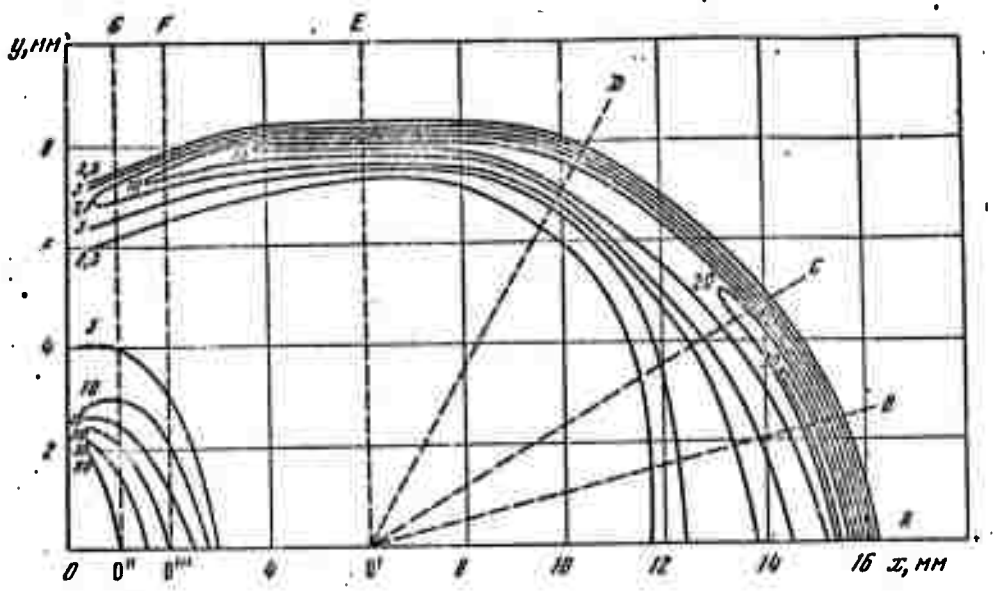

Fig. 16. N_e profiles in a shock wave, x $10^{17}/cm^3$. Energy = 6 j, elapsed time = 95 nsec after end of laser pulse. Origin of coordinates is beam focal point.

c. Schlieren Method

A limiting factor in the interferometry method just described is its inability to distinguish variations in compression layer thickness. This is theoretically possible by interferometry, but would require extremely precise optics as well as laborious calculations; a preferable method used by Basov is the Schlieren photo technique shown in Fig. 17. With an optical knife-edge placed at the focus of objective (5), any variation in refractive index in the illuminated plasma would register as an increase or decrease in film darkening (7), thus generating an intensity pattern which could be analyzed photometrically to yield refractive index gradient in the compression region. Using this method, Basov was also able to establish a range of 0.3 to 0.6 mm as the width of the compression region (these figures actually represent the resolution limits of the technique). A typical Schlieren photo series is given in Fig. 18 for four increasing pressures, and illustrates the sharp variation in refraction at the higher pressures. Basov concludes that the Schlieren method is an order of magnitude more sensitive than the interferometry method in this application.

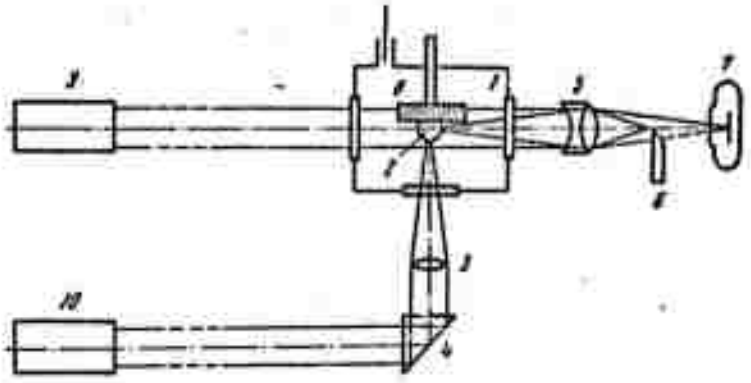

Fig. 17. Apparatus for Schlieren photography of laser flare.

1-chamber; 2-flare; 3-focus lens; 4-deflector; 5-objective; 6-knife-edge; 7-film; 8-carbon target; 9-ruby; 10-Nd laser.

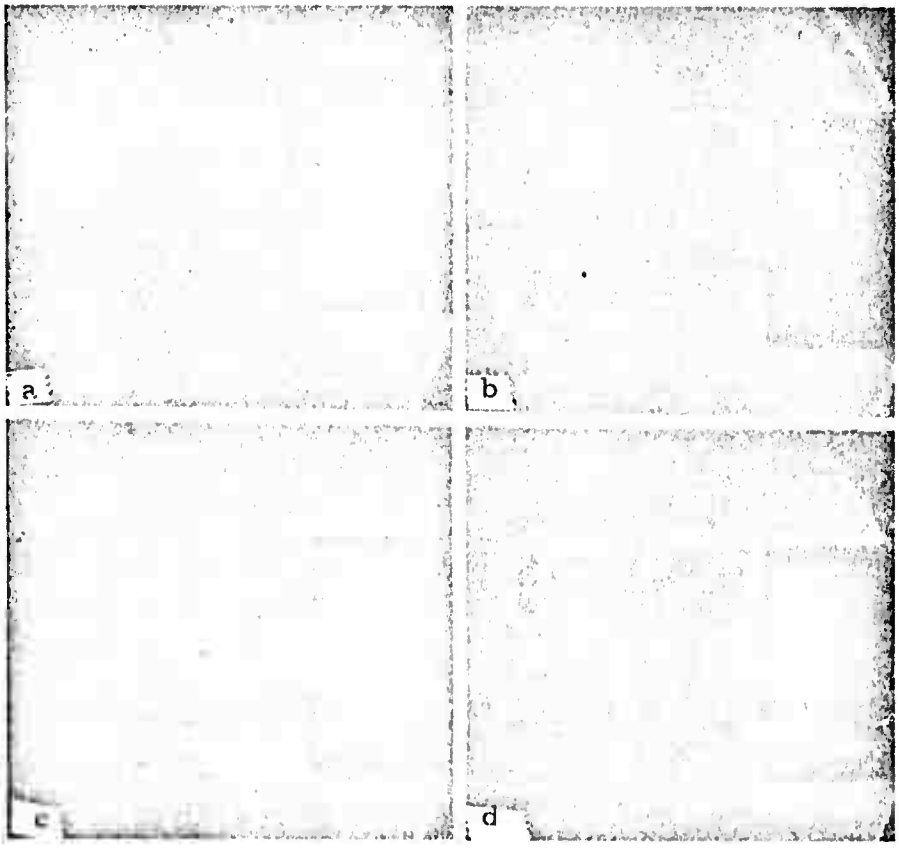

Fig. 18. Schlieren photos of flares from a carbon target, 100 nsec after pulse end.
Pulse energy = 6j, τ = 20 nsec, exposure = 3 nsec.
a - 2×10^{-2} torr; b - 1 torr; c - 2 torr; d - 4 torr.

d. Particle Emission Measurements

A technique for measuring some plasma parameters by monitoring particle emission, already mentioned by Basov as a generally earlier stage in laser plasma studies, is next briefly reviewed. Referring to a previous report of his (20), Basov describes a probe method for recording variation in emitted particle density and polarity in the course of flare expansion. Electrons are emitted from the plasma, leaving a net positive charge region behind; probe data are given illustrating the polarity change with time, from which the growth rate of the flare radius can be determined. For a Nd laser power of 200 Mw at 3j, the dispersion velocity is shown in one example to reach 1.4×10^7 cm/sec.

e. Magnetic Field Measurements

The emf induced by a laser plasma expanding through a transverse magnetic field has been used for determining flare parameters (21, 22). The schematic form for this is given in Fig. 19, and a brief reference to experimental results from it is given by Basov. A critical factor in the success of this technique is the compensation for the space charge which accumulates on the current-measuring electrodes, 1 and 2 in Fig. 19.

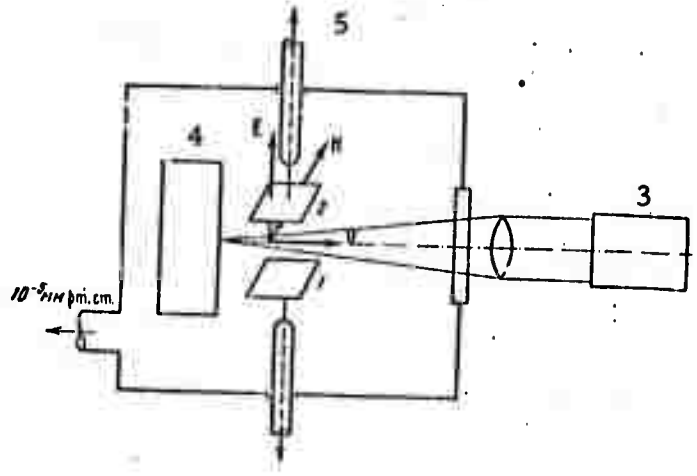

Fig. 19. Measuring flare parameters with a transverse magnetic field.
1, 2 - current electrodes; 3 - laser; 4 - target;
5 - to compensating circuitry.

Basov suggests several compensation circuits for this, and briefly describes some diagnostic results obtained when using a field on the order of 1 koe. With some simplifications it can be shown that dispersion velocity will then be a direct function of induced emf, and from conductivity the electron density and temperature can be found.

A question arises in this technique as to the possible distorting effects of the applied field to plasma development. Basov produces shadow photos of plasmas with and without an external field, showing that, at least for his experimental conditions, the field had negligible effect; this is in contradiction to the finding of Linlor (21), but Basov suggests Linlor was led to an erroneous conclusion from a lack of adequate time resolution.

f. Measurement of Recoil and Reactions in the Target Mass

A final measurement method briefly discussed involves the recoil imparted to the target by the laser action. The recoil can be measured by various methods, including the pendulum technique described by Basov, from which ejecta mass can be calculated. There is evidence that local pressures at the target surface reach the order of 10^5 atm during the laser pulse, which generates a compressional shock wave in the target material. Basov establishes that it is the unloading of this compression which primarily generates the specific recoil pulse, and which forces the bulk of the ejecta in a direction opposite to the beam. This is clearly demonstrated in a sequence of shadow photos in which the target was 10 micron Al foil covering a hole in a metal cylinder wall. Data are also presented to show that specific impulse has only a weak dependence on beam intensity, i.e. $P/E \sim q^{-\alpha}$ where α varies over a range of 0.1 to 0.3.

Conclusions

In summarizing their results, Basov et al reiterate some of the values obtained for laser plasma parameters, and again stress the success of their shadow and interferometry techniques in obtaining this data. The high frame resolution thus has permitted a more detailed analysis of plasma propagation rate and geometry, shock wave configuration, and local densities and temperatures of plasma particles.

Aside from the pure research into laser-target interactions, the results obtained suggest some interesting possibilities in other applications. Thus in addition to the CTR possibilities already referred to, Basov points to the feasibility of generating a cumulative shock wave effect by using a multiple target face, as in Fig. 8. The emission properties of the plasma suggest its use as a local electron or very pure ion source in related applications. Finally, the techniques can in general be applied to thermodynamic studies of evaporation of highly refractive materials, without requiring the complex apparatus otherwise needed at such high temperatures and pressures.

REFERENCES

1. Basov, N. G., O. N. Krokhin, and G. V. Sklizkov. Study of the dynamics of heating and expansion of a plasma formed by focusing powerful laser radiation on materials. IN: AN SSSR. Fizicheskiy institut imeni P. N. Lebedeva. Trudy no. 52, 1970. Kvantovaya radiofizika, 171-236.

2. Honig, R. E., J. R. Woolston. Applied Physics Letters, 2, no. 7, 1963.

3. Lichman, D., J. F. Ready. Physics Review Letters, 10, no. 8, 1963.

4. Linlor, W. I. Applied Physics Letters, 3, 210, 1963.

5. Haught, A. F., D. H. Polk. Physics of Fluids, 9, 2047, 1966.

6. Opower, H., E. Burlefinger. Physics Letters, 16, 37, 1965.

7. Cobb, J. K., J. J. Murray. Bull. Amer. Phys. Soc., 9, 536, 1964; J. F. Ready. Bull. Amer. Phys. Soc., 9, 536, 1964.

8. Bogdankevich, O. V., V. Yu. Sudzilovskiy, and A. A. Lozhnikov. ZhTF, v. 35, 1965, 2052.

9. Ascoli-Bartoli, U., C. De Michelis, E. Mazzucato. Rept. Conf. Plasma Physics and Controlled Nuclear Fusion Research, Culham, 1965, CN-21/77.

10. Weichel, H., P. V. Avizonis. Appl. Physics Letters, 9, 334, 1966.

11. Bruce, C. W., J. Deacon, D. F. Vonderhaar. Appl. Physics Letters, 9, 164, 1966.

12. Dolgov-Savel'yev, G. G., M. I. Pergament, M. M. Stepanenko, and A. I. Yaroslavskiy. IN: Sbornik. Diagnostika plazmy, part 2. Atomizdat, 1969.

13. Kaskadnyye EOPy. Sbornik. M. M. Vutslov, ed. (transl.), 1965.

14. Fawcett, B. C., A. H. Gabrel, F. E. Ions, N. J. Peacock, P. A. H. Saunders. Proc. Phys. Soc., 88, 1051, 1966.

15. Basov, N. G., V. A. Boyko, Yu. P. Voynov, E. Ya. Kononov, S. L. Mandel'shtam, and G. V. Sklizkov. ZhETF P, v. 5, 1967, 177; v. 6, 1967, 849.

16. Gregg, D. W., S. J. Thomas. J. Appl. Physics, 37, 2787, 1966.

17. Askar'yan, G. A. and Ye. M. Moroz. ZhETF, v. 43, 1962, 2319.

18. Sedov, L. I. Methods of similarity and dimensionality in mechanics. Izd-vo nauka, 1965.

19. Nemchinov, I. V. Prikladnaya mekhanika i matematika, v. 31, 1967, 300.

20. Basov, N. G., V. A. Boyko, V. A. Dement'yev, O. N. Krokhin, and G. V. Sklizkov. ZhETF, v. 51, 1966, 989.

21. Linlor, W. I. Phys. Rev. Letters, 12, 383, 1964.

22. Sucow, E. W., G. L. Pack, A. V. Phelps, A. J. Engelhardt. Phys. Fluids, 10, 2035, 1967.

SOURCE ABBREVIATIONS

DAN SSSR	-	Akademiya nauk SSSR. Doklady
FiKhOM	-	Fizika i khimiya obrabotki materialov
F-KhMM	-	Fiziko-khimicheskaya mekhanika materialov
FTP	-	Fizika i tekhnika poluprovodnikov
FTT	-	Fizika tverdogo tela
IAN Fiz	-	Izvestiya AN SSSR. Seriya fizicheskaya
I-FZh	-	Inzhenerno-fizicheskiy zhurnal
KhVE	-	Khimiya vysokikh energiy
KSpF	-	Kratkiye soobshcheniya po fizike
MiTOM	-	Metallovedeniye i termicheskaya obrabotka materialov
MZhiG	-	Akademiya nauk SSSR. Izvestiya. Mekhanika zhidkosti i gaza
OiS	-	Optika i spektroskopiya
PTE	-	Pribory i tekhnika eksperimenta
RiE	-	Radiotekhnika i elektronika
TVT	-	Teplofizika vysokikh temperatur
ZhETF	-	Zhurnal eksperimental'noy i teoreticheskoy fiziki
ZhETF P	-	Pis'ma v zhurnal eksperimental'noy i teoreticheskoy fiziki
ZhPMTF	-	Zhurnal prikladnoy mekhaniki i tekhnicheskoy fiziki

ZhPS	-	Zhurnal prikladnoy spektroskopii
ZhTF	-	Zhurnal tekhnicheskoy fiziki

AUTHOR INDEX